Characterizing Geological and Geochemical Properties of Selected Gas Shales and Their Thermal Maturation in the Black Warrior Basin, Alabama

by

Christopher Scott Marlow

A thesis submitted to the Graduate Faculty of
Auburn University
in partial fulfillment of the
requirements for the Degree of
Master of Science

Auburn, Alabama
August 2, 2014

Copyright 2014 by Christopher Marlow

Approved by

Ming-Kuo Lee, Chair, Robert B. Cook Professor, Department of Geology and Geography
Lorraine Wolf, Professor, Department of Geology and Geography
David T. King Jr., Professor, Department of Geology and Geography
Richard Esposito, Principal Research Geologist, Southern Company

Abstract

This study will focus on selected gas shale's, geological and geochemical properties in Alabama's Black Warrior Basin, which contains Cambrian through Mississippian shales; these gas-shales that may potentially produce up to 800 trillion cubic feet of natural gas.

This study was performed from a multidisciplinary standpoint where several important aspects of gas-shale production were examined where both industrial and environmental concerns of gas-shale were addressed. Environmental concerns were restricted to aspects of gas-shale production that could potentially contaminate groundwater. Considering industry concerns, special attention was paid to the hydrocarbon development in each of the gas-shales studied. To do this, several techniques were utilized to (1) characterize the variations in gas-shale mineralogy's, (2) quantify the concentration of trace elements (e.g., those with potential impacts to drinking water), (3) characterize and correlate key organic compounds (i.e., biomarkers) extracted from shales, (4) model the thermal history and hydrodynamic evolution of the basin, and (5) understand how new regulations involving hydraulic fracturing may potentially affect the industrial practices of protecting groundwater supplies.

X-ray diffraction (XRD) and X-ray fluorescence (XRF) techniques were used to characterize the variations in gas shale mineralogy and quantify the concentration of trace elements, especially those with potential to impact potable groundwater if mixing of brine fluids and groundwater occur. The XRD results show that these shales contained varying amounts of quartz, calcite, and sulfide minerals (e.g., pyrite and arsenopyrite). Elevated concentrations of

certain trace elements such as arsenic (As) and lead (Pb) are found in all but the Cambrian Conasauga Shale, which is dominated by carbonate minerals (up to 50% by weight). The Neal (Floyd) Shale has the highest sulfide mineral and As contents. Trace metals tend to concentrate in fine-grained sulfide minerals, which commonly serve as the major sinks for toxic metals such as As and Pb under reducing environments. These particular toxic metals are currently regulated by groundwater regulations in Illinois, Colorado, and Pennsylvania, during gas-shale production.

Similarities in gas fragmentographs of all three biomarkers associated with m/z 191, 217, and 218 suggest a common source of organic carbon for the Devonian Chattanooga Shale and Cambrian Conasauga Shale. By contrast, significantly different biomarker signatures of the Mississippian Neal (Floyd) Shale indicate that organic matter in this younger unit is likely derived from a different source. Geophysical logs (gamma logs) were used to correlate hydro-geologic units in the basin. A three dimensional hydro-stratigraphic framework of the Black Warrior Basin was reconstructed; utilizing this hydro-stratigraphic framework, a two-dimensional transect across the basin was modeled for thermal and hydrologic evolution. The modeling results indicate that major over-pressurization within the Black Warrior Basin occurred during the rapid deposition of the thick Pottsville Formation (Pennsylvanian). It was during Pennsylvanian that the majority of the Neal (Floyd) and Chattanooga shales reached the oil window; the gas window in these units was not reached until the erosion of the Upper Pottsville Formation during Late Pennsylvanian.

Table of Contents

Abstract ii

List of Tables vii

List of Figures viii

Chapter 1: Introduction 1

Chapter 2: Site Location and Background 4

Gas-Shale reservoirs 7

Mineralogy 8

Heavy metals/radio nuclides 9

Redox geochemistry 9

Permeability/porosity 10

Total organic carbon 12

Petroleum Bio-markers 13

Thermal maturation 13

Chapter 3: Materials and Methods 17

Core sample collection 17

X-ray diffraction (XRD) analysis 17

X-ray fluorescence (XRF) analysis 18

Organic matter extraction and biomarker analysis 21

Geophysical log analysis and basin modeling 22

Chapter 4: Results and Discussion 26
Inorganic Geochemistry 26
Aluminum 30
Arsenic 32
Lead 35
Mercury 38
Sulfur 40
Iron 43
Wellbore, Pit, and Base Line Water Testing 47
Potential USDW Degradation and Economic Impact Due to Gas-Shale Production 48
Subsurface Monitoring and Contaminant Modeling 49
Future Impact Due to Colorado, Pennsylvania, and Illinois Base Line Water Testing 50
Metal enrichment in the Black Warrior Basin Shale's 52
Mineralogy 59
Organic geochemistry 68
Chattanooga Shale, Greene County Alabama 68
Conasauga Formation, St. Claire County Alabama 73
Neal (Floyd) Shale, Pickens County Alabama 78
Petroleum Bio-markers 83
Chattanooga Shale, Greene County Alabama 83
Conasauga Formation, St. Claire County Alabama 88
Neal (Floyd) Shale, Pickens County Alabama 89
Reconstruction of hydro-stratigraphic sections 94

Basin hydraulic evolution, overpressurization, and thermal maturation 101

Modeling results..... 104

Discussion Summary 119

Conclusions..... 120

References 126

Appendix1. Script written for and utilized in Basin2 modeling thermal maturation, overpressurization, and hydraulic evolution of the Black Warrior Basin..... 131

List of Tables

Table 1. TTI values and thermal maturation 14

Table 2. Depth and location of well permit #s 2191 and 1780 14

Table 3. Location and depth of drill cores 17

Table 4. XRF settings used in elemental analysis..... 19

Table 5. ICP-MS standard for elemental analysis 20

Table 6. Permit #s, well name, and location of down hole geophysical logs 23

Table 7. Wellbore and baseline water testing requirements 51

Table 8. Containment pit requirements..... 52

Table 9. Illinois water testing requirements for hydraulic fracturing 52

Table 10. ANEF values for selected EPA regulated elements..... 55

List of Figures

Figure 1. Black Warrior Basin location and study area 6

Figure 2. Log-linear relationship of porosity and permeability 11

Figure 3. TTI index for stratigraphic units present in well permit #s 2191 and 1780 16

Figure 4. Locations of Black Warrior Basin down-hole geophysical logs 25

Figure 5. Spectral signature from the Neal (Floyd) Shale in Greene County 27-29

Figure 6. Aluminum concentrations for each shale 31

Figure 7. Arsenic concentrations for each shale 34

Figure 8. Lead concentrations for each shale..... 37

Figure 9. Mercury concentrations for each shale..... 39

Figure 10. Sulfur concentrations for each shale..... 42

Figure 11. Iron concentrations for each shale..... 45

Figure 12. Arsenic, lead, and sulfur concentrations versus iron concentrations..... 46

Figure 13. ANEF for the Chattanooga Shale in Greene County..... 56

Figure 14. ANEF for the Conasauga Shale in Shelby County..... 56

Figure 15. ANEF for the Conasauga Shale in St. Claire County..... 57

Figure 16. ANEF for the Devonian Shale in Hale County 57

Figure 17. ANEF for the Neal (Floyd) Shale in Greene County 58

Figure 18. ANEF for the Neal (Floyd) Shale in Pickens County 58

Figure 19. 2θ spectrum for the Chattanooga Shale in Greene County 62

Figure 20. 2θ spectrum for the Conasauga Shale in Shelby County..... 63

Figure 21. 2θ spectrum for the Conasauga Shale in St. Claire County..... 64

Figure 22. 2θ spectrum for the Devonian Shale in Hale County 65

Figure 23. 2θ spectrum for the Neal (Floyd) Shale in Pickens County 66

Figure 24. 2θ spectrum for the Neal (Floyd) Shale in Greene County 67

Figure 25. Hydrocarbon compound identified in the Chattanooga Shale in Greene County 69

Figure 26. Spectral signature of the hydrocarbon compound extracted from the Chattanooga Shale in Greene County 70

Figure 27. M/Z ratios of extracted organics from the Chattanooga Shale in Greene County 71

Figure 28. Gas Chromatograph of extracted organics from the Chattanooga Shale in Greene County..... 72

Figure 29. Hydrocarbon compound identified in the Conasauga Shale in St. Claire County 74

Figure 30. Spectral signature of the hydrocarbon compound extracted from the Conasauga Shale in St. Claire County..... 75

Figure 31. M/Z ratios of extracted organics from the Conasauga Shale in St. Claire County ... 76

Figure 32. Gas Chromatograph of extracted organics from the Conasauga Shale in St. Claire County..... 77

Figure 33. Hydrocarbon compound identified in the Neal (Floyd) Shale in Pickens County.... 79

Figure 34. Spectral signature of the hydrocarbon compound from the Neal (Floyd) Shale in Pickens County 80

Figure 35. M/Z ratios of extracted organics from the Neal (Floyd) Shale in Pickens County ... 81

Figure 36. Gas Chromatograph of extracted organics from the Neal (Floyd) Shale in Pickens County..... 82

Figure 37. Gas Fragmentograph of m/z 191 bio-marker for the Chattanooga Shale in Greene County and the Conasauga Shale in St. Claire County..... 85

Figure 38. Gas Fragmentograph of m/z 217 bio-marker for the Chattanooga Shale in Greene County and the Conasauga Shale in St. Claire County..... 86

Figure 39. Gas Fragmentograph of m/z 218 bio-marker for the Chattanooga Shale in Greene County and the Conasauga Shale in St. Claire County 87

Figure 40. Gas Fragmentograph of m/z 191 bio-marker for the Neal (Floyd) Shale in Pickens County 91

Figure 41. Gas Fragmentograph of m/z 217 bio-marker for the Neal (Floyd) Shale in Pickens County 92

Figure 42. Gas Fragmentograph of m/z 218 bio-marker for the Neal (Floyd) Shale in Pickens County 93

Figure 43. Panel diagram of well permit #s 1800 and 1810 96

Figure 44. Reconstructed surfaces of the Chattanooga Shale and Neal (Floyd) Shale within the Black Warrior Basin 97-100

Figure 45. Transect of the Black Warrior Basin modeled in Basin2 102

Figure 46. Present day stratigraphic cross section of the Black Warrior Basin 103

Figure 47. Black Warrior Basin modeling results at 505 m.y. 109

Figure 48. Black Warrior Basin modeling results at 480 m.y. 110

Figure 49. Black Warrior Basin modeling results at 350 m.y. 111

Figure 50. Black Warrior Basin modeling results at 323 m.y. 112

Figure 51. Black Warrior Basin modeling results at 248 m.y. 113

Figure 52. Black Warrior Basin modeling results at 75 m.y. 114

Figure 53. Black Warrior Basin modeling results at present day 115

Figure 54. Calculated oil window, through time, for the Conasauga Formation, Chattanooga Shale, and Neal (Floyd) Shale 116

Figure 55. Calculated oil percentage generated, through time, for the Conasauga Formation, Chattanooga Shale, and Neal (Floyd) Shale 117

Figure 56. Calculated gas window, through time, for the Conasauga Formation, Chattanooga Shale, and Neal (Floyd) Shale 118

INTRODUCTION

Unconventional oil and gas exploration and development is in the very early stage in Alabama and most of this is being currently directed at the state's Cambrian through Mississippian shale reservoirs (Pashin et al., 2011). Shale is considered an unconventional reservoir due to its nature as a reservoir body as well as its very low porosity and permeability (Miskimins, 2009; Jarvie et al., 2007). For unconventional reservoirs to be economically viable, secondary fracture systems must be present or induced through hydraulic fracturing (Miskimins, 2009; Jarvie et al., 2007). Hydraulic fracturing technologies and implementation have surpassed current regulations due to a lack of scientific understanding of fracturing fluids-rock interaction and the potential release of heavy metals, radionuclides, and organic compounds from metal- and organic-rich shales (Alley, et. al, 2011; Coveney, 1989; Perkins, 2012).

The potential soci-economic impact of gas-shale production is staggering, according to the Energy Information Administration (EIA) gas-shale accounted for 14% of gas production in the United States in 2004 and by 2030 it is projected that gas-shale will account for approximately 53% of new electricity (Myers, 2012). Further research must progress in the realm of unconventional reservoirs to understand reservoir viability and potential geologic and geochemical interactions caused by exploiting this vast hydrocarbon resource.

With this in mind, the largest oil and gas reservoirs within Alabama are located in the Black Warrior Basin (Figure 1) where 800 trillion cubic feet of natural gas are potentially held in three gas-shales: the Cambrian Conasauga Shale, the Devonian Chattanooga Shale, and the

Mississippian Neal (Floyd) Shale (Pashin et al., 2011). The Neal (Floyd) Shale is the stratigraphic equivalent of two high-yield unconventional reservoirs, namely the Fayetteville Shale of the Arkoma Basin and the Barnett Shale of the Fort Worth Basin (Pashin et al., 2011).

When developing gas-shale, one must consider the regulations that are either being emplaced or may potentially be emplaced. Of major concern are regulations concerning gas-shale production and potential contamination of groundwater resources and how this is related to the inorganic/organic geochemistry and mineralogy within shales. One particular element that Colorado, Pennsylvania, and Illinois require to be tested is arsenic. Arsenic is of special concern because of its negative health effects (Smith et al., 2012; Soeder and Kappel, 2009).

This research project will focus on characterizing three gas-shale units in the Black Warrior Basin. Of special interest is the mineralogy of the various reservoir bodies, levels of heavy metals present, organic compounds in the reservoirs, permeability and porosity, stratigraphy and spatial distribution of shales, and thermal history and basin hydrodynamics.

The hydrocarbons within gas-shale generally lack analysis beyond the particular types of organic compounds, the amount of free gas, and total organic carbon present; however, biomarker fingerprinting the organic carbon of the hydrocarbons has not been conducted in previous studies. This research will move forward the understanding of source of organic matter in the various shales by petroleum biomarker analysis.

Mineralogical, geochemical, and hydrological properties of various shales in the Black Warrior Basin reflect their depositional and thermal history. The geological, geochemical, and hydrological characteristics of shales could be investigated using mineralogy, bulk geochemistry, petroleum biomarker, and porosity/permeability analyses. Metal-rich gas shales with potential environmental implications may be identified by bulk geochemical analysis.

Key gas-production shale units with unique hydrogeophysical properties may be revealed by geophysical logs and hydrologic analysis. Geophysical data could be used in conjunction with stratigraphy and geochemical data for basin hydrology and thermal modeling.

This study was performed from a multidisciplinary standpoint were several important aspects of gas-shale production were examined where both industrial and environmental concerns of gas-shale were addressed. Environmental concerns were restricted to aspects of gas-shale production that could potentially contaminate groundwater. Considering industry concerns, special attention was paid to the hydrocarbon development in each of the gas-shales studied. To do this, several techniques were utilized to (1) characterize the variations in gas-shale mineralogies, (2) quantify the concentration of trace elements (e.g., those with potential impacts to drinking water), (3) characterize and correlate key organic compounds (i.e., biomarkers) extracted from shales, (4) model the thermal history and hydrodynamic evolution of the basin, and (5) understand how new regulations involving hydraulic fracturing may potentially affect the industrial practices of protecting groundwater supplies.

This study first explored the fundamental geologic properties and organic geochemistry of major shale units in Black Warrior Basin. Stratigraphic cross sections were correlated using geological and geophysical logs and these sections were then used to model the thermal and hydrodynamic evolution of the basin; basin modeling results shed lights on hydrocarbon generation and migration, overpressuring by sedimentation processes, as well as overall oil and gas production potential and timing in the Black Warrior Basin. Future study should focus on characterizing pore-connectivity of shales; such hydrologic properties control fluid and hydrocarbon migration and thus are of great interest to energy and environmental industry.

BACKGROUND

Geologic Setting

The Black Warrior Basin, evolved from a Late Paleozoic foreland depression, is located in northeast Mississippi and northwest Alabama (Figure 1). The Black Warrior Basin's structure is mainly controlled by two orogenic events and a doming event, the Ouachita Orogeny to the southwest, the Appalachian Orogeny to the southeast, and the Nashville Dome to the north (Carroll, et al., 1995). Folding, faulting, and major fracture systems within the Black Warrior Basin were influenced by tectonic stresses on weakly deformed, sub-horizontal strata that dip uniformly to the southwest (Thomas, 1988; Pashin and Groshong, 1998; Groshong , et. al. 2010; Pashin, et al., 2011). Along the margin of the Black Warrior Basin bordering the Appalachian Mountains are a series of thrust faults, which strike northeast (Pashin, 2008).

The Black Warrior Basin first developed in response to the spreading of the Laurentian platform, following by subsequent deposition on the Alabama Promontory during Precambrian through Cambrian Iapentan rifting (Thomas, 1988; Pashin and Groshong, 1998; Groshong et al., 2010). Dominant faulting type throughout the Black Warrior Basin is expressed through normal faults, striking northwest, that exhibit vertical displacement up to 1,000 feet and extend laterally for up to ten miles (Pashin et al., 2011).

During Cambrian, the Conasauga Formation was deposited in a graben due to the Iapetan rifting event that occurred from Late Precambrian to Early Cambrian. During later thrusting

associated with the Appalachian orogeny, thick sections of Conasauga Shale were deposited (Thomas, 2001; Thomas and Bayona, 2005).

Devonian shale of the Black Warrior Basin are dominated by the Chattanooga Shale, which was deposited during Middle to Late Devonian. The distribution of Chattanooga Shale is wide-spread, representing the deposition in an euxinic basin created as a cratonic extension of the Acadian foreland basin (Pashin et al., 2010). Chattanooga Shale is dominantly produced along the southeastern margin of the Black Warrior Basin where the basin borders the Appalachian thrust belt (Pashin, 2008; 2009; Pashin, et. al., 2010; Haynes et al., 2010).

Secondary development of the Black Warrior Basin occurred along the southwestern part of the Alabama promontory during Mississippian, as a result of the Ouachita Orogeny (Thomas, 1977). However, major sediment loads were not delivered to southwestern section of the Black Warrior Basin until the beginning of Pennsylvanian (Pashin, 2004).

Deposition of the Neal (Floyd) Shale during Mississippian resulted in a complex that involves interbedded siliclastic and carbonate rock types. It is suggested that the Neal section of the shale body was deposited in a continental slope and ocean-floor environment (Cleaves and Broussard, 1980; Pashin, 1993; 1994).

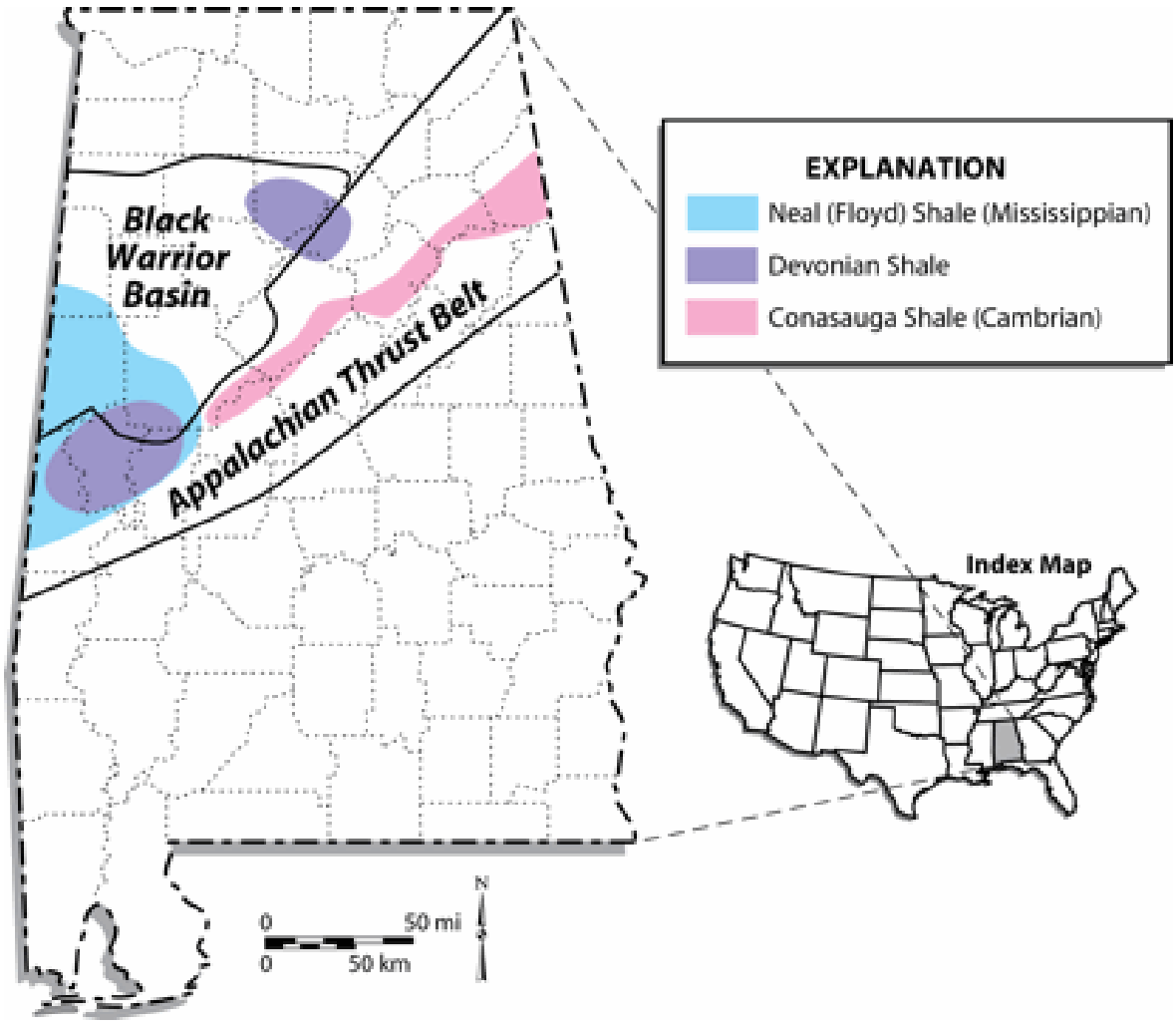

Figure 1. Generalized diagram of the study area of the Black Warrior Basin (Modified from Pashin, 2008)

Gas-Shale Reserviors

The Middle to Upper Cambrian Conasauga Formation ranges in thickness from 1,500 to 3,000 feet; however, due to deformation, thickness may reach 12,000 feet at certain localities influenced by downwarping of normal faults (Thomas and Bayona, 2005). Shale is dominant in the lower sections of the formation, whereas limestone and dolostone dominate in the upper reaches of the formation (Pashin et al., 2011). Oil production has been restricted mainly to shale and limestone sections (Pashin et al., 2011).

The Middle to Upper Devonian Chattanooga Formation is an organic-rich black shale unit (Rheams and Neathery, 1988). The Chattanooga is easily identified in gamma ray logs due to its relatively high radioactivity, associated with fine-grain minerals enriched in radioactive isotopes. In the southwestern margin of the basin a deposition center is present, representing the possibly of major plays of oil and gas.

The Neal (Floyd) Shale is equivalent to the highly productive Barnett Shale found in the Fort Worth Basin and the Fayetteville Shale located in the Arkoma Basin (Pashin et al., 2011). An important section of lower Floyd is referred the Neal Shale; this section contains abundant organics and is a probable source of oil and gas (Pashin, 1994; Carroll et al., 1995). Within the Mississippian stratigraphic section of the Black Warrior Basin, the Neal Shale has the potential to be the largest gas shale reservoir. The Neal Shale can be delineated from the Chattanooga Shale by its relatively lower gamma-ray signature in geophysical logs (Pashin et al., 2011).

Mineralogy

The mineralogy varies considerably in three main gas-shale units in the Black Warrior Basin. Within the Conasauga Shale, carbonates dominate the bulk mineralogy with calcite ranging from 8-49% by weight. Quartz percentages vary from 12-20%, whereas clay minerals constitute 12-50% of the mineralogy (Pashin et al., 2011). Within the Chattanooga Shale quartz is the dominant mineral present with a range of 34-54%, whereas clay minerals range from 27-42% and calcite where present, can be as high as 14%. Within the Neal (Floyd) Shale the bulk mineralogy primarily consists of clay minerals, while quartz varies from 25 - 47% and calcite and dolomite, where present, are at negligible percentages (Pashin et al., 2011).

A possible analog for ideal mineralogical make up for unconventional Black Warrior Basin reservoirs are high yield sections in the Barnett Shale. Maximum production in the Barnett Shale occurs where the shale is approximately 45% quartz, 27% clay, 8% carbonates, 7% feldspar, 5% organic matter, 5% pyrite, and 3% siderite (Bowker, 2003; 2002). This composition allows the reservoir body to behave in a brittle manner when hydraulically fractured. The well-formed induced fracture networks allow for the connection of pore throats which increases the permeability and potential recovery of free hydrocarbons (Jarvie, et al., 2007). Where secondary micro-fractures have occurred naturally the hydraulic fracturing potential has been dramatically reduced due to secondary infilling of calcite. Not only does a high quartz and carbonate content increase the overall fracturing potential but also they have a very low gas-sorbing capacity. Thus larger percentages of quartz and carbonate may allow increased amounts of free gas to be produced during hydraulic fracturing (Wang and Carr, 2012).

Heavy Metals/Radionuclides

The Marcellus Shale in the Appalachian Basin has shown elevated amounts of arsenic, barium, radionuclides, as well as other heavy metals that may impact local drinking water (Soeder and Kappel, 2009). Injection of solvents and chemicals into a formation may lead to increased water-rock interaction and subsequent leaching of hosting shale and release of toxic elements (e.g., arsenic, vanadium, and uranium) into pore fluids (Soerensen and Cant, 1988; Dale and Fardy, 1984; Aunela-Tapola et al., 1998). It is thus important to quantify the concentration of trace elements to order to find more productive and environmentally responsible ways to explore the gas shale.

Redox Geochemistry

Due to the potential for contamination of groundwater resources by trace elements (e.g., arsenic) during the production of gas-shale, it is imperative to understand the correlation between shale mineralogy, geochemistry, trace metal content, and how the mobility of toxic elements may be affected by the redox and pH conditions. Both the redox and pH conditions found in the formation fluids will affect the speciation and mobility of arsenic (Beaulie and Ramirez, 2013; Smedley and Kinniburgh, 2002). Water-rock interaction involving sorption or de-sorption of arsenic are highly dependent on the concentration of iron, sulfur, as well as the Eh-pH values (Kao et al., 2013). This in turn will affect the stability of main mineral phases present (e.g., sulfide and oxide solids) which serve as major sinks of trace elements to be sorbed onto, or incorporated within mineral's structure (Saunders et al., 2008).

It has been proposed that pyrite is the most important mineral for the sorption or co-precipitation of arsenic (Kao et al., 2013; Mandal et al., 2009; 2012; Saunders et al., 2008; La Force et al., 2000); Arsenic may also be precipitated in biogenic pyrite by sulfate reducing bacteria (Saunders et al., 1997). Once arsenic bearing sulfides are formed and stable under sulfate reducing conditions, the arsenic should remain immobile (Saunders et al., 2008). The stability of Fe-sulfides generally decreases as pH decreases or Eh increases. The oxidation of Fe-sulfides will result in the release of iron, sulfuric acid, as well as arsenic from the sulfide minerals. It has been shown that high concentrations of arsenic are often correlated with those of dissolved iron in fluids as both are released simultaneously from pyrite (Saunders et al., 2008).

If the redox conditions at which pyrites are stable within a gas-shale are altered, possibly due to the fracking-induced oxidation, there stands to be a potential release of arsenic and other elements (e.g., lead) that are found within sulfides. If hydrologic mixing occurs between the shale formation fluids and potable groundwater sources, the socio-economic and environmental impact could be significant.

Permeability/Porosity

Shale bodies generally have an extremely low intrinsic permeability; as low as 10^{-16} darcy has been recorded for the Marcellus Shale. However, typical permeability values of shales in the Black Warrior Basin fall into the range of approximately 10^{-7} darcy (Kwon et al. 2004a; 2004b; Neuzil, 1986; 1994; Soeder, 1988). Within the three gas-shale reservoirs average permeability values vary from 1.33×10^{-7} darcy for the Conasauga Formation, to 2.37×10^{-7} darcy for the Devonian Chattanooga Shale, and to 1.47×10^{-7} darcy for the Neal (Floyd) Shale, all of which are consistent with their expected low permeability nature (Pashin et al., 2011).

Considering porosity values of a major gas-shale, the Barnett Shale has an average porosity of 6% (Jarvie et al., 2007). Within the Black Warrior Basin the Conasauga Formation has porosity values that range from 1.4-5.4%. The Devonian Chattanooga shale has porosity values that range from 1.2-2.5%. The Neal (Floyd) Shale has the highest natural porosity with values that range from 2.2-7.7% (Pashin et al., 2011).

In general there is a log-linear relationship between porosity and permeability (Figure 2), however at any given porosity the permeability within clay or a shale body can vary by several orders of magnitude due to the presence of fractures or fracture networks. There is a general trend that for every 13% reduction in porosity there is an order of magnitude drop in permeability (Neuzil, 1994). A major uncertainty when measuring permeability is the scale of the flow system measured. When measuring values of permeability at small-scales, the main control will be original depositional arrangement of clay minerals, resulting in relatively small permeability variance; however, when measuring values over regional geologic provinces, permeability will be enhanced by the presence of fractures or conduit networks (Neuzil, 1994).

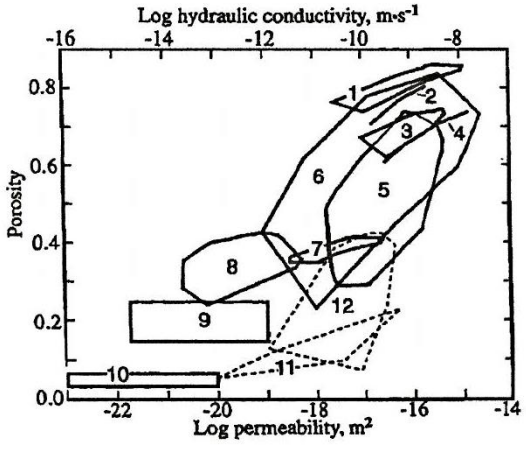

Figure 2. Log-Linear relationship shown between porosity and permeability. Numbered fields represent correlation between porosity and permeability for various experiments (Modified from Neuzil, 1994).

Fracture networks can allow orders of magnitude differences in permeability in all directions. Within the Black Warrior Basin, shale bodies have fracture networks consisting of orthogonal, systematic and cross joints (Pashin et al., 2011). The systematic joints tend to be much more laterally continuous, whereas the cross joints are more sinuous and terminate when intersecting systematic joints (Pashin et al., 2011).

The low porosity and permeability nature of unconventional shale reservoirs implies that they must be hydraulically fractured to produce economically viable resources (Myers, 2012). During the hydraulic fracturing process millions of liters of fracturing fluids are pumped into the targeted unit at pressures that can reach 69,000 kPa (PADEP, 2011). The hydraulic fracturing of the shale creates up to 9.2 million square meters of surface area accessible from a horizontal well (King, 2010; King et al., 2008). However, it has been noted in the Marcellus Shale that fractures have propagated as much as 500 m into overlying, non-target formations (Fisher and Warpinski, 2011). These fractures that protrude into overlying layers can work as conduits for advetive and dispersive transport of heavy metals and radionuclides into aquifer systems. The over-pressurization that occurs during the hydraulic fracturing process will also facilitate rapid movement of fluids from target formations to overlying and surrounding formations (Lacombe et al., 1995).

Total Organic Carbon (TOC)

The presence of organic carbon within an unconventional reservoir tends to increase the porosity, and furnish the material to be converted into oil and gas through thermal maturation (Zhang et al., 2012). The fundamental element of oil and gas generation potential lies in the TOC present within a given reservoir body (Wang and Carr, 2012). In the three gas-shale reservoirs within the Black Warrior Basin, TOC percentages range from 0.2%-1.8% with an average value

of 0.5% for the Conasauga Shale measured in Dawson 34-3-1. The Chattanooga Shale values range from 2.9%-7.6% with a mean value of 4.8% measured in Lamb 1-3 #1. The Neal (Floyd) Shale has TOC values that range from 2.3%-4.0% with a mean value of 3.3% measured in Lamb 1-3 #1 (Pashin et al., 2011).

Petroleum Bio-Markers

As crude oil and gas degrade due to microbial interactions and environmental alteration, particular hydrocarbon compounds, known as biomarkers, will remain stable and largely unchanged throughout geologic time (Natter et al., 2012). These biomarkers (e.g., terpanes, hopanes, and steranes) have been used to correlate organic matter in reservoirs to their initial sources (Wang and Stout, 2007). Stable carbon isotopes can also be used to characterize the sources of organic matter in reservoir rocks. This process is possible due to the different pathways that carbon is fixated in plants (Natter et al., 2012) during photosynthesis. Plants that utilize a photosynthetic pathway are C3 plants; while plants that utilize the Hatch-Slack pathway are C4 plants. Plants utilizing the C3 pathway typically have significantly lower $\delta^{13}C$ isotopic signatures when compared to those of C4 plants (Natter et al., 2012). Thus, when examining the biomarker and stable carbon isotope signatures of organic matter in the shales, it is possible to evaluate the possible sources and geochemical evolution of hydrocarbons.

Thermal Maturation

When quantifying thermal maturation of source rocks the most influential factors are time and temperature (Bethke et al., 1993). In 1971, Lopatin defined the Time-Temperature Index (TTI) of a potential source rock representing thermal maturities developed over time at different temperatures (T_k, in Kelvins):

$$TTI = \int_t 2^{(T_k/10 - 37.815)}\, dt \qquad (1)$$

Waples (1980) further assigned a quantitative measure to correlate TTI with oil and gas generation windows (Table 1).

Table 1. TTI values and corresponding thermal maturation stage.

TTI	Thermal Maturation Stage
15	Onset of oil generation
75	Peak oil generation
160	End of oil generation
500-1,000	Deadline for preserving oil
1,500	Deadline for preserving wet gas
> 65,000	Deadline for preserving Dry gas

Within the Black Warrior Basin, The TTI values of Chattanooga Shale were calculated in two wells, PN 2191 and PN 1780 (Table 2). It was found that maturation of kerogen was rapid, reaching a maximum between 290 m.y. to 200 m.y. ago; correlating to the deepest burial of Pottsville Formation (Carroll et al., 1995). However, in well PN 2191 the base of Chattanooga Shale was located above the depth interval of peak oil-generation window, indicating that most of the shale at this location is thermally immature. The deeper Chattanooga Shale in well PN 1780 (Figure 3) fell into the gas generation window, indicating that the shale was thermally mature at this location since 200 m.y. ago (Carroll et al.,1995).

Table2. Permit number, depth, and location of wells.

Permit number	Depth	Longitude	Latitude	County
2191	4688 feet	-88.03758	33.8409	Lamar
1780	7000 feet	-88.04983	33.1115	Pickens

Within the Black Warrior Basin, there is a trend of increasing thermal maturation from northwest to southeast, as indicated by vitrinite reflectance values (Pashin et al., 2011). Where

the largest amount of conventional oil has been produced in Lamar and Pickens counties, vitrinite reflectance increases in a uniform manner with depth, indicating that depth of burial, as well as variations in the geothermal gradient, have had the greatest influence on thermal maturation (Pashin et al., 2011). Within the Big Canoe Creek Field, vitrinite reflectance values for the Conasauga shale ranged from 1.1 to 1.9, indicating that most of the reservoir body currently falls into the gas production window (Pashin et al., 2011).

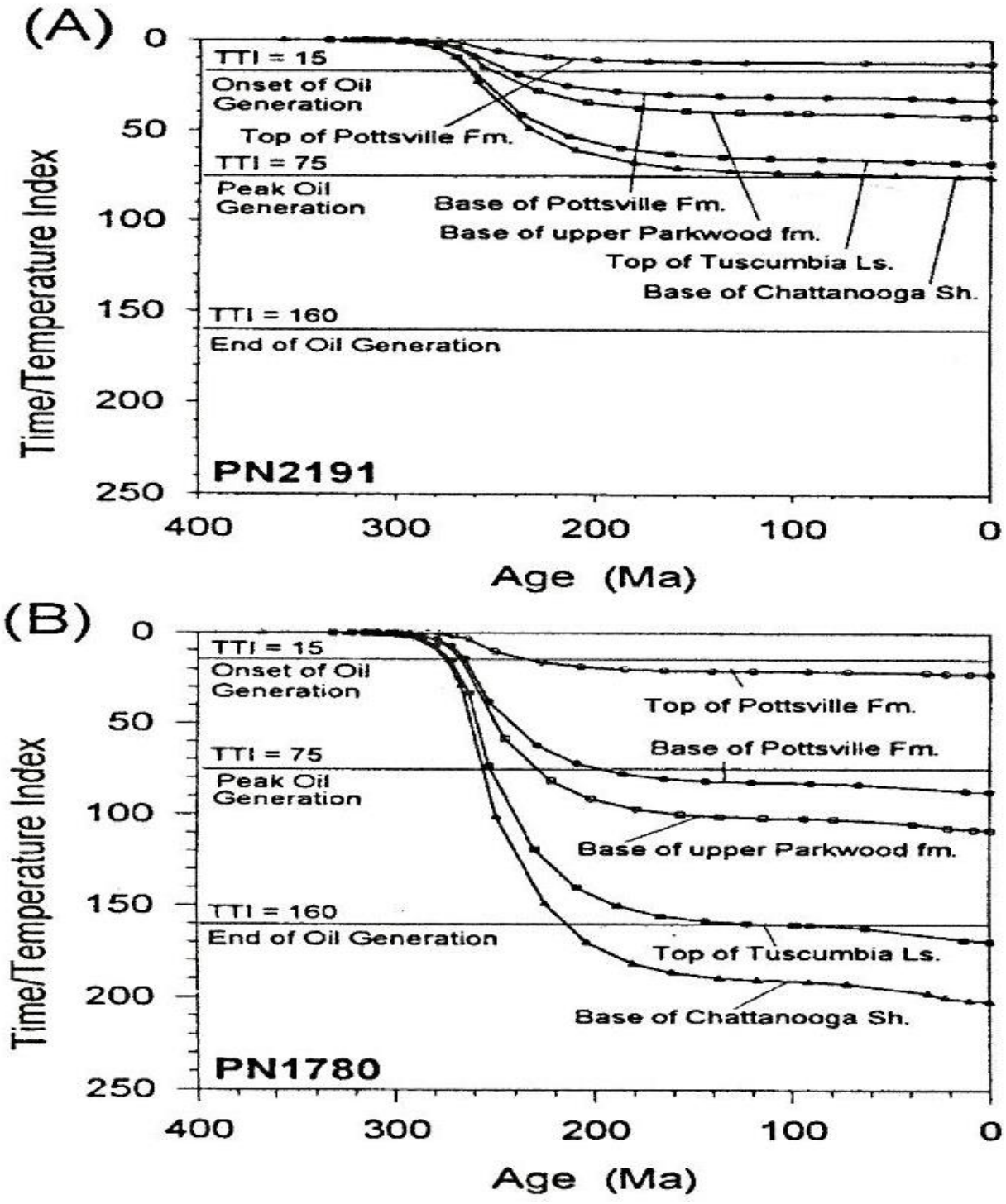

Figure 3. Calculated TTI index for various stratigraphic units present in wells PN 2191 and PN1780 (Modified from Pashin et al., 2011).

MATERIALS AND METHODS

Core Sample Collection

During November 2012, shale samples were collected from seven oil and gas drill cores (Table 3) stored in the Core Warehouse of the Alabama Geological Survey. From these seven drill cores, 36 sub-samples, from varying depths, were processed for various geological, geochemical, and hydrological analyses. The cores analyzed include 10 samples from the Conasauga Shale, three samples from Chattanooga Shale, seven samples of the Devonian Shale, and 16 samples from the Neal (Floyd) Shale.

Table 3. Location, depths, and permit #s of drill core samples used in this study.

Formation	County	Depth (top)	Depth (bottom)	Permit #	Longitude	Latitude
Conasauga	St. Clair	7540 feet	7577 feet	15720	-86.22214	33.85764
Devonian	Hale	10301 feet	10362 feet	3939	-87.70136	32.76762
Neal (Floyd)	Greene	7996 feet	8055.1 feet	15075	-87.85457	33.08227
Neal (Floyd)	Greene	9013 feet	9073 feet	15668	-87.74112	33.00451
Conasauga	Shelby	14, 1698 feet	14,197 feet	3518	-86.52885	33.28967
Chattanooga	Greene	8,441 feet	8,446 feet	3800	-87.87437	32.63802
Neal (Floyd)	Pickens	6,650 feet	6,568 feet	14289	-88.06002	33.20421

X-Ray Diffraction (XRD) Analysis

About 1-10 grams of shales from each sub-sample were processed for a period of 40 minutes using a mortar and pestle. To avoid cross contamination the mortar and pestle were scrubbed using soap and water after each sample was prepared. The XRD analysis measured the bulk weight percentage of silicate, carbonate, sulfide, clay minerals, as well as other minerals present within each sample. As previously discussed, differences in mineralogy (quartz,

carbonate, sulfide, iron oxide contents) are known to influence trace element contents and make a great difference in hydraulic fracturing operation.

XRD analysis was conducted using a Bruker D2 Phaser XRD in the Geology and Geography Department at Auburn University. Samples were run from 2 theta values of 10 degrees to 90 degrees with a 3800 step interval, resulting in a total time of 20 minutes for each sample analysis. This time step and 2 theta angle allows for the non-clay minerals present within each sample to be identified with a relative high degree of accuracy while being time efficient.

The mineral composition of the samples was determined by a peak search and match procedure using DIFFRAC.EVA software. Furthermore, XRD pattern also reveals semi-quantitative make-up of a material since the areas under the peak reflect the amount of each phase present in the sample.

X-Ray Fluorescence (XRF) analysis

XRF analysis of shale samples was performed by an Elemental Tracer IV-ED handheld unit in the Geology and Geography Department at Auburn University. Sample preparation consists of creating a fresh surface on the same set of samples collected from the Alabama Geological Survey. For each sample, three different filter, voltage, and amperage setting (Table 4) were used for targets different element groups. Analyses were repeated at three locations on each sample, near the front, rear, and center of each sample. The elemental compositions of each sample were averaged from values measured at three locations. Each filter, voltage, and current setting used allowed for different suite of elements to be analyzed (Table 4).

Table 4. Voltage, amperage, filter, and vacuum setting used for each applicable element in XRF analysis.

Voltage (KeV)	Amperage (µA)	Filter #	Elements	Vacuum
15	55	2	Na-Fe	Yes
40	18	1	Fe-U	No
45	30	3	As, Hg, Pb, etc.	No

The XRF technology analyzes the energy emission of characteristic fluorescent X-rays from a sample that has been excited by bombarding with high-energy (i.e., short-wavelength) X-rays. The XRF technology can quantify the elemental composition of a material because each element has unique electronic orbitals of characteristic energy and the intensity of each characteristic radiation is directly related to the amount of each element in the material. Major elements and most trace elements (Ba, Cr, Co, Cu, Mo, Nb, Ni, Pb, Rb, Sr, U, Th, V, Y, Zn, Se, As, etc) of shale samples, in the range of parts per million (ppm), were measured at Auburn University's XRF and XRD laboratory. The instrument takes a sample reading from a very small area (about 3 × 4 mm) with a small distance to the target so that potential heavy metal/trace element zones can be recognized in high detail. The Elemental Tracer IV-ED has been calibrated by various international shale standards (i.e., GBW07107, SARM-41, SCO-1, SDO-1, etc.) for quantitative elemental analysis. For this study a standard was set by an ICP-MS analysis (Table 5) of a representative sample from the Neal (Floyd) Shale, Greene County, so that a quantitative measurement of elemental concentrations in all samples could be obtained. This ICP-MS analysis was performed at the commercial laboratory Spectrum Analysis.

Table 5. ICP-MS standard for selected elements.

Element	Concentration (ppm or weight %)
Aluminum (Al)	0.29 %
Arsenic (As)	20.8 ppm
Lead (Pb)	22.5 ppm
Mercury (Hg)	0.11 ppm
Sulfur (S)	2.26 %
Iron (Fe)	1.94 %
Molybdenum (Mo)	2.4 ppm
Copper (Cu)	143.1 ppm
Zinc (Zn)	96.0 ppm
Silver (Ag)	<0.1 ppm
Nickel (Ni)	68.0 ppm
Cobalt (Co)	13.7 ppm
Manganese (Mn)	90.0 ppm
Gold (Au)	<0.5 ppm
Thorium (Th)	3.0 ppm
Strontium (Sr)	90.0 ppm
Cadmium (Cd)	<0.1 ppm
Antimony (Sb)	2.0 ppm
Bismuth (Bi)	0.4 ppm
Vanadium (V)	29.0 ppm
Calcium (Ca)	1.3 %
Phosphorus (P)	0.04%
Lanthanum (La)	6.0 ppm
Chromium (Cr)	9.0 ppm
Magnesium (Mg)	0.67%
Barium (Ba)	63.0 ppm
Titanium (Ti)	0.002%
Boron (B)	17.0 ppm
Sodium (Na)	0.052%
Potassium (K)	0.21%
Tungsten (W)	<0.1ppm
Scandium (Sc)	4.8 ppm
Thallium (Tl)	0.2 ppm
Gallium (Ga)	1.0 ppm
Selenium (Se)	1.8 ppm
Tellurium (Te)	0.4 ppm

Organic Matter Extraction and Biomarker Analysis

In order to fingerprint the source of organic matter in shales, organic compounds were extracted from shales, at Auburn University's Geology and Geography department, based on the EPA method 3570 on microscale solvent extraction (USEPA, 2002). In this method, 2.5 grams of anhydrous sodium sulfate is first added to a pre-cleaned glass extraction tube which has a polytetrafluoroethylene (PTFE) screw cap. Three grams of crushed shales are measured and transferred into the tarred extraction tube. 10 mL of dichloromethane (DCM) is then added to the extraction tube. The tubes need to be agitated vigorously until slurry is free flowing for 10 min at 250 rpm. More sodium sulfate can be added as necessary to produce free-flowing, finely divided slurry. The organic phase is then transferred to DCM by rotating them for at least 24 hours in an orbital rotator. The organic phase is centrifuged at 3000 rpm for 10 minutes. Liquid phase (supernatant) is transferred with a Pasteur pipette to glass vial. The liquid phase is filtered using glass syringe and syringe filter (0.2 µm PTFE) to another glass vial. The organic phase in solvent is then dried under a vent hood with nitrogen gas for approximately 30 minutes. One and one-half mL of Hexane-MTBE 1:1 solution is added to dried organics in glass vial. After 10 minutes, the extract is transferred to 2 mL amber GC vial. The vials containing the solutions were stored in the freezer until analysis by the gas chromatograph mass spectroscopy. Sample preparation was performed at Auburn University's Civil Engineering department.

Extracted organic compounds were analyzed using an Agilent 5975C gas chromatograph mass spectrometer (GC-MS) in a full-scan mode at Auburn University. Additionally, selected

samples were analyzed for petroleum biomarkers, with specific mass to charge ratios (m/z) of 191, 217, and 218, under much higher sensitivity by GC-MS Selected Ion Mode at ACTLAB. Data was processed at Auburn University's Pharmacy school utilizing ChemStation software.

Geophysical Log Analysis and Basin Modeling

Approximately forty down-hole geophysical logs were collected from the Alabama Oil and Gas Board (Table 6). Down-hole geophysical logs are available in six counties (Figure 4). Log types consist of gamma-ray, spontaneous potential, conductivity, resistivity, neutron bulk density, and neutron porosity. Using the software package Neuralog, various logs were converted from raster files to digital outputs by tracing individual logs from each well. These digital outputs were then converted to file formats that are suitable for PETRA software for 3-D spatial analysis and stratigraphy correlation.

Gamma logs were then used to correlate hydro-geologic units, focusing on the Conasauga Shale, Chattanooga Shale, and the Neal (Floyd) Shale. Correlations were done with the Software package PETRA. A three dimensional hydro-stratigraphic section of the Black Warrior Basin was completed using this technique. From this hydro-stratigraphic section, a two dimensional north-to-south transect across the entire basin was modeled for thermal and hydrologic evolution using Basin2 modeling software (Bethke et al., 1993). The modeled transect represents a section of the Black Warrior Basin with abundant down-hole geophysical and geologic data. The basin modeling is centered on evaluating the thermal maturation and potential development of over-pressurization due to sediment compaction. Oil-generation and gas-generation windows were also calculated using the TTI model method described above.

Table 6. Permit #s, well names and locations of selected geophysical logs in the Black Warrior Basin. The second columns numbers correlate to locations of geophysical logs in Figure 4.

Permit	#	Well Name	Lat.	Long.	County
15241	1	Sumter Farm and Stock, Inc. 04-10 No. 1	32.91152	-88.29867	Sumter
3597	2	Sumter Farm and Stock Co. 33-15 #1	32.92097	-88.29915	Sumter
1160	3	James B. Hill #1	32.821557	-88.210098	Sumter
1040	4	J.J. Hagerman #1	32.98267	-88.30412	Sumter
16220	5	Caldwell 19-15 #1 ST	32.68846	-87.81838	Greene
16221	6	Tate 9-4 #1	32.6412	-87.89489	Greene
15668	7	Lamb 1-3H No. 1	33.00451	-87.74112	Greene
15075	8	Weyehaeuser No. 2-43-4202	33.08227	-87.85457	Greene
14673	9	Bayne Etheridge 36-9 #1	32.66203	-87.8308	Greene
10010	10	Weyerhaeuser 2-3 #1	33.09607	-87.85663	Greene
3800	11	Arco/Amoco Et Al- Ethel M. Koch 10-6 #1	32.63802	-87.87437	Greene
1810	12	James W. Sterling Et Al #17-14	32.96905	-88.01753	Greene
16066	13	Cain 6-6 #1	33.08637	-87.5128	Tuscaloosa
16065	14	JWR 25-14-04	33.26927	-87.32906	Tuscaloosa
16183	15	Westervelt 19-2H #1	33.04468	-87.50938	Tuscaloosa
14971	16	JWR 28-05-02	33.27324	-87.2816	Tuscaloosa
13680	17	Bolton 1-4 #1A	33.51241	-87.43834	Tuscaloosa
13387	18	Alawest 2-3 #1	33.51322	-87.45047	Tuscaloosa
13388	19	Bane 36-14 #1	33.51731	-87.43535	Tuscaloosa
16184	20	Lee 26-12	33.02772	-88.27422	Pickens
14371	21	Parker 3-16 # 1	33.16757	-88.19051	Pickens
14319	22	Eric Smith 18-12 #1	33.31505	-88.0442	Pickens
8599	23	Chicken Swamp Branch Gas	33.4564	-88.07608	Pickens
6922	24	Lizzie Johnson Et Al 15-16 #1	33.49163	-88.19153	Pickens
6809	25	Betty Wilcox 17-12 #1	33.49355	-88.23822	Pickens
5787	26	Melrose Timber Co. Inc. 2-15 #1	33.34732	-88.3636	Pickens
2580	27	Andrew C. Wade 26-1 #1	33.20469	-88.06501	Pickens
1800	28	George M. Collins # 5-11	33.1671	-88.02157	Pickens
1792	29	B.E. Turner #32-10	33.44293	-87.91381	Pickens
1763	30	Francis Bell Exum #7-8	33.24765	-88.13628	Pickens
1634	31	Robinson Et. Al. #1	33.31809	-88.18026	Pickens
1087	32	J.G. Lee #1	33.02773	-88.27526	Pickens
4100	33	Mother 13-15 #1	34.34087	-86.90556	Morgan
2794	34	Skidmore 36-1 #1	34.39113	-86.58231	Morgan
3097	35	Leroy Jones 14-10#1	33.6653	-88.07631	Lamar

2527	36	Weyerhaeuser #1	33.69054	-87.98549	Lamar
3939	37	Burke 29-7 No. 1	32.76742	-87.70123	Hale
9515	38	Teco Injection Well #26-8-224A-4400	32.93927	-87.54321	Hale
13389	39	U.S. Steel Corporation 21-13 #1	33.36588	-87.07329	Jefferson

Figure 4. Locations of Black Warrior Basin down-hole geophysical logs. Latitudes, longitudes, permit #s, and counties available in Table 6.

Results and Discussion

Inorganic Geochemistry

The geochemical analysis done in this study consists of measuring concentration of selected EPA regulated elements (e.g., arsenic, lead, iron, sulfur, and aluminum) in shales at varying depths using XRF technology. Special attention was paid to these elements due to new groundwater regulations concerning these elements when hydraulic fracturing gas-shale (Table 5). Elemental concentrations are measured in either parts per million (ppm) or in weight percentage (%). Concentrations (C) of trace elements in all samples are calculated from the standard sample of the Neal (Floyd) shale (Table 5) using the following equation:

$$C_{sample} = C_{ICP-MS} \times \frac{A_{sample}}{A_{standard}} \quad (2)$$

Here C_{sample} and $C_{ICP\text{-}MS}$ represent concentrations of a given element in a sample and the Neal Floyd standard (measured by ICP-MS). A_{sample} and $A_{standard}$ are the total areas under the XRF peaks of the same element in a sample and the Neal (Floyd) standard. The energy dispersive spectrum of the Neal Floyd standard sample is shown in Figure 5a-c. The XRF analysis resulted in peaks for trace elements for Fe, Mn, As, Pb, Hg, Al, Se, Cu, Zn, Ni, Sr, Ba, Ti, and V, along with Ca, K, S and silica. Several of these trace elements are regulated by the EPA and are on the list of primary drinking water standards.

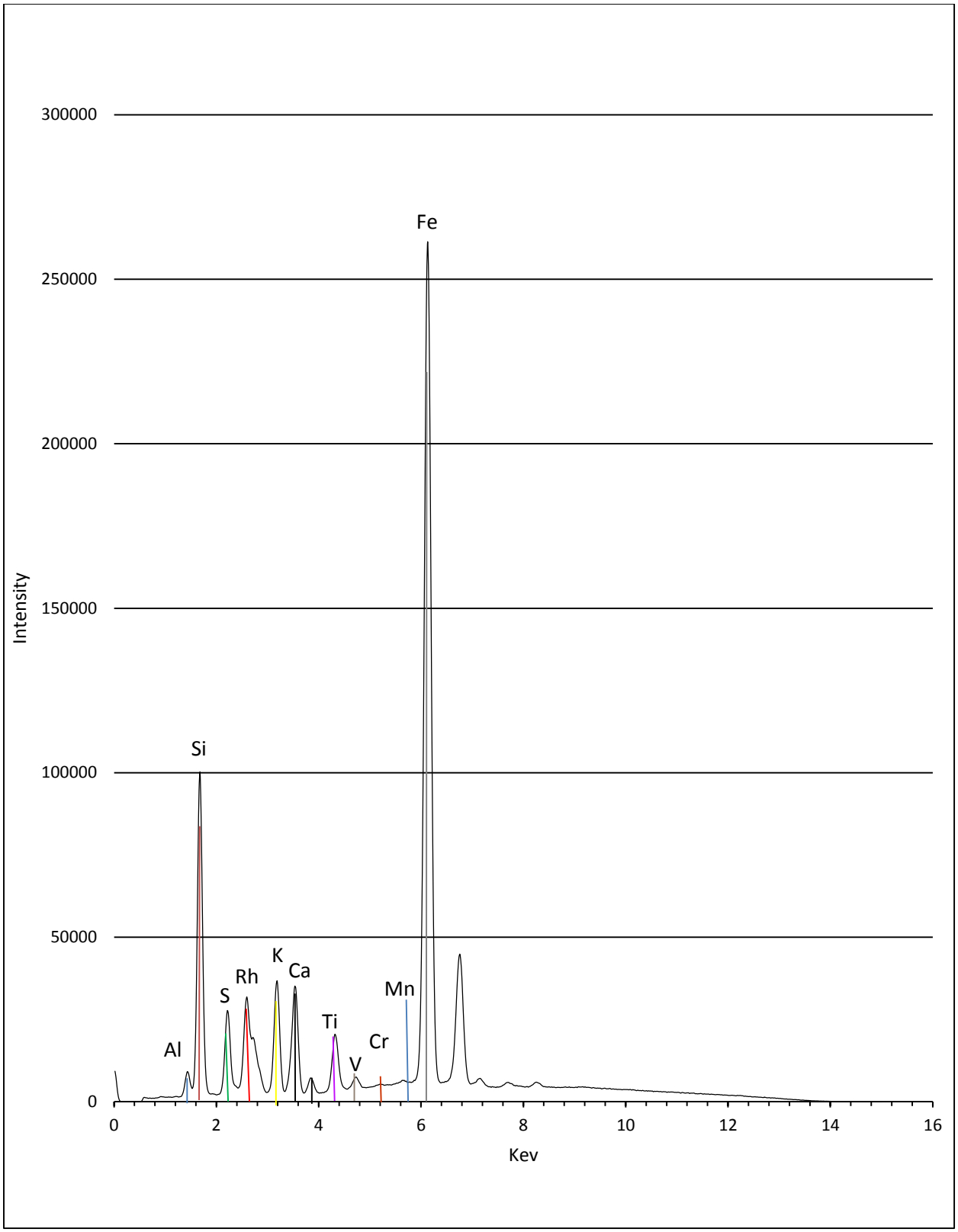

Figure 5a. X- ray fluorescent spectral signature from the Neal (Floyd) Shale in Greene County which targeted elements Na-Fe utilizing settings of 15 Kev, 55µA, filter #2, and a vacuum.

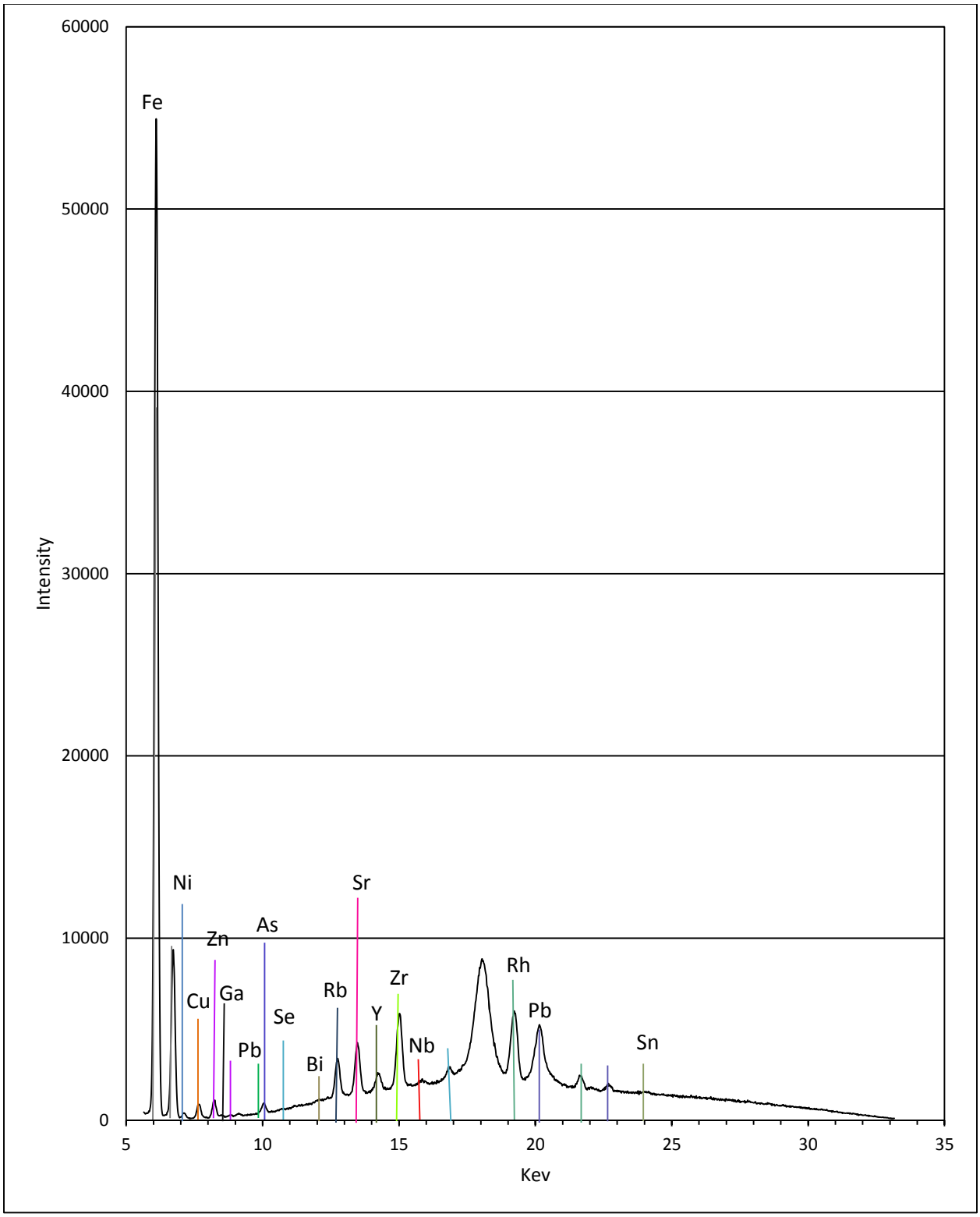

Figure 5b. X- ray fluorescent spectral signature from the Neal (Floyd) Shale in Greene County which targeted elements Fe-U utilizing settings of 40 KeV, 18 µA, filter #1, and no vacuum.

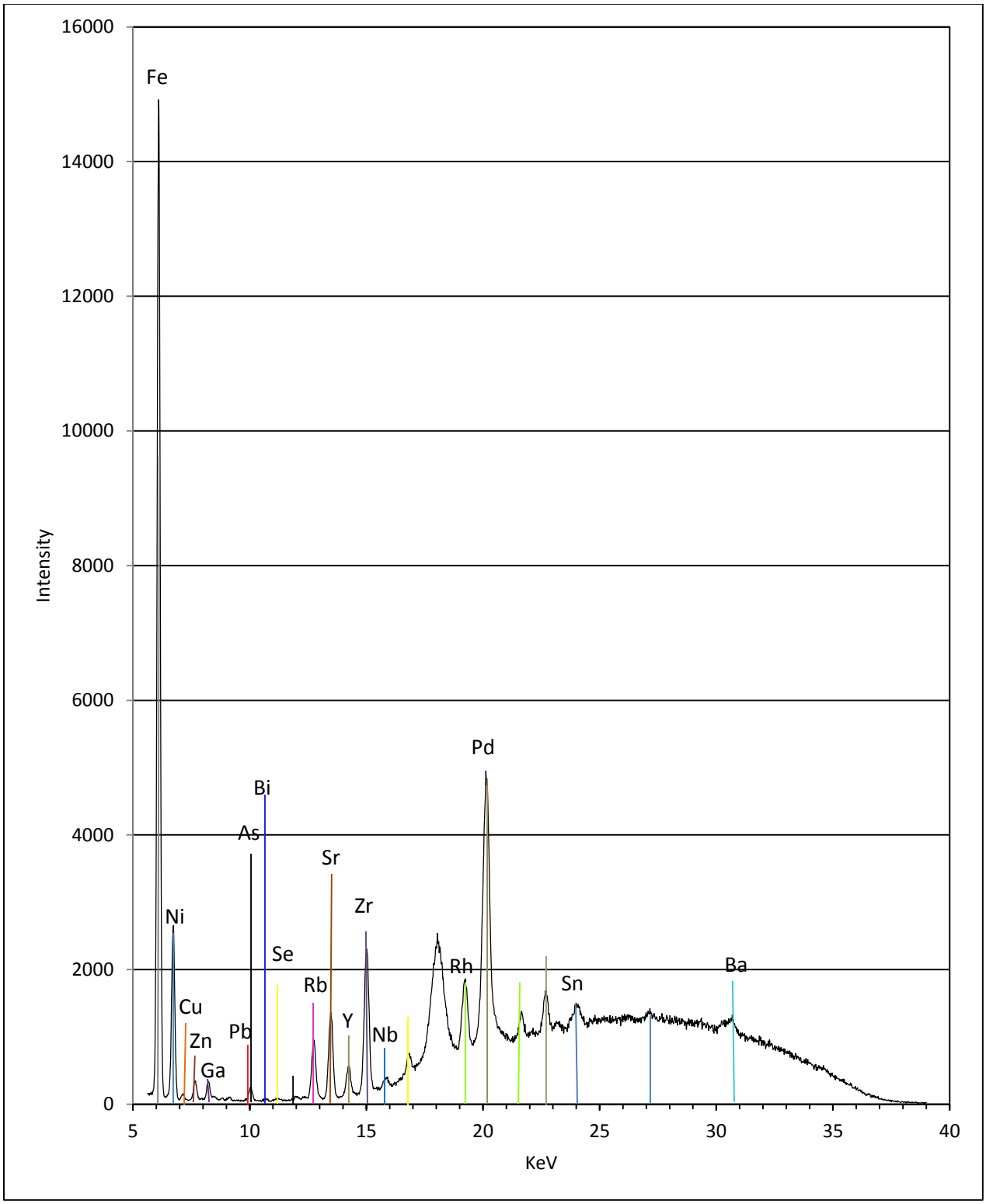

Figure 5c. X- ray fluorescent spectral signature from the Neal (Floyd) Shale in Greene County which targeted elements As, Pb, Hg, Ba ect., utilizing settings of 45 Kev, 30 µa, and no vacuum.

Aluminum

Concentrations of Al in all shale samples are significantly lower than the average of Earth's crust (about 9.30 % by weight). For the Chattanooga Shale, Greene County, aluminum concentrations varies from approximately 0.33% to 0.44% (Figure 6a). The Conasauga Shale, Shelby County, contains the least amount of Al among the all shale units analyzed (Figure 6b). Concentrations vary from 0.00% to approximately 0.04% by weight. However, the Al concentration of the Conasauga Shale in St. Claire County varies from 0.12% at a depth of 7557 feet to 0.51% at a depth of 7553 feet (Figure 6c). This is slightly higher than concentrations in Shelby County (Figure 6b).

A possible explanation for relatively low Al concentration within the Conasauga Shale is the large amount of calcium carbonates present. This is especially true if carbonate rich section are either being targeted for analysis or the sample analyzed represents a predominantly carbonate-rich section of this shale. This interpretation is backed by XRD data (see Conasauga Shale mineralogy) which shows large amounts of carbonates in this shale.

In the Devonian shale, of Hale County, concentrations of Al range from 0.29% to 0.32%, at depths of 10,336 and 10,349 feet, respectively (Figure 6d). In the Neal (Floyd) Shale, in Pickens and Greene County, similar ranges of Al concentrations are found, 0.45% to 0.75% for Pickens County and 0.20% to 0.92% in Greene County (Figure 6e-f).

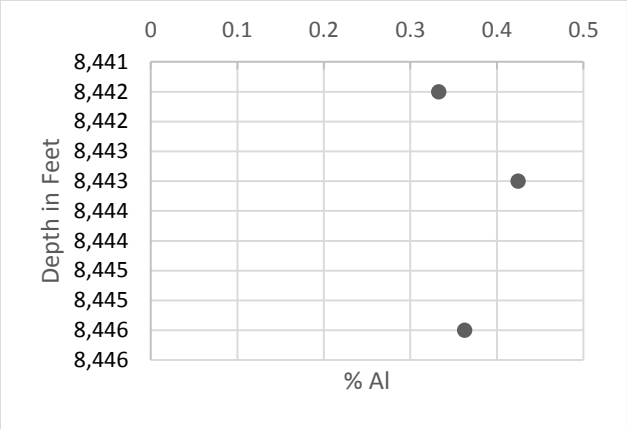

Figure 6a. Concentration of Al for Chattanooga Shale in well permit # 3800, Greene County.

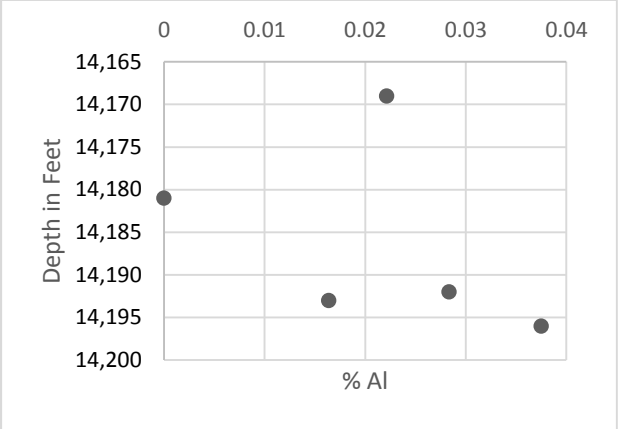

Figure 6b. Concentration of Al for Conasauga Shale in well permit # 3518, Shelby County.

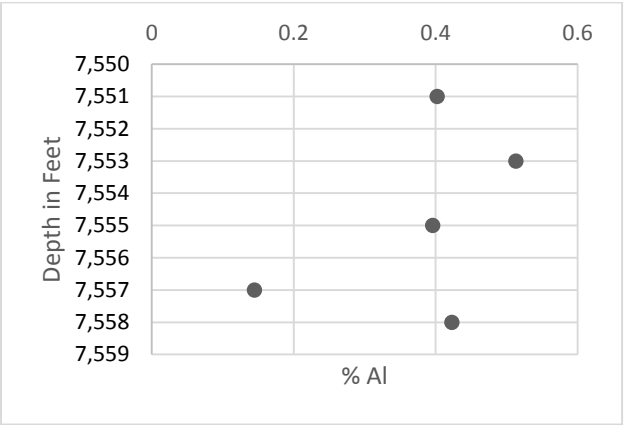

Figure 6c. Concentration of Al for Conasauga Shale in well permit # 15720, St. Claire County.

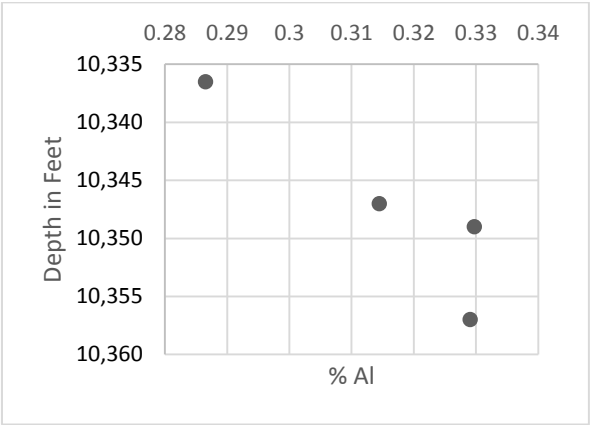

Figure 6d. Concentration of Al for Devonian Shale in well permit # 3939, Hale County.

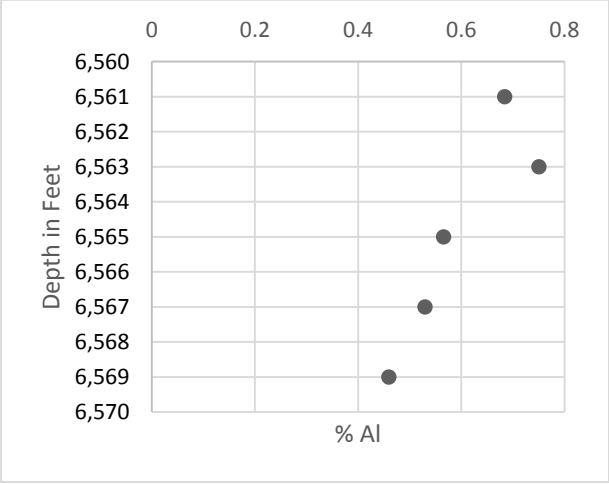

Figure 6e. Concentration of Al for Neal (Floyd) Shale in well permit # 14289 Pickens County.

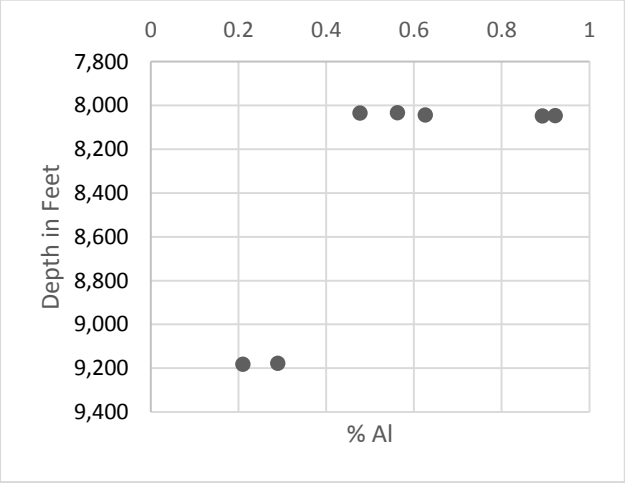

Figure 6f. Concentration of Al for Neal (Floyd) Shale in well permit # 15668, Greene County.

Arsenic

Arsenic concentrations vary from 0.00 to 20.80 ppm (Figure 7 a-e). A few samples have As concentrations significantly higher than those in granite (about 2 ppm), basalt (about 2 ppm), and sandstone (about 1 ppm) whereas certain concentrations fall below the detection limits (a few ppm) of the XRF instrumentation. The average arsenic concentration in shales reported in literature is roughly 13 ppm (Drever, 1997).

In the Chattanooga Shale, Greene County, the As concentrations range from 13.18 to 14.26 ppm with one sampling point falling below the lower detection limit of the instrumentation (Figure 7a). Within the Conasauga Shale, Shelby County and St. Claire County, all of the measured concentrations fall below the detection limit, suggesting that arsenic is very low in shales dominated by carbonate minerals (Figure 7 b-c).

The Devonian shale, Hale County, has one recorded As concentration above the minimum detection limit (Figure 7d). This is found at a depth of 10,336.5 feet with a concentration of 10.60 ppm.

Two shales have relatively high concentrations of As; these are the Neal (Floyd) Shale, Pickens County, and the Neal (Floyd) Shale, Greene County (Figure 7e-f). In the Neal (Floyd) Shale, Pickens County, As concentrations are as high as 12.95 ppm (Figure 7e); As concentrations in the Neal (Floyd) Shale, Greene County, range from 12.38 ppm to 20.80 ppm (Figure 7f). However, there are several locations within this gas-shale close to As-rich depth

intervals do not show detectable As contents. These results indicate a heterogeneous distribution of arsenic within the shales.

Special attention must be placed on the presence of As within gas shales. As mobility is highly sensitive to redox geochemical conditions (Lee et al., 2005). Saunders et al (2008) indicated that As is mobile under Fe-reducing conditions, immobile under sulfate-reducing conditions. The geochemical environments may become more oxidized through the hydraulic fracturing process, as a result, arsenic, which is either sorbed or co-precipitated onto pyrite mineral structure, could potentially be released into the surrounding formation water or brine fluids by pyrite oxidation. Considering this coupled with the EPA's minimum contaminant levels of As in groundwater, 0.010 ppm, there is the potential for large amounts of As to be released into the brine fluids when oxidizing conditions are induced with the hydraulic fracturing. It is enough concern that three states, Illinois, Colorado, and Pennsylvania, require baseline and subsequent testing of the groundwater with As as one of the elements that must be quantified.

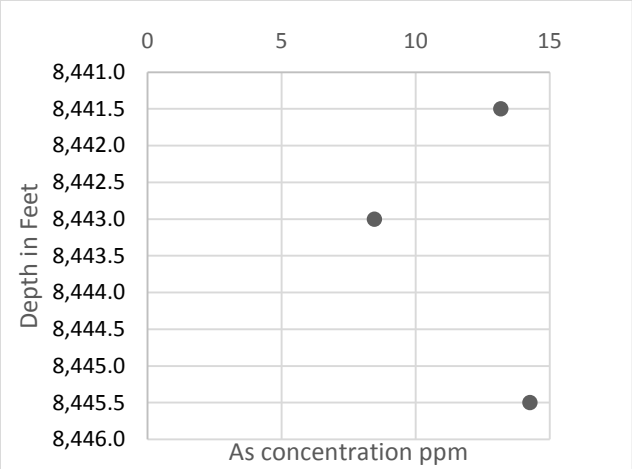

Figure 7a. Concentration of As for Chattanooga Shale in well permit # 3800, Greene County.

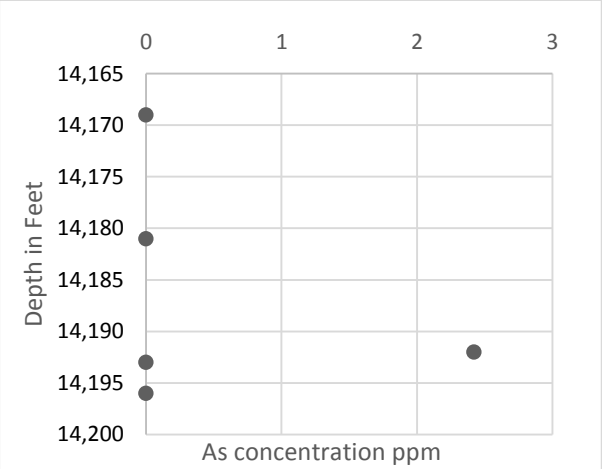

Figure 7b. Concentration of As for Conasauga Shale in well permit # 3518, Shelby County.

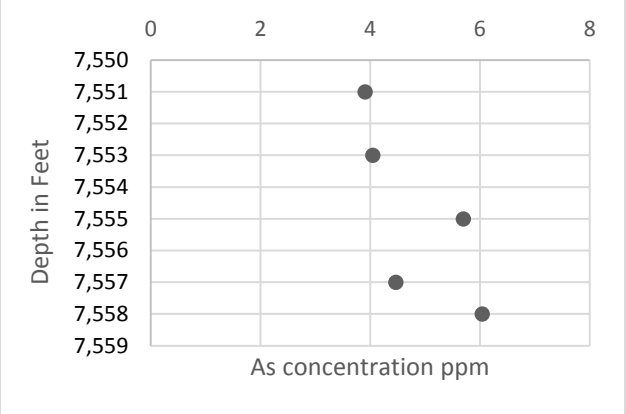

Figure 7c. Concentration of As for Conasauga Shale in well permit # 15720, St. Claire County.

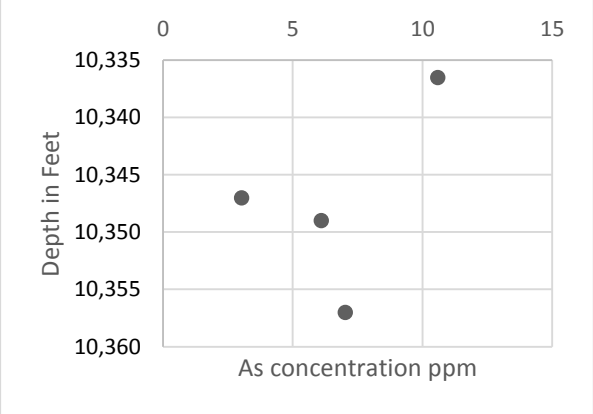

Figure 7d. Concentration of As for Devonian Shale in well permit # 3939, Hale County.

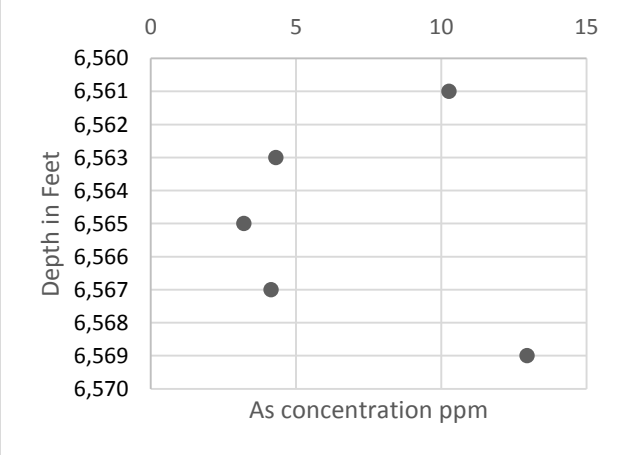

Figure 7e. Concentration of As for Neal (Floyd) Shale in well permit # 14289 Pickens County.

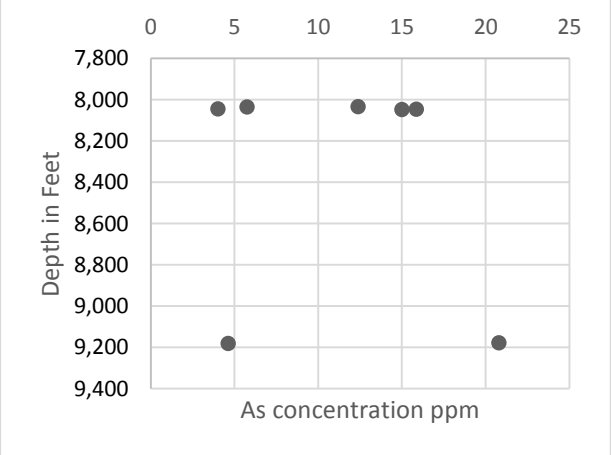

Figure 7f. Concentration of As for Neal (Floyd) Shale in well permit # 15668, Greene County.

Lead

Lead concentration in shales appears to vary with depth and ranges from below detection limits of the instrumentation (< 10 ppm) to 98.25 ppm (Figure 8 a-e). The average lead concentration in shales reported in literature is approximately 20.00 ppm (Drever, 1997). The Chattanooga Shale, Greene County, has a large variance of Pb concentrations that range from 21.52 ppm at 8,445.5 feet to 98.25 ppm at 8441 feet (Figure 8a).

The Conasauga Shale, Shelby County, has lead concentrations that fall below the detection limit of the equipment (Figure 8b). In contrast, the Conasauga Shale, St. Claire County has higher Pb concentrations, ranging from 12.66 ppm to 33.26 ppm (Figure 8c). This result indicates a heterogeneous distribution of lead within the shales. The Conasauga Shale is known for high amounts of carbonates within the upper sections. Carbonate-rich sections of shales generally have very low lead content.

The Devonian Shale, Hale County, has a wide range of Pb concentrations. Concentrations range from 30.57 ppm at a depth of 10,336.5 feet and 12.07 ppm at a depth of 10,349 feet (Figure 8d).

The Neal (Floyd) Shale, Pickens County and Greene County, have varying concentrations of Pb (Figure 8 e-f). Concentrations vary in the Neal (Floyd) Shale, Pickens County, from 12.38 ppm at a depth of 6551 feet to 32.69 ppm at a depth of 6563 feet (Figure 8e). The Neal (Floyd) Shale, Greene County, has similar Pb concentrations to those found in the Neal (Floyd) Shale, Pickens County (Figure 8e-f). A low value of 13.18 ppm is found at a depth of 8044 feet and a high value of 24.18 ppm is found at a depth of 8035 feet. Two deeper samples at

9181.5 feet and 9178 feet however, have relatively low Pb concentrations with respect to shallow samples.

With the EPA's maximum concentration of 0.015 ppm for lead allowed in drinking water, the potential for contamination of Pb in groundwater is quite large; this is based upon the combination of high lead contents in shales, the potential communication of produced fluids with USDWs, and surface contamination from mechanical failure.

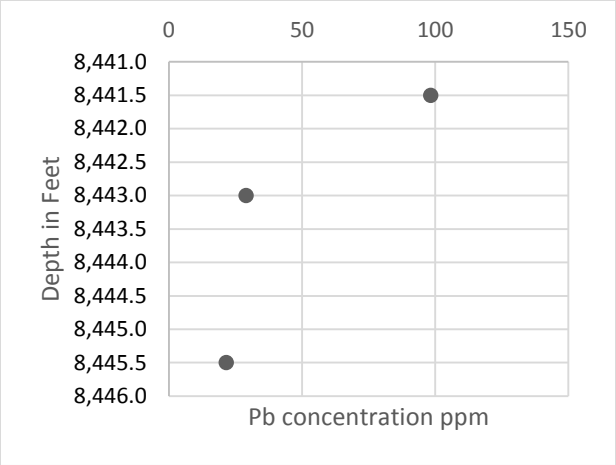

Figure 8a. Concentration of Pb for Chattanooga Shale in well permit # 3800, Greene County.

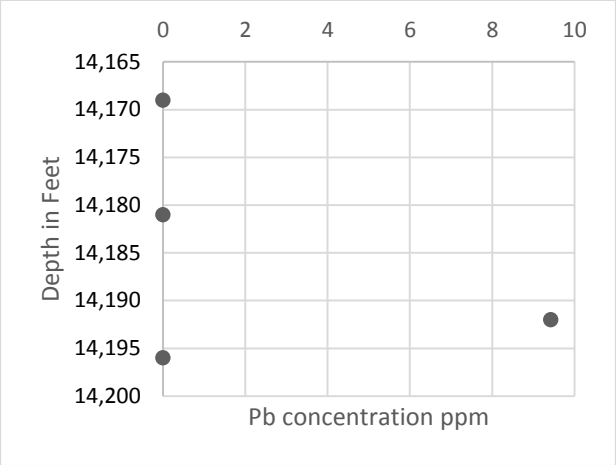

Figure 8b. Concentration of Pb for Conasauga Shale in well permit # 3518, Shelby County.

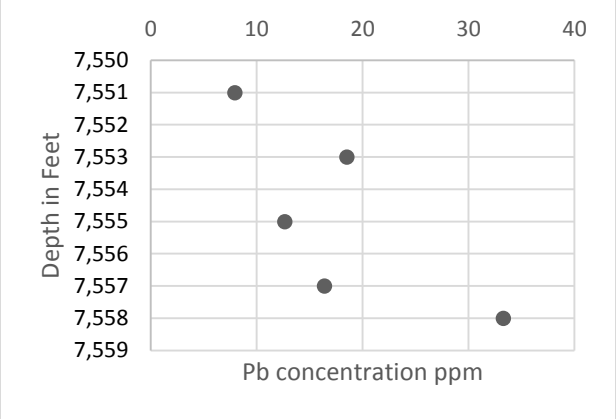

Figure 8c. Concentration of Pb for Conasauga Shale in well permit # 15720, St. Claire County.

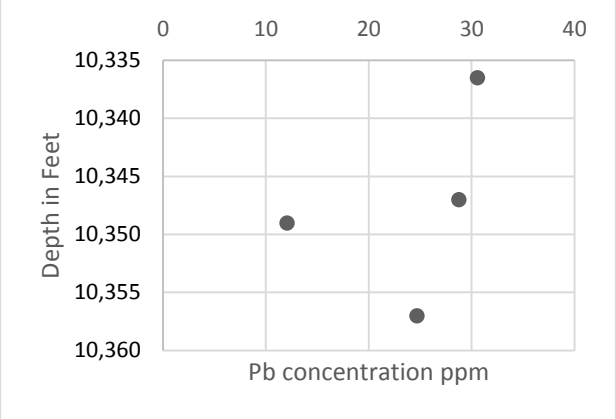

Figure 8d. Concentration of Pb for Devonian Shale in well permit # 3939, Hale County.

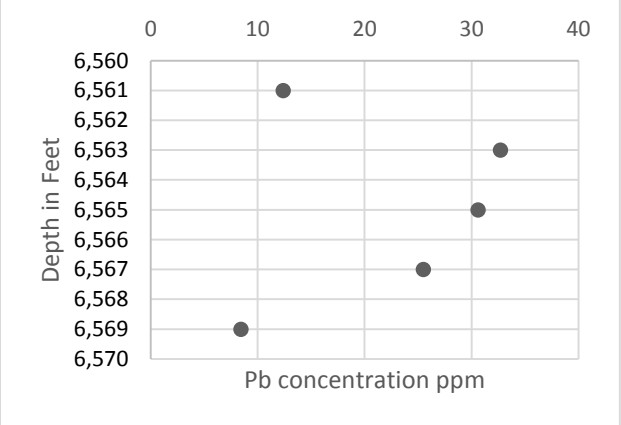

Figure 8e. Concentration of Pb for Neal (Floyd) Shale in well permit # 14289 Pickens County.

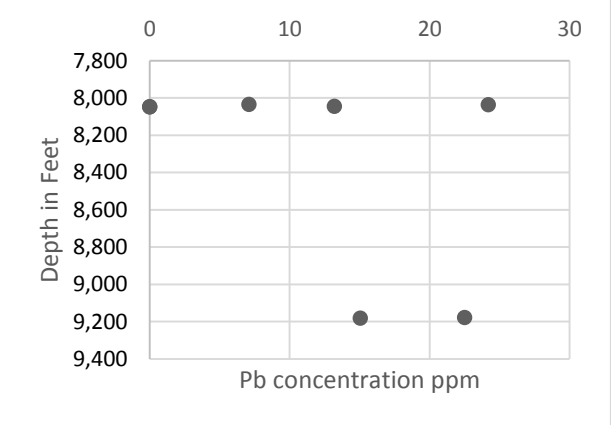

Figure 8f. Concentration of Pb for Neal (Floyd) Shale in well permit # 15668, Greene County.

Mercury

Mercury concentration in shales appears to vary with depth and ranges from 0.00 to 73.41 ppm (Figure 9 a-b). The average mercury concentration in shales reported in literature is about 0.4 ppm (Drever, 1997). Two shales had concentrations of mercury (Hg) that were above the detection limit; these were the Devonian Shale in Hale County and the Neal (Floyd) Shale in Greene County (Figure 9 a-b).

The Devonian Shale within Hale County has substantial concentrations of Hg (Figure 9a). The lowest concentration is found at a depth of 10,357 feet with a concentration of 17.73 ppm while the highest concentration is 58.74 ppm at a depth of 10,349 feet.

In the Neal (Floyd) Shale located in Greene County there are also very high levels of Hg (Figure 9b). The highest concentration of 73.41 ppm is found at a depth of 8048 feet and the lowest concentration of 13.5 ppm is found at a depth of 8034 feet (Figure 9b). Large Hg concentration heterogeneity exists within this shale body.

Current EPA standard dictate that no more than 2 parts per billion (ppb) of Hg can be present in drinking water. With mercury's extreme health effects and the potential for large quantities present in the shales, special attention must be paid when it comes to proper care of produced fluids as well as cutting from the well bore.

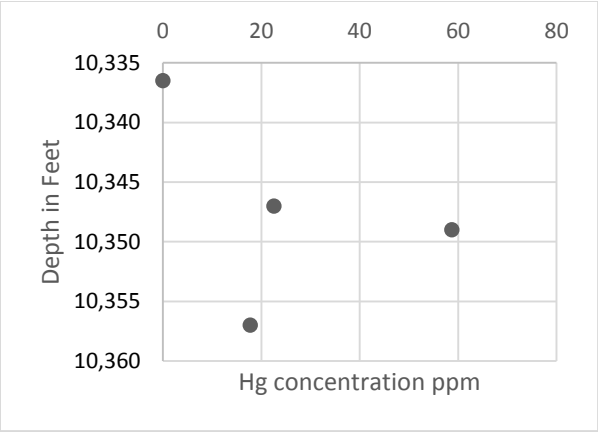

Figure 9a. Concentration of Pb for Devonian Shale in well permit # 15668, Greene County.

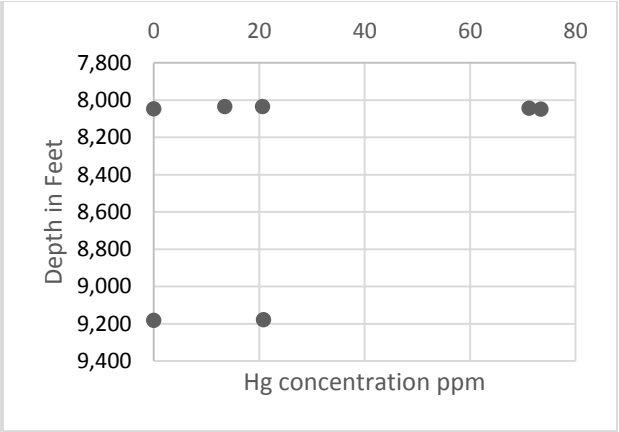

Figure 9b. Concentration of Pb for Neal (Floyd) Shale in well permit # 15720, St. Claire County.

Sulfur

Sulfur concentration in shales appears to vary with depth and ranges from 0.00 to 6.82 % (Figure 10 a-e). The average sulfur concentration in shales reported in literature is about 2.60 % (Karl and Karl, 1961). The Chattanooga Shale, Greene County, has relatively high concentrations of sulfur (Figure 10a). The highest concentration of 5.21% occurs at a depth of 8441.5 feet; the lowest concentration of about 2.78% is found at a depth of 8443 feet.

The Conasauga Shale within Shelby County has very low concentrations of sulfur (<0.40%) (Figure 10b). This is consistent with the low amounts of Fe, and other trace metals found in this shale body; sulfur tends to have high geochemical affinity with Fe. Moreover, high amounts of calcium carbonates are present in this shale. The lowest concentration of sulfur in this shale is about 0.15%, found at a depth of 14,196 feet, while the highest concentration is 0.33%, found at a depth of 14,192 feet. This is consistent with the mineralogy results of this study as there are insignificant sulfide minerals present (see Conasauga Shale Shelby County mineralogy section).

Sulfur concentrations in the Conasauga Shale, St. Claire County (Figure 10c), are significantly higher those in the carbonate-rich shale Conasauga Shale, Shelby County (Figure 10b). The lowest concentration in this shale is about 1.05% at a depth of 7551 feet, while the highest concentration of 6.82% is found at a depth of 7555 feet. It should be noted that As and Pb concentrations are also significantly higher in St. Claire County than those in Shelby County.

The concentrations of sulfur in the Devonian Shale, Hale County, ranging from 1.26% to 5.88 %, are significantly higher than those of the Conasauga Shale in Shelby County (Figure

10d). As and Pb concentrations are also significantly higher in the Devonian Shale than those in Conasauga Shale, Shelby County. Concentrations of sulfur in the Neal (Floyd) Shale, Pickens County, range from 1.94% at a depth of 6,563 feet to 3.24% at a depth of 6,565 feet (Figure 10e). Concentrations of sulfur in the Neal (Floyd) Shale, Greene County, vary from a maximum of 4.89% to a minimum of 1.40%; these concentrations are found at depths of 8035 feet and 9181.5 feet, respectively (Figure 10f).

It is imperative to quantify the amount of sulfur within each of these shale bodies' due to the strong geochemical affinity for trace metals to be sorbed or incorporated into common sulfide minerals. Sulfide minerals are common in shales typically deposited under highly reducing environments. Natural occurring metal and metalloid sulfide minerals include pyrite (FeS_2, most common), galena (PbS), sphalerite (ZnS), cinnabar (HgS), as well as the arsenic sulfides realgar (AsS), orpiment (As_2S_3), and arsenopyrite (FeAsS). The low solubility of these minerals makes them effective in removing trace metals (e.g., As and Pb) from formation water.

As stated before these minerals are very redox sensitive and a change of the redox state from the injection of fracturing fluid into shale could make these minerals unstable, thus facilitating the release of toxic elements into the brine fluid. This fluid may then be returned as produced water to the surface where it has the potential to contaminate groundwater through either mechanical failure in cementation or casing or human failure at the surface.

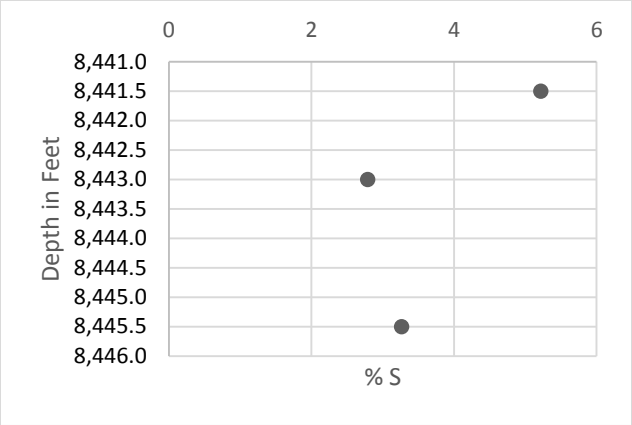

Figure 10a. Concentration of S for Chattanooga Shale in well permit # 3800, Greene County.

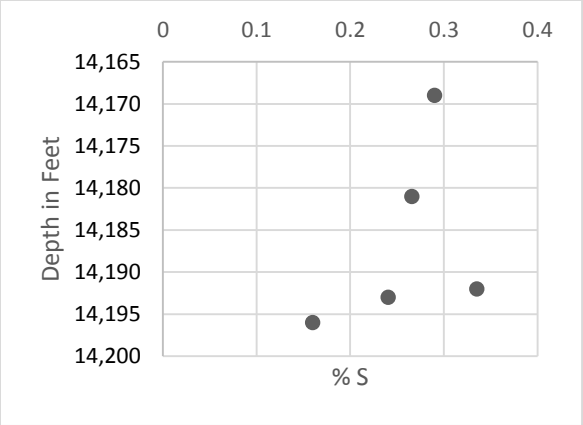

Figure 10b. Concentration of S for Conasauga Shale in well permit # 3518, Shelby County.

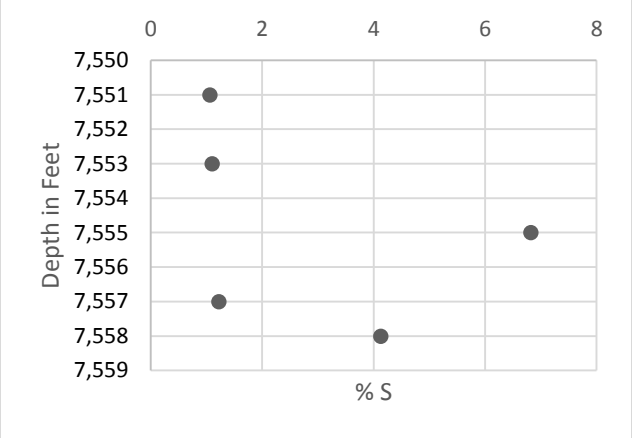

Figure 10c. Concentration of S for Conasauga Shale in well permit # 15720, St. Claire County.

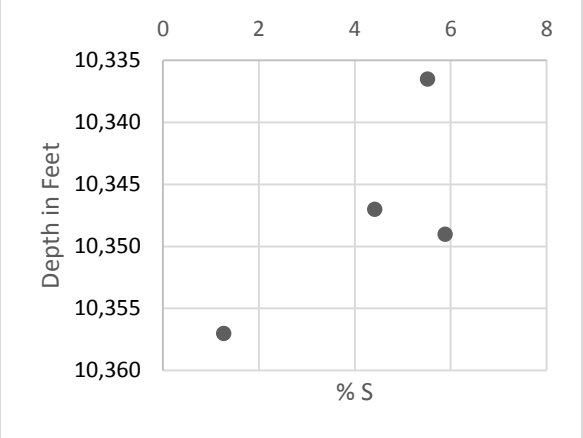

Figure 10d. Concentration of S for Devonian Shale in well permit # 3939, Hale County.

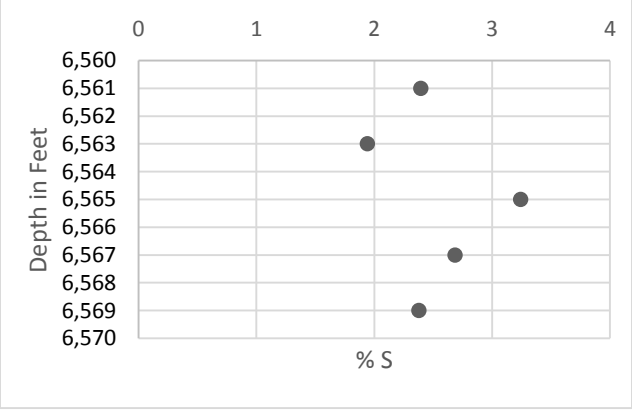

Figure 10e. Concentration of S for Neal (Floyd) Shale in well permit # 14289 Pickens County.

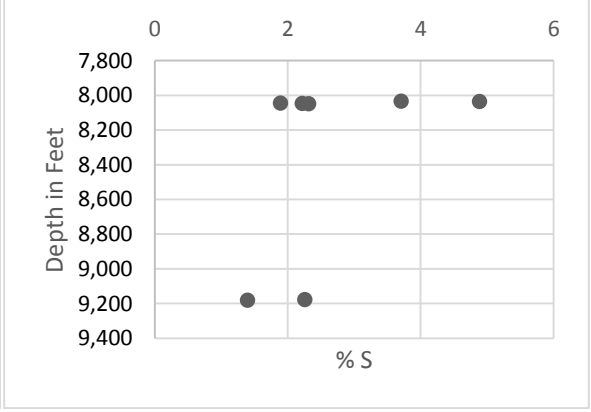

Figure 10f. Concentration of S for Neal (Floyd) Shale in well permit # 15668, Greene County.

Iron

Iron concentration in shales appears to vary with depth and ranges from 0 .08% to 4.49% (Figure 11 a-f). The average Fe concentration in shales reported in literature is 4.72 % (Karl and Karl, 1961). Fe concentrations in the Chattanooga Shale within Greene County range from 4.49% at a depth of 8441.5 feet to 2.41% at a depth of 8444.5 feet (Figure 11a).

The Conasauga Shale located in Shelby County has considerably lower Fe concentrations as compared to those in the Greene County (Figure 11b). Iron concentrations range from a low of 0.08% at a depth of 14,181 feet to a high concentration of 0.36% at a depth of 14,192 feet. This result is consistent with the high amounts of calcium carbonates present in this section of the Conasauga Shale (see Conasauga Shale Shelby County mineralogy section). The low iron content corresponds well with low concentrations of metals such as Pb and As which has strong geochemical affiliation with Fe (Figures 8b and 7b).

The Conasauga Shale in St. Claire County (Figure 11c) also has higher concentrations of Fe as compared to the Conasauga Shale in Shelby County. In St. Claire County, Fe concentrations range from 0.67% at a depth of 7557 feet to 2.19% at a depth of 7553 feet.

The Fe concentration in the Devonian shale in Hale County spans a narrow range; a low of 1.68% is present at a depth of 10,347 feet and a high of 1.86% is present at a depth of 10,349 feet (Figure 11d).

The maximum concentration of Fe within the Neal (Floyd) Shale, located in Pickens County, is 2.63 % at a depth of 6561 feet (Figure 11e). The lowest concentration of 1.77 % is found a depth of 6565 feet. Iron concentration in the Neal (Floyd) Shale within Greene County

range from a high value of 2.72% at a depth of 8034 feet to a low concentration value of 1.39% at a depth of 9181.5 feet (Figure 11f).

The concentration of Fe within each of the shale bodies reflect the abundance of iron-bearing minerals (e.g., Fe sulfides, Fe oxides, Fe carbonate, Fe-rich silicate, etc). The iron-bearing minerals have strong geochemical affinity to sorb trace metals onto their surfaces or incorporate these trace metals into their crystalline structure. There is a strong trend for increasing concentrations of As, Pb, and S with increasing concentrations of Fe (Figure 12 a-c) with R^2 values of 0.29 for S, 0.36 for Pb, and 0.36 for As (Figure 12 a-c).

The transformation of Fe-bearing minerals under changing redox conditions may control mobility and concentrations of trace metals in groundwater. For example, a large quantity of trace metals could be introduced into the groundwater as pyrite becomes oxidized. Weathering of Fe-rich silicate minerals and reduction of Fe oxides also releases Fe and trace metals into groundwater (Saunders et al., 2008). The metal-rich fluid then has the potential to contaminate underground drinking water supplies (USDWs) from a multitude of scenarios, such as cementation failure, well bore failure, or intimate contact of produced fluids with the surface due to human or mechanical failure. Because of this the regulations involving hydraulic fracturing gas-shale must be considered.

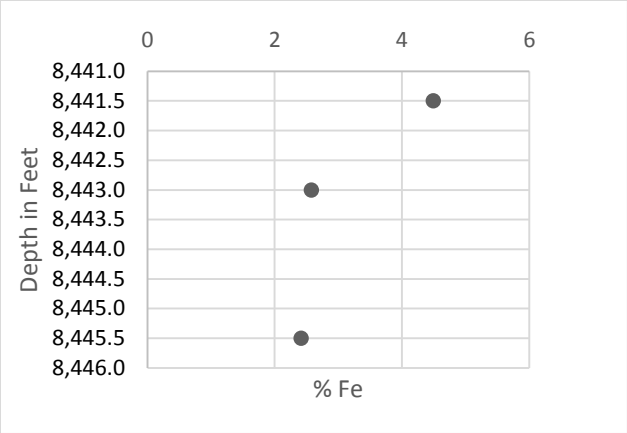

Figure 11a. Concentration of Fe for Chattanooga Shale in well permit # 3800, Greene County.

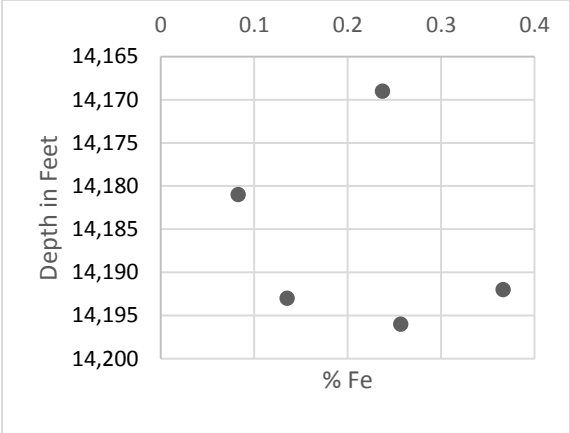

Figure 11b. Concentration of Fe for Conasauga Shale in well permit # 3518, Shelby County.

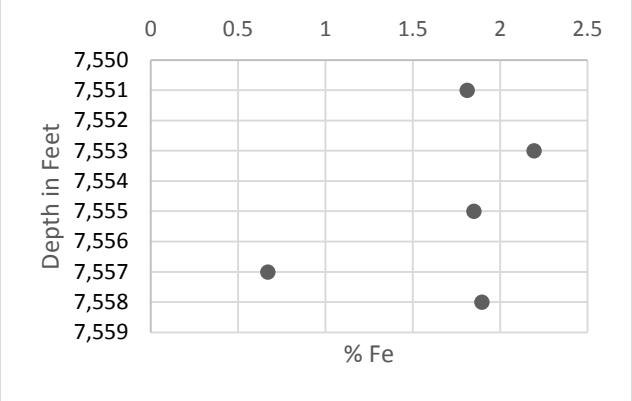

Figure 11c. Concentration of Fe for Conasauga Shale in well permit # 15720, St. Claire County.

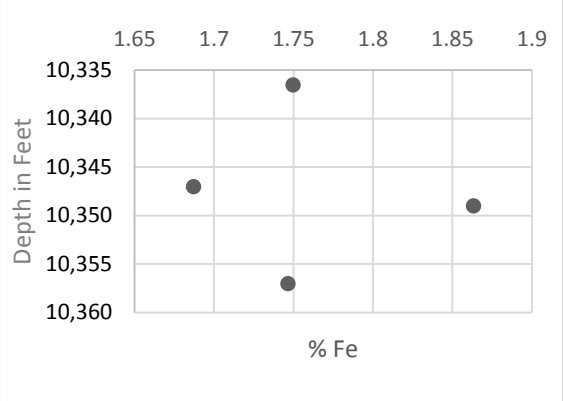

Figure 11d. Concentration of Fe for Devonian shale in well permit # 3939, Hale County.

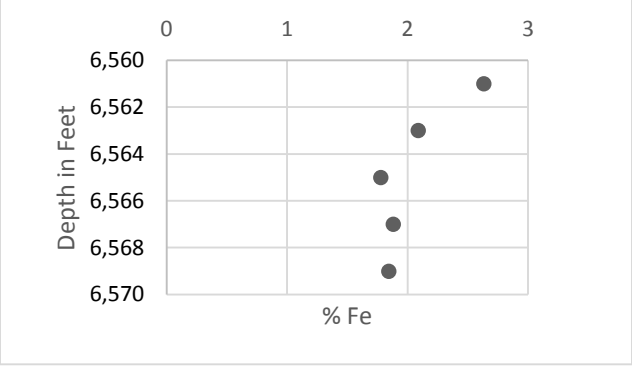

Figure 11e. Concentration of Fe for Neal (Floyd) Shale in well permit # 14289 Pickens County.

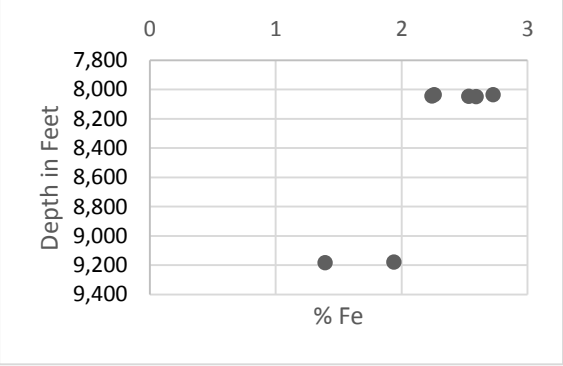

Figure 11f. Concentration of S for Neal (Floyd) Shale in well permit # 15668, Greene County.

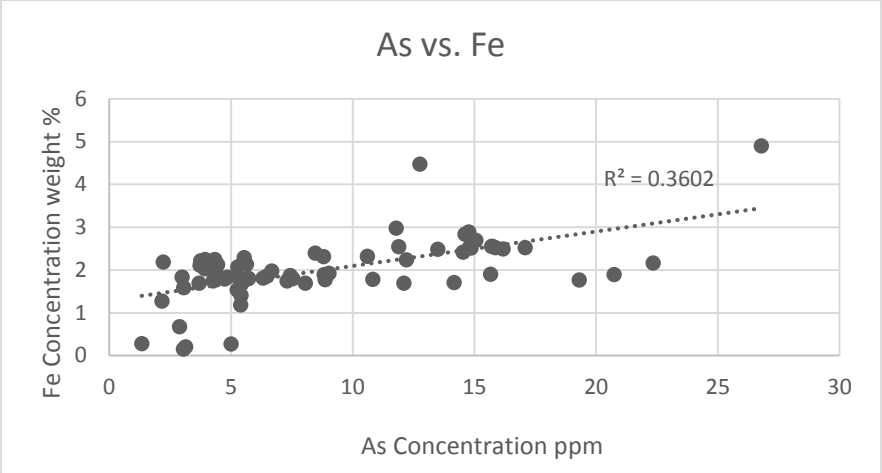

Figure 12a. Correlation of As concentrations (ppm) and Fe concentrations (weight %) for all shales investigated.

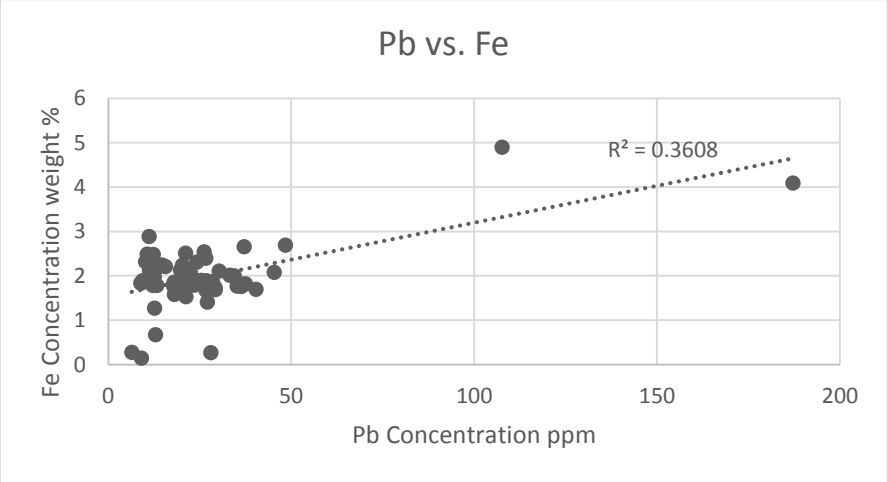

Figure 12b. Correlation of Pb concentrations (ppm) and Fe concentrations (weight %) for all shales investigated.

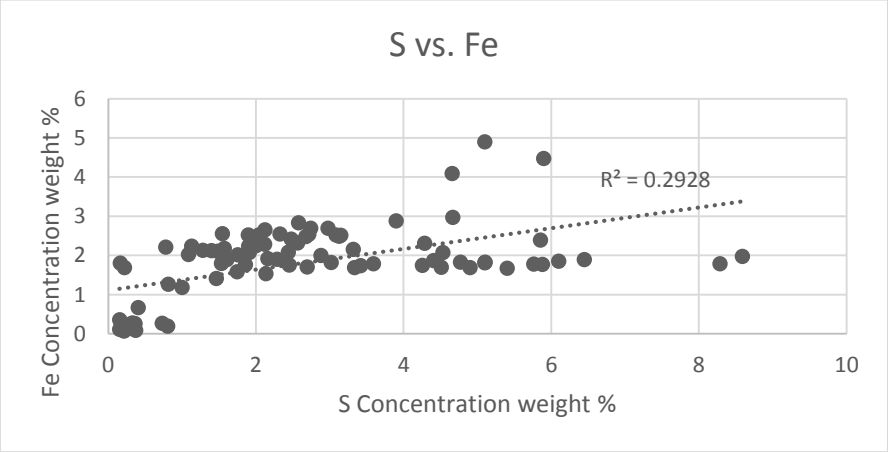

Figure 12c. Correlation of S concentrations (weight %) and Fe concentrations (weight %) for all shales investigated.

Wellbore, Pit, and Base Line Water Testing Regulations

This section reviews relevant environmental regulations on gas-shale hydraulic fracturing operation. The new hydraulic fracturing technologies used for shale oil and gas production requires specific protocols or guidelines for environmental protection, which have not been properly reviewed and formulated. Throughout state and federal regulations, there exists a related regulations required for wellbore construction (e.g. casing, cementation, mechanical integrity test, and cement evaluation logs) (Table 7) and pit construction (Table 8).

A major concern involving wellbore integrity occurs during the cementing process; when fresh cement encounters natural gas from non-producing horizons there is potential for high pressure gas to cut channels in the cement, allowing for communication of deep reservoirs with shallow underground source of drinking groundwater or USDWs. As of now, there is not a proof test that can be done to inspect if channeling has occurred, or inspect the quality of the cement/rock contact. This is a major concern for the potential contamination of USDWs (Ingraffea, 2010).

Wellbore construction and pit construction is essentially standard for each state; however, baseline water testing is not. Only three states, Pennsylvania, Illinois, and Colorado, require this testing (Table 7).

Potential USDW Degradation and Economic Impact Due to Gas-shale Production

When producing shale-gas there are two main areas of potential USDW contamination; 1) communication of hydrocarbons and formation waters from producing and non-producing formations to USDWs due to improper cementing and casing, and 2) migration of flowback fluids and produced fluids from the containment pit into USDWs. It has been found that there is a failure rate of about 6.5% in well casings (Ingraffea, 2010). Failure can be either casing failure or failure of the cement to isolate USDWs from the migration of fluids or contaminants (Ingraffea, 2010). This number may seem small, however, when considering the dynamics of shale-gas production and the amount of wells that must be drilled in order for gas plays to remain economical this stands as a significant potential for contamination (Ingraffea, 2010; Berman, et al., 2012)

With current federal and state regulations, only three states (e.g. Pennsylvania, Colorado, and Illinois) require determinations if the contamination within USDWs is due to the production of shale-gas or naturally occurring (background or from an unidentified source). Presented in Table 8 are Illinois state baseline water testing requirements.

As illustrated in Table 9, water sampling in Illinois is quite extensive, and while not a probable large expense for any one well, the culmination of testing could possibly lead to a larger overhead expenditure for shale-gas development.

If there is contamination from either the wellbore or the containment pit, the source will need be determined and the appropriate action will take place. This is because natural occurring

contamination would be differentiated from contamination from production. These regulations allow for a proactive position as opposed to a reactive position.

One testing requirement that Colorado has put into place states that if methane concentration is found within a well over 1 mg/L, isotope analysis will be conducted on C^{12} and C^{13} ratios, as well as H^1 and H^2 ratios. Particular ratios of these stable isotopes indicate either a biogenic or thermogenic formation of the gas. From this it will be possible to determine if the methane in the groundwater was either produced from natural bacterial activities in groundwater or natural gas seeping from a producing zone into groundwater (Colorado Oil and Gas Conservation Commission, 2012).

Subsurface Monitoring and Contaminant Modeling

Recent EPA regulations, 40 CFR 146.6(a) (2) and 40 CFR 144.41, would require the monitoring and modeling of subsurface flow to determine the likelihood of USDW contamination from contaminant migration. The process of modeling is extremely complex, involving extensive literature review as well as collection of raw geological and hydrologic data, the prediction of contamination scenarios (i.e., fluid migration through a fault, well bore failure), the actual model (i.e. geomechanical model, transport model) and analysis of the model quality. Subsurface monitoring would consist of pressure monitoring; where an increase in pressure could indicate the migration of gas or potential casing failure, both of which could be detrimental to USDWs (Briskin and Stephen, 2013).

The practice of subsurface contaminant modeling introduces many unknown complexities and would require extensive work and expenditures on top of the overhead allocated for production. As of now, EPA's regulatory arm only extends to those wells that are hydraulically fractured using diesel fuel, thus negating regulations for companies that

hydraulically fracture rocks with water based fluid. However, if future hydraulic fracturing operations fall under the Clean Water Act (CWA), operations would be required to follow these preemptive guidelines, potentially causing a dramatic cost increase for "business as usual" practices.

Future Impact Due to Colorado, Pennsylvania, and Illinois Base-Line Water Testing

Colorado, Pennsylvania, and Illinois have recently passed the most comprehensive regulations concerning the practice of hydraulic fracturing, namely the requirement of baseline water testing as well as other requirements not presented in this paper. These new regulations (i.e., baseline water testing) will potentially set the precedent for standards to be put forth for the regulation of shale-gas production in the United States.

These new regulations could serve as a double-edged sword, that is, if contamination is confirmed by the baseline and subsequent testing at a site, it could possibly limit hydraulic fracturing practices in the United States. However, this testing could also confirm the industry's stance on hydraulic fracturing; it is a safe practice and does not commonly impact USDWs. This could result in encouraging the opening of new shale-gas opportunities in states where moratoriums have been placed upon hydraulic fracturing (e.g., Marcellus shale in New York State and municipal bans in parts of Colorado).

New baseline water testing regulations could have an impact on the cost of producing gas-shale. With well failure rates coupled with the amount of wells that must be drilled, the potential for contamination due to shale-gas production increases. If all state and federal regulations come up to par to Illinois, Colorado, and Pennsylvania regulations, additional accountability will be placed on all potential contamination as a result of producing shale-gas.

This coupled with a large public dissent concerning hydraulic fracturing has the potential to impact the proliferation of unconventional gas production.

The concerns of groundwater contamination have created great uncertainty on future gas-shale development. This uncertainty stems largely from inadequate knowledge on shales' mineralogy, fractures, mechanic properties, porosity, permeability, and chemical (trace metal) composition.

Table 7. Wellbore and baseline water testing requirements for Colorado, Illinois, and Pennsylvania. (Colorado Oil and Gas Conservation Commission, 2012; Bradley et. al., 2013; Pennsylvania Department of Environmental Protection, 2012)

Regulating Body	Casing	Cementation	Mechanical integrity Test	Cement Evaluation Log	Baseline Water Testing
Colorado	Required to protect all USDWs.	Must protect all aquifers and have a minimum compressive strength after 24 and 72 hours.	The production casing must be pressure tested with pressures similar to those expected.	A cement bond log shall be run on all production casing.	Required for new permitted oil and gas well in a ½ mile radius from the well bore.
Illinois	Must isolate all USDWs.	Cement must conform to current industry standards published by the American petroleum institute.	A pressure test demonstrating less than or equal to a 5% pressure drop after 30 minutes	A radial cement bond evaluation log must be run on each well. If cementation is found inadequate, it must be remediated.	Required in a 1,500 feet radius extending out from the well bore.
Pennsylvania	Required to protect all USDWs from fluid migration.	Cementing must secure the casing in the wellbore, isolate the wellbore from fresh groundwater, and contain any pressure from drilling, completion and production.	A pressure test demonstrating less than or equal to a 10% pressure drop after 30 minutes	None required.	Required in a 1,000 feet radius from the well bore.

Table 8. Containment pit requirements for Colorado, Illinois, and Pennsylvania. (Colorado Oil and Gas Conservation Commission, 2012; Bradley, J., et. al., 2013; Pennsylvania Department of Environmental Protection, 2012)

Regulating Body	Use of Pits Allowed	Pit construction requirements
Colorado	Yes, however, only in emergency situations.	Must not allow any communication of contaminants and aquifers or USDWs.
Illinois	Yes, however only for temporary storage due higher than expected flow back.	The synthetic liner must have a minimum thickness of 24 mils, capacity of at least 110% of maximum volume of anticipated recovered fluid.
Pennsylvania	Yes, however only for temporary containment.	Pits must be constructed with synthetic flexible liner that has a permeability value no greater than 1 x 10-7 cm/sec.

Table 9. Illinois water testing requirements for hydraulically fractured wells (Bradley, et al., 2013)

Water properties and dissolved gasses to be tested	pH, total dissolved solids, dissolved methane, dissolved propane, dissolved ethane, alkalinity, and specific conductance.
Anions and Elements to be tested	Chloride, sulfate, arsenic, barium, calcium, chromium, iron, magnesium, selenium, cadmium, lead, manganese, mercury, and silver.
Benzenes to be tested	Benzene, toluene, etheylbenzene, and xylene. (BTEX)
Radioactivity to be tested	Gross alpha and beta particles.
Responsible testing body	Either a licensed engineer (P.E.) or a licensed Geologist (P.G.). Analysis must be conducted at an independent testing laboratory.
Sampling frequency	Baseline, 6 months, 18 months, and 30 months.

Metal Enrichment in Black Warrior Basin Shale's

The concentrations of selected elements of gas-shales in the Black Warrior Basin were normalized (Table 10) using the aluminum normalized enrichment factor (ANEF);

$$\frac{Me_{sample}/Al_{sample}}{Me_{crust}/Al_{crust}} = \text{ANEF} \qquad (2)$$

Here Me represent trace metals in shale samples and Al (aluminum) is the selected reference metal in Earth's crust. ANEF determines the enrichment or depletion of an element relative to the reference aluminum. Since there are no known anthropogenic sources of aluminum to

sediments or rocks, any metals with substantial terrigenous inputs would have positive ANEF anomalies. ANEF may also provide useful insights on reactivity relationship such as the retention of chalcophile metals in sediments or minerals via bacterial sulfate reduction and formation of sulfide solids.

The Chattanooga Shale located in Greene County (Figure 13 and Table 10) is highly enriched in most trace elements but three (Hg, Ba, and Mn). The enrichment factor is greater than 100 for As, Cu, and S; Pb, Fe, Zn, and Ca also display relatively high ANEF values (>10). The high ANEF values suggest that this shale represent a significant sink for trace elements.

The Conasauga Shale located in Shelby County (Figure 14 and Table 10), shows astronomically high enrichment values for several of the elements (e.g., Ca, Cu, and S). This is most likely the result of targeting a carbonate-rich section of the sample being analyzed; little or almost no aluminum present in the sample causes these anomalously high ANEF results.

The Conasauga Shale in St. Claire County are enriched in As, Cu, and Pb with ANEF factors greater 10 (Figure 15 and Table 10). These data match nicely with the enrichment of sulfur and iron, which is consistent with the hypothesis that iron sulfide minerals such as pyrite represent major sinks for arsenic as well as lead. When comparing this section of the Conasauga Shale with the section found in Shelby County, (Figure 14 and Table 10), we can denote that there is a considerable difference in the enrichment of elements such as Ca, Cu, Fe, S, and Mn. In the case of calcium, there are five orders of magnitude difference between the two shales; however, the enrichment factors of arsenic are similar.

The Devonian Shale in Hale County (Figure 16 and Table 10), exhibits similar enrichments of As, Cu, S, Fe, and Pb to those found in the Conasauga Shale. However, there is a considerable enrichment of Hg present within this shale with ANEF values near 10,000

The Neal (Floyd) Shale in Greene County (Figure 17 and Table 9) shows great enrichment S, As, Cu, and Hg (ANEF>100). Other trace elements such as Fe, Pb, V, and Zn also display relatively high ANEF values (>10).

The Neal (Floyd) Shale in Pickens County (Figure 18 and Table 10) has one element S with an ANEF value greater than 100. Other trace elements such as As, Cu, Pb, Zn, and V also display relatively high ANEF values (>10).

The highest enrichment factor of As (ANEF> 100) and Pb (ANEF > 65) is found in the Chattanooga Shale in Greene County. It should be noted that very high enrichment factor of sulfur is found in all the shales. This result supports the hypothesis that the sulfide minerals are abundant and represent the primary sinks for the toxic trace metals arsenic, lead, and mercury.

Table 10. Aluminum enrichment factor for selected EPA regulated elements for the Chattanooga Shale, Conasauga Shale, Devonian Shale, and the Neal (Floyd) Shale.

Element	Chattanooga Shale, Greene Co	Conasauga Shale, Shelby Co	Conasauga Shale, St. Claire Co	Devonian shale, Hale Co	Neal (Floyd), Pickens Co	Neal (Floyd), Greene Co
As	128.1	66.3	59.9	83.9	48.4	93.2
Ba	6.4	0.00	1.4	5.0	1.4	1.8
Ca	22.9	3063209.0	201.8	62.2	8.8	8.1
Cu	129.3	320487.3	154.9	115.5	78.3	113.4
Fe	22.0	5196.3	11.3	14.1	8.7	11.5
S	850.0	539055.4	655.0	1118.7	358.8	457.0
Pb	64.6	30.4	25.6	35.3	16.6	15.2
Mn	4.8	9777.4	8.3	4.3	3.2	3.4
Hg	0.000	0.000	0.000	9821.8	0.000	6173.7
V	2.8	24.7	7.3	18.6	10.3	11.8
Zn	11.6	169.2	18.4	57.0	65.9	0.000

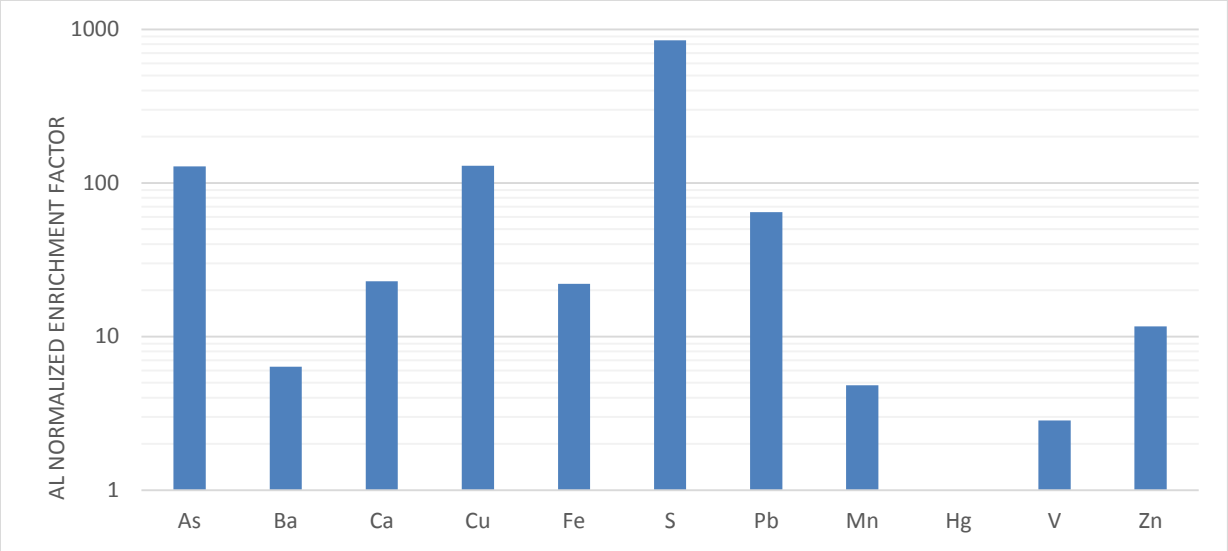

Figure 13. Aluminum normalized enrichment factor for the Chattanooga Shale, Greene County.

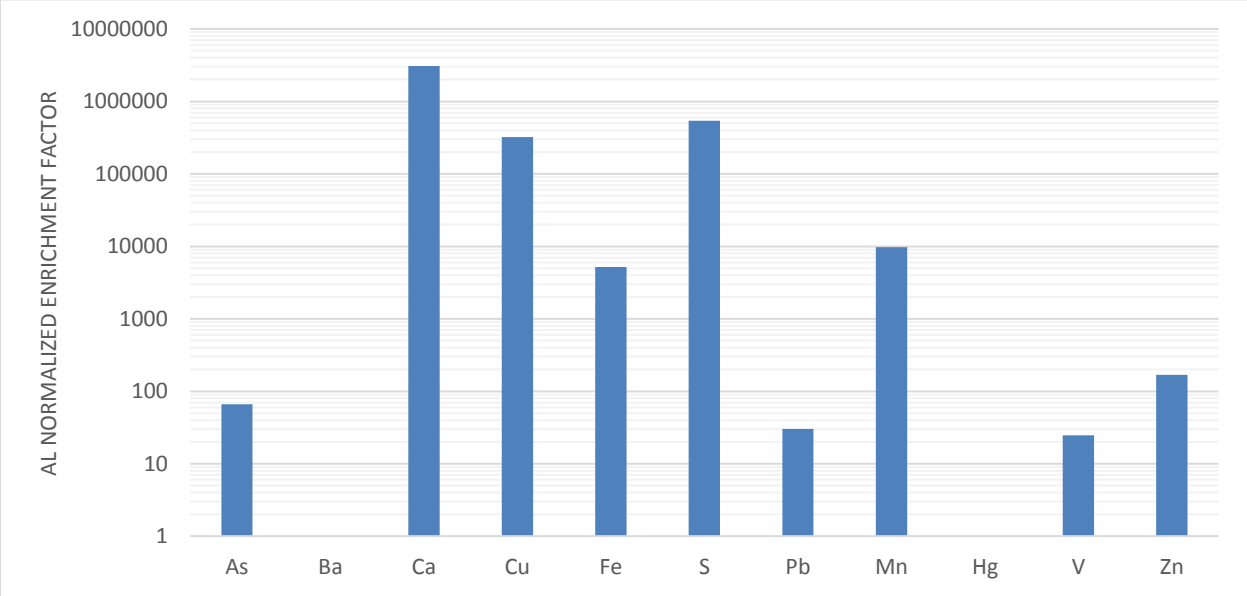

Figure 14. Aluminum normalized enrichment factor for the Conasauga Shale, Shelby County.

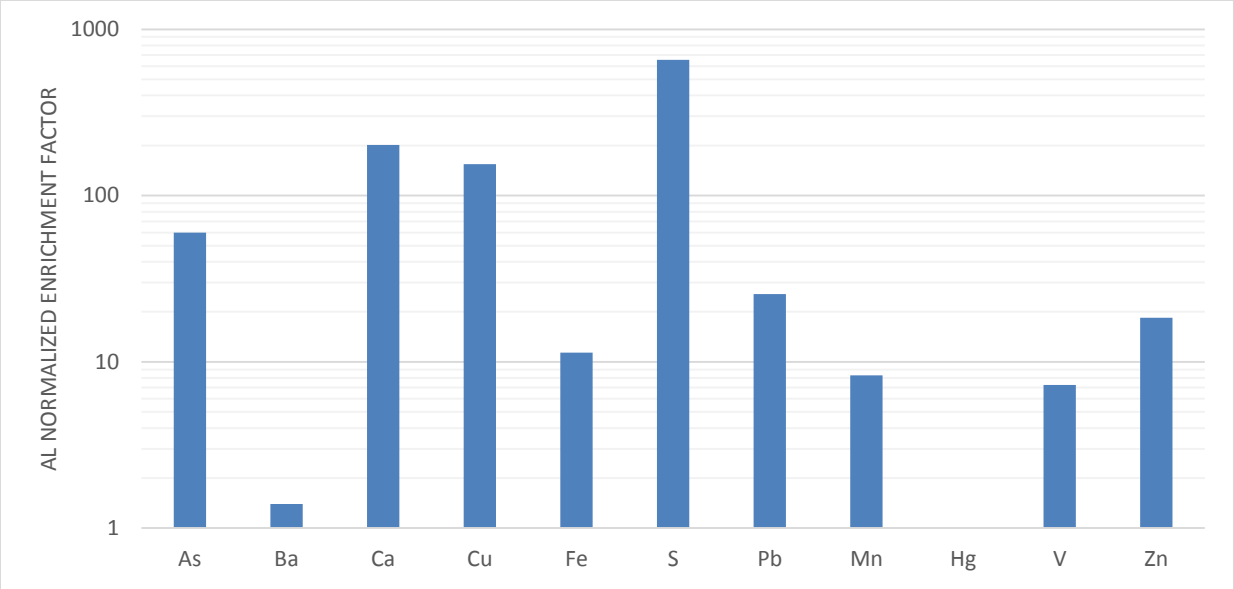

Figure 15. Aluminum normalized enrichment factor for the Conasauga Shale, St. Claire County.

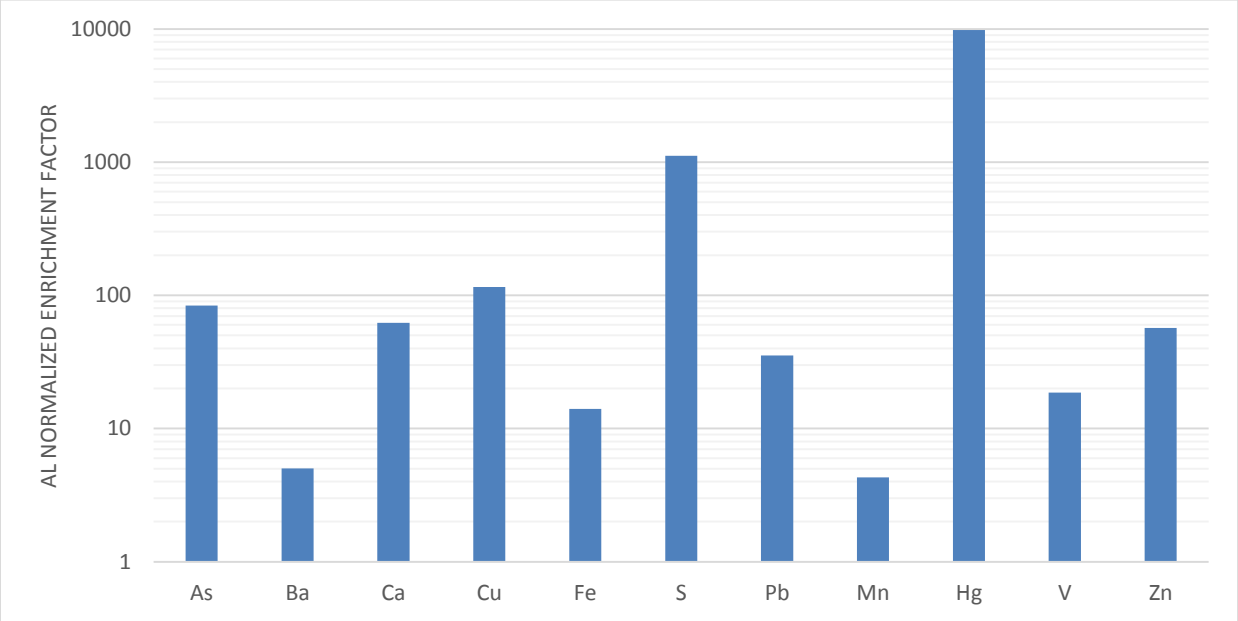

Figure 16. Aluminum normalized enrichment factor for the Devonian shale, Hale County.

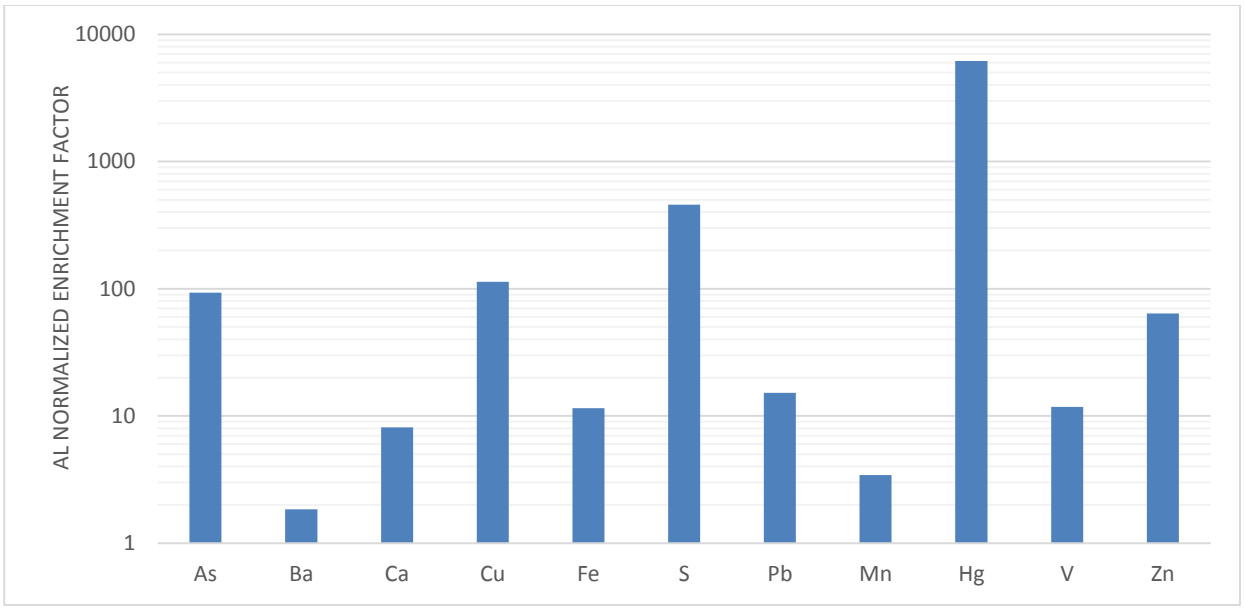

Figure 17. Aluminum normalized enrichment factor for the Neal (Floyd) Shale, Greene County.

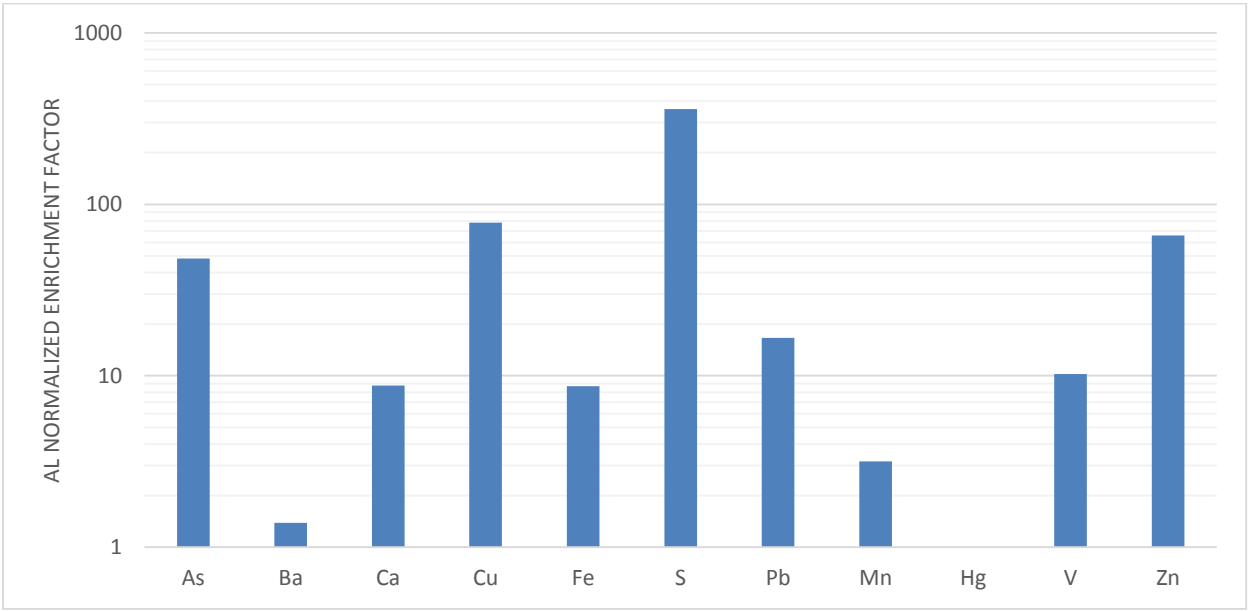

Figure 18. Aluminum normalized enrichment factor for the Neal (Floyd) Shale, Pickens County.

Mineralogy

X-ray diffraction (XRD) analyses of shales were performed on selective sections of three shale units. Powdered XRD pattern were recorded using Bruker D2 Phaser with Ni-filtered Cu Kα radiation at 30 kV and 10 mA. Samples were scanned from 2θ of 10° to 90^0 for 4500 steps at 0.3° sec per step. Identification of clay minerals, which requires preparation of oriented sample, was not performed in this study.

Mineralogical components of the Chattanooga Shale, Greene County (Figure 19), consist mainly of quartz, with accessory sulfide minerals pyrite and marcasite as well as carbonate minerals (calcite and dolomite). Mineralogical composition correlates well with bulk geochemistry analysis of shales. The presence of iron sulfides (i.e., pyrite) is consistent with the abundance of sulfur and iron in this shale (see inorganic geochemistry section) and the positive geochemical correlation between S with Fe (Figure 12c). Other sulfide minerals enriched in Zn and Cu were also identified.

Mineralogical make-up of the Conasauga Shale, Shelby County (Figure 20), is dominated by various carbonates (e.g., magnesium rich calcite, pure calcite, calcium rich dolomite, pure dolomite) with minor amount of quartz. Sulfide minerals are not identified in the XRD spectrum. The lack of sulfides is consistent with the results of bulk geochemical analysis in which there are low Fe, As, Pb, and S (Figure 12a, 12b, 12c) contents in this shale.

Carbonates (e.g., calcite and dolomite) are the main mineralogical constituent in the Conasauga Shale, St. Claire County (Figure 21). Muscovite and magnetite are present as accessory minerals. Muscovite is a common phyllosilicate mineral enriched in Al and K. X-ray

fluorescence analysis also shows the presence of Al and K in this sample. Sulfide mineral assemblages are absent in this sample. Magnetite (Fe_3O_4), a common naturally occurring Fe oxide, is the primary source of Fe in this sample.

Mineralogy in the Devonian shale, Hale County (Figure 22), is dominated by quartz, calcite, and dolomite. Fe-rich sulfide (pyrite) and oxide are accessory minerals. Iron sulfides and iron oxides provide an appropriate mineralogy for trace metal sinks. With increasing iron content an increase in Pb and S is expected; this is confirmed by linear the correlation between of Fe and Pb and bulk geochemical data (Figure 12 b-c).

Dominate mineralogy of the Neal (Floyd) Shale consist of quartz; major accessory minerals include dolomite, calcite, pyrite, and Fe-oxides (Figure 23). Minor silicate minerals (e.g., albite) were also identified. Iron oxides and iron sulfides would be expected with the Fe- and S-rich nature of this shale (see inorganic geochemistry section). Bulk geochemistry data (Figure 12 a-c) indicate that Pb and As may be contained within Fe sulfide minerals. Mineralogy of the Neal (Floyd) Shale, Greene County (Figure 24) is very similar to the Neal (Floyd) Shale, Shelby County (Figure 23). Quartz is the dominant mineral and accessory minerals consist of pyrite, dolomite, and magnetite. Other sulfide minerals enriched in Zn were also identified. The enrichment of sulfide minerals is consistent with the results of bulk geochemical analysis exhibiting high Fe, As, S, Pb and Hg contents (Figures 7-11).

To fully understand the potential environmental impact of producing shales that are rich in sulfides and iron oxides, we must fully characterize the mineral contents and bulk geochemistry of shale. As shown above, there are high concentrations of toxic elements (e.g., As, Pb, etc.) held within minerals in these shales. These minerals are inherently sensitive to changes in redox conditions and pH states. When hydraulic fracturing fluid is introduced into the shale

the conditions under which the minerals exhibit stability may be changed. This in turn will potentially lead to disintegration or break down of the minerals structure, causing the release of toxic elements into groundwater. There is also the possibility of expedited fluid-minerals interactions due to the unique makeup of the fracturing fluid, which is not in thermal or chemical equilibrium with hosting shales.

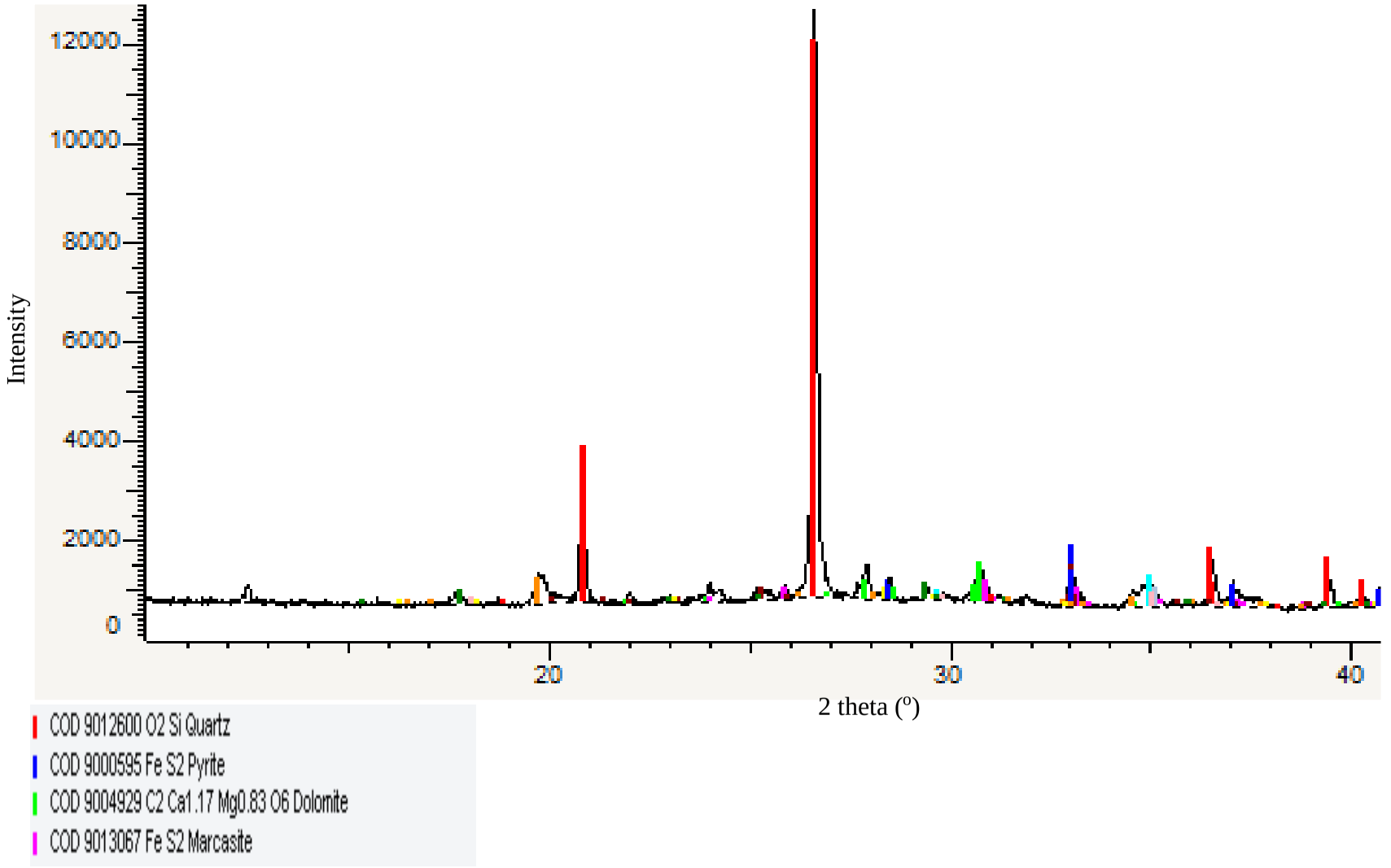

Figure 19. 2Θ spectrum for the Chattanooga Shale, Greene County.

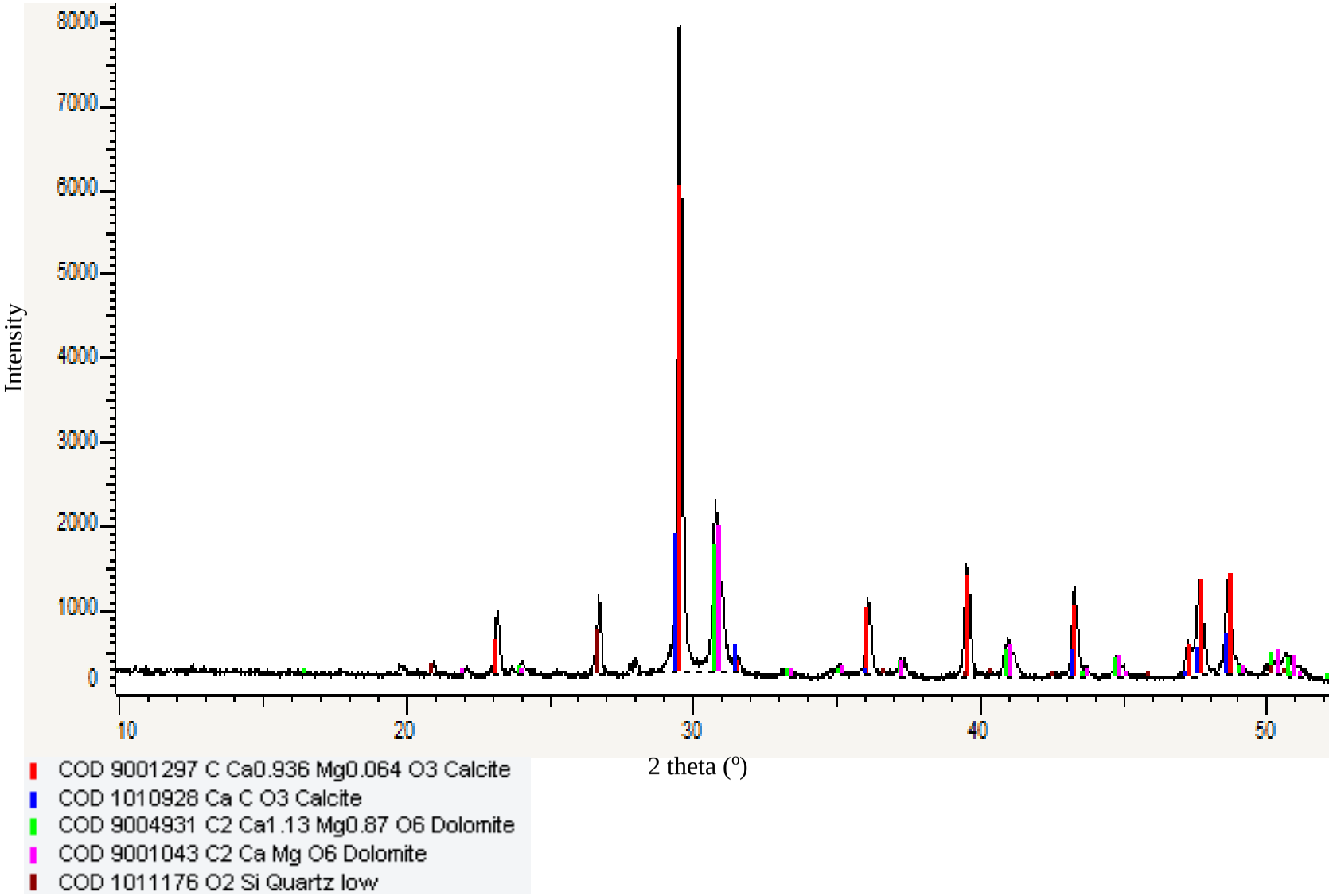

Figure 20. 2Θ spectrum for the Conasauga Shale, Shelby County.

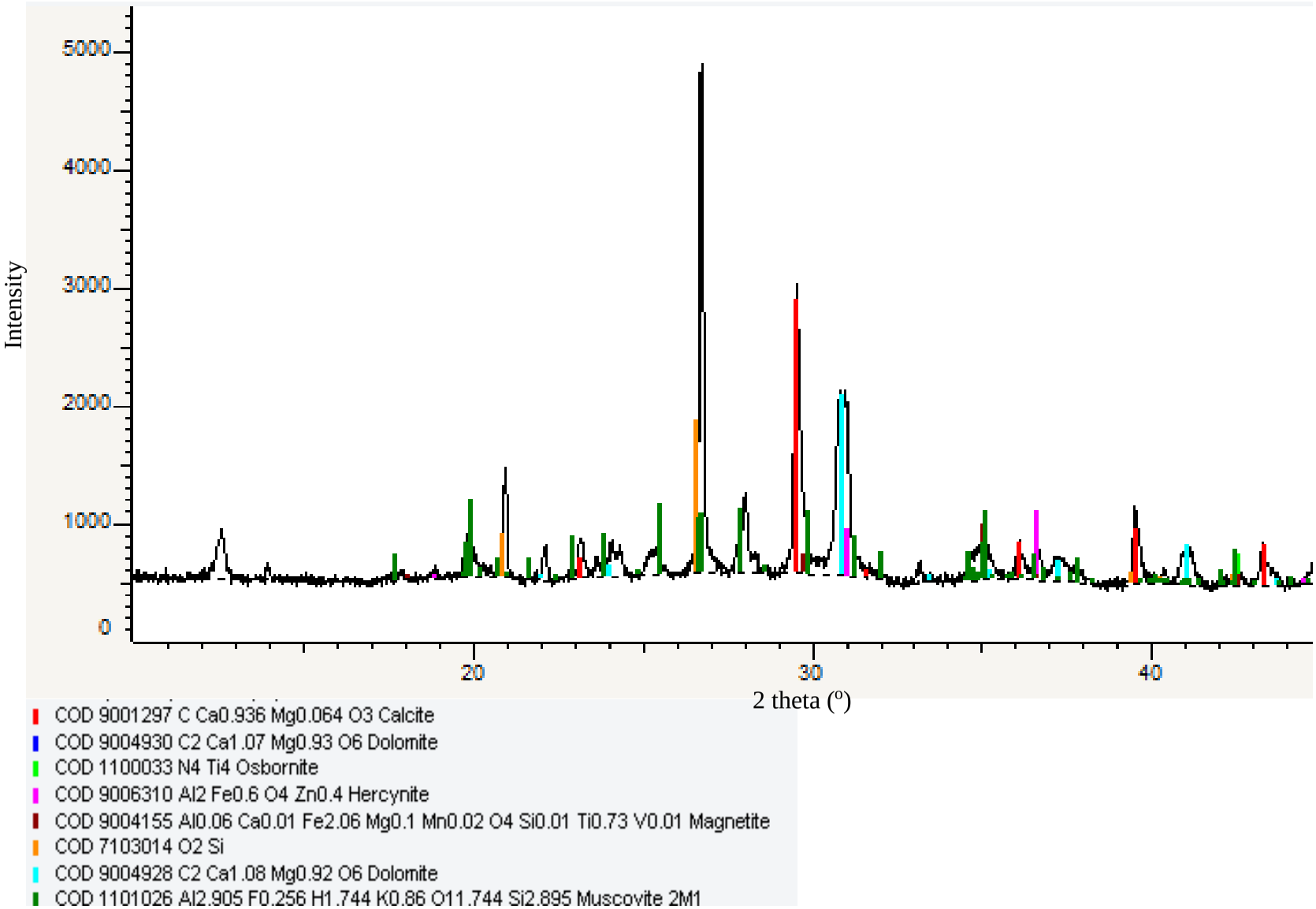

Figure 21. 2Θ spectrum for the Conasauga Shale, St. Claire County.

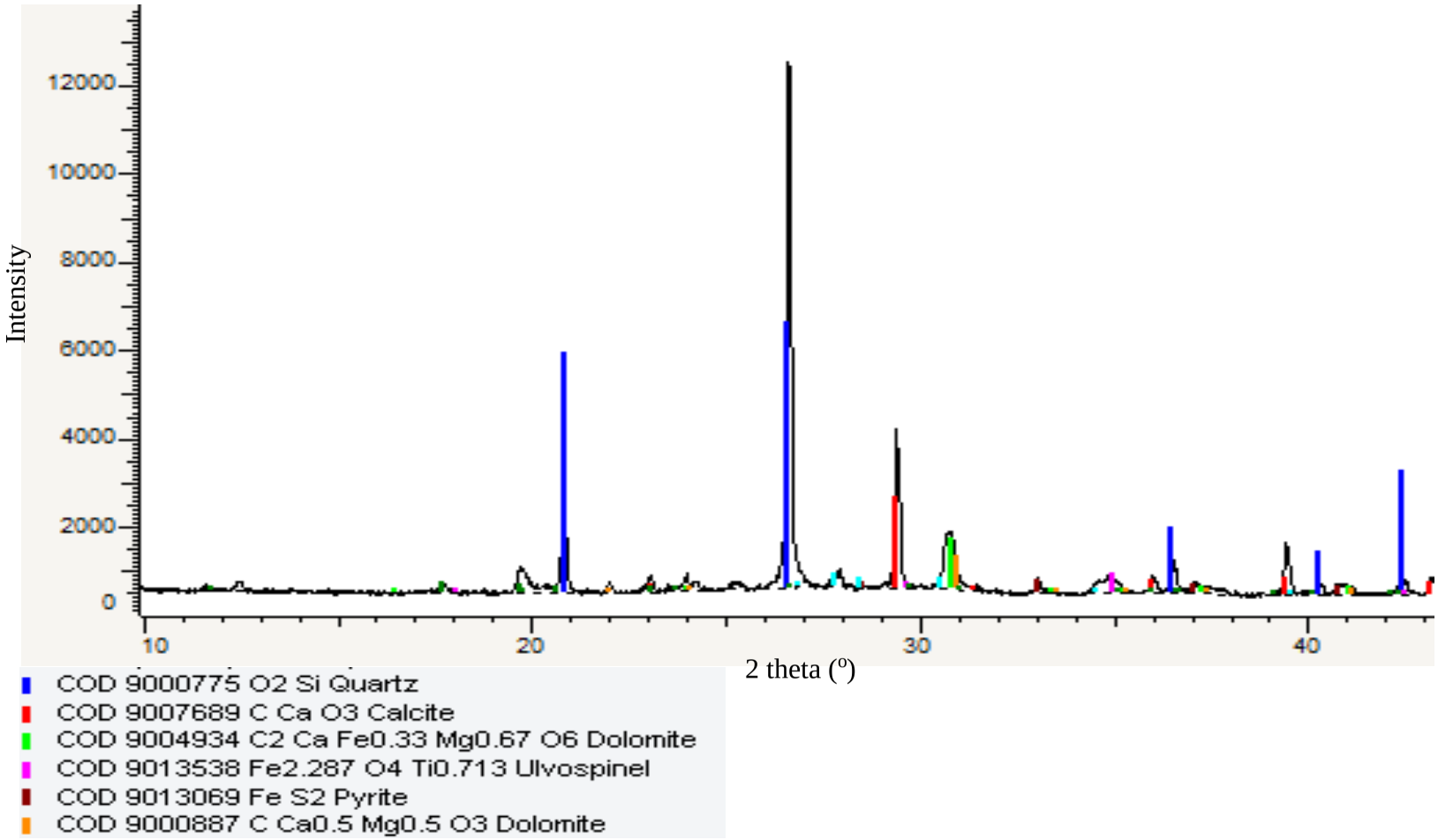

Figure 22. 2Θ specturm for the Devonian Shale, Hale County.

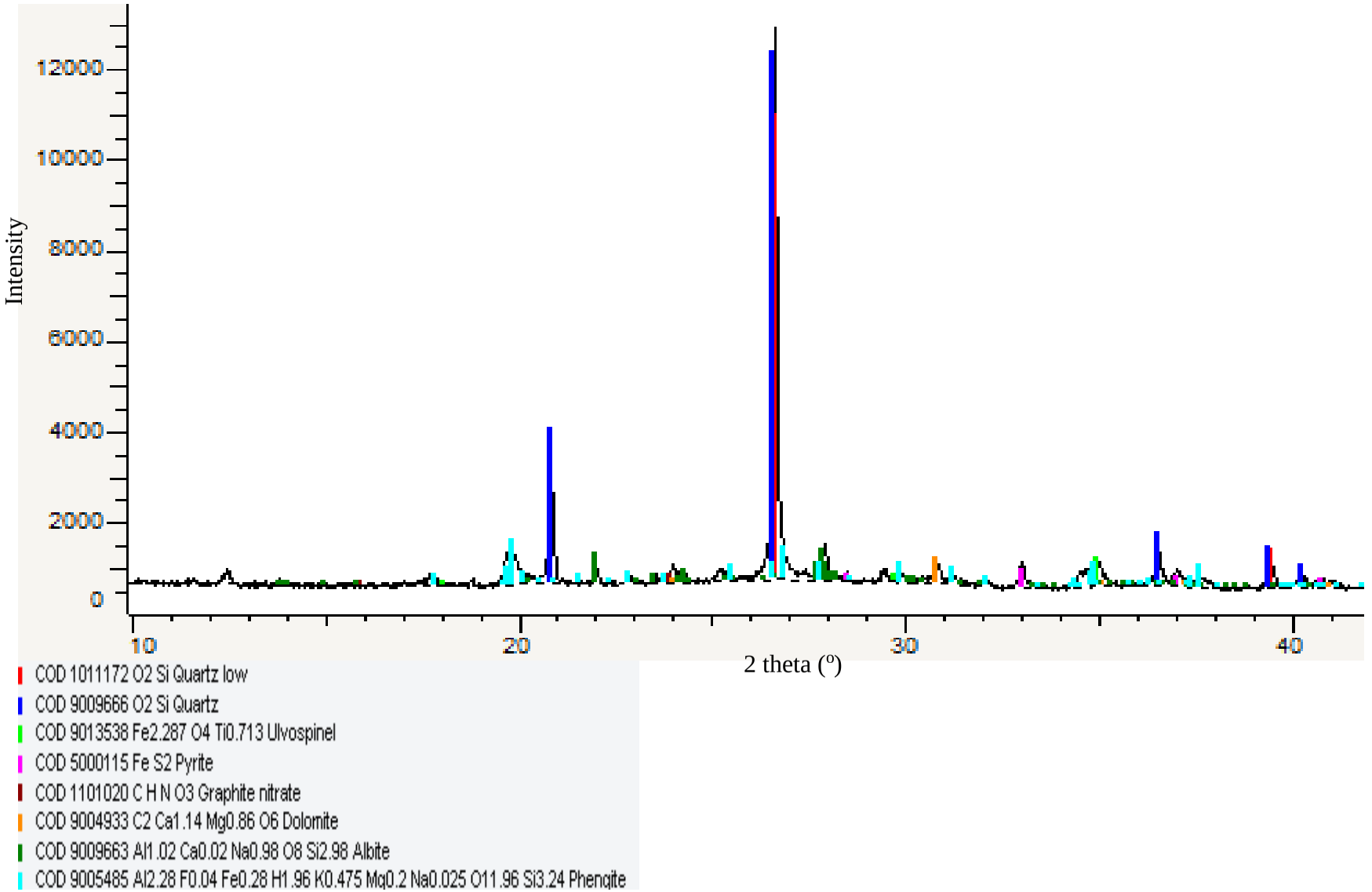

Figure 23. 2Θ spectrum for the Neal (Floyd) Shale, Pickens County.

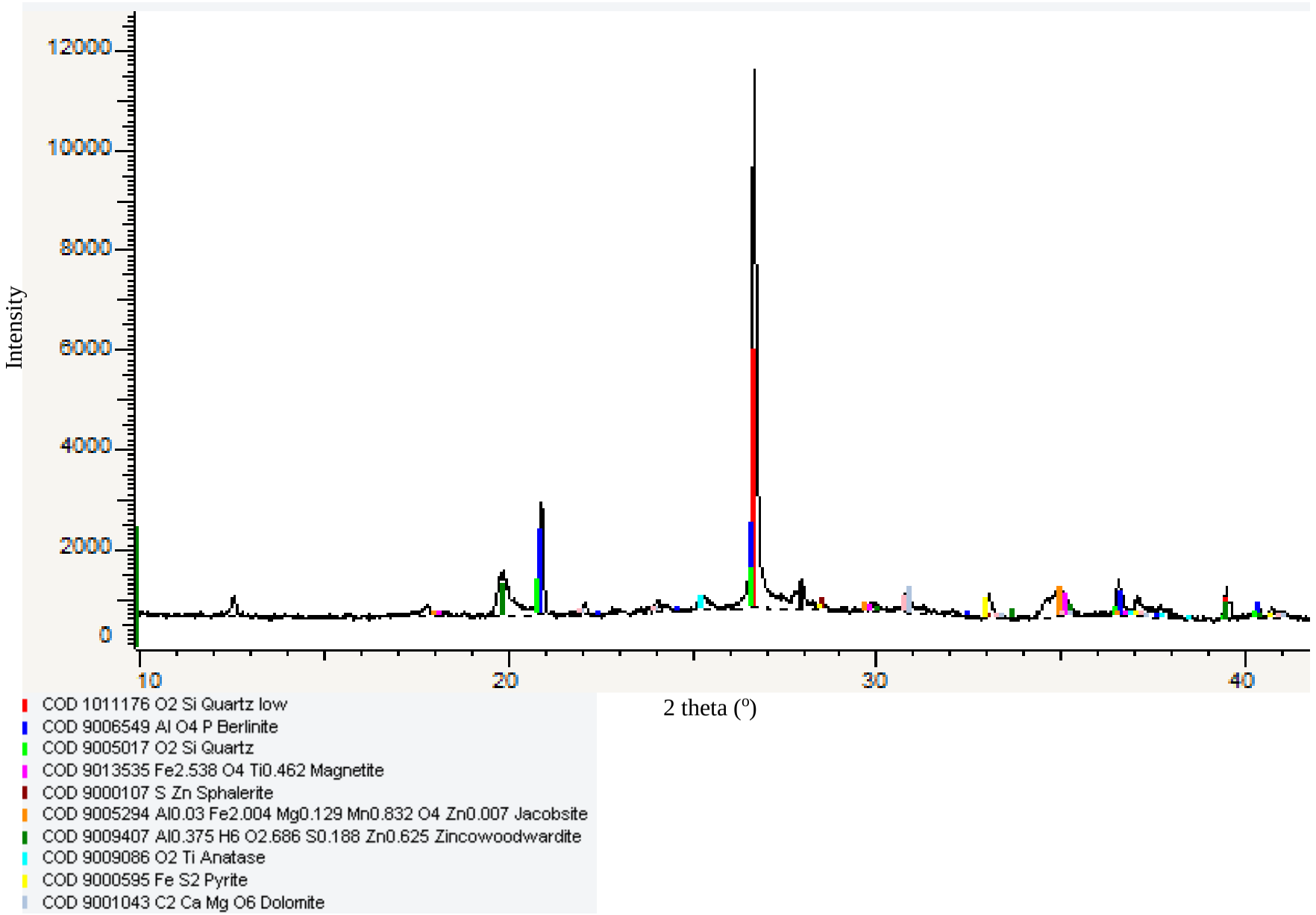

Figure 24. 2Θ spectrum for the Neal (Floyd) Shale, Greene County

Organic Geochemistry

Chattanooga Shale, Greene County

Full scan gas chromatography mass spectroscopy (GC-MS) results indicate the presence of hentriacontanone ($C_{31}H_{62}O$) in the Chattanooga Shale, Greene County in well permit #3800 (Figure 25). Hentriacontanone was identified by comparison of idealized (standard) and actual spectral signatures of extracted organic compounds (Figure 26). The spectral signature shows that the extracted organics are dominated by compounds with m/z ratios of 71, 85, 194, 211, 239, 255, 267, 281, 295, 309, and 323 (Figure 27). Spectral signatures of both light and heavy sections of the hydrocarbon match very well, implying the stability of hentriacontanone through geologic time (Figure 26, 27). Full scan gas chromatograph shows that organic compounds with very light molecular weight (< 9 minutes) are not presented (Figure 28), indicating this group of light hydrocarbon has been degraded in the geologic past. The complete gas chromatogram (Figure 28) shows the occurrence of many high peaks between 9-40 minutes, with highest-intensity peaks associated with heavier compounds in the 34-36 minute range.

For production and environmental concerns identification of reservoir hydrocarbons is essential. Gas migration from reservoir rock to overlying groundwater is of major concern. This study indicates that gas chromatographs of specific organic compounds present in contaminated groundwater may fingerprint their initial sources in shales. With regulations becoming stricter, in regards to groundwater contamination from the hydraulic fracturing process, geochemical correlation and fingerprinting of specific organic compounds (i.e., biomarkers) within shales will allow for responsibility to be placed if gas migration does occur.

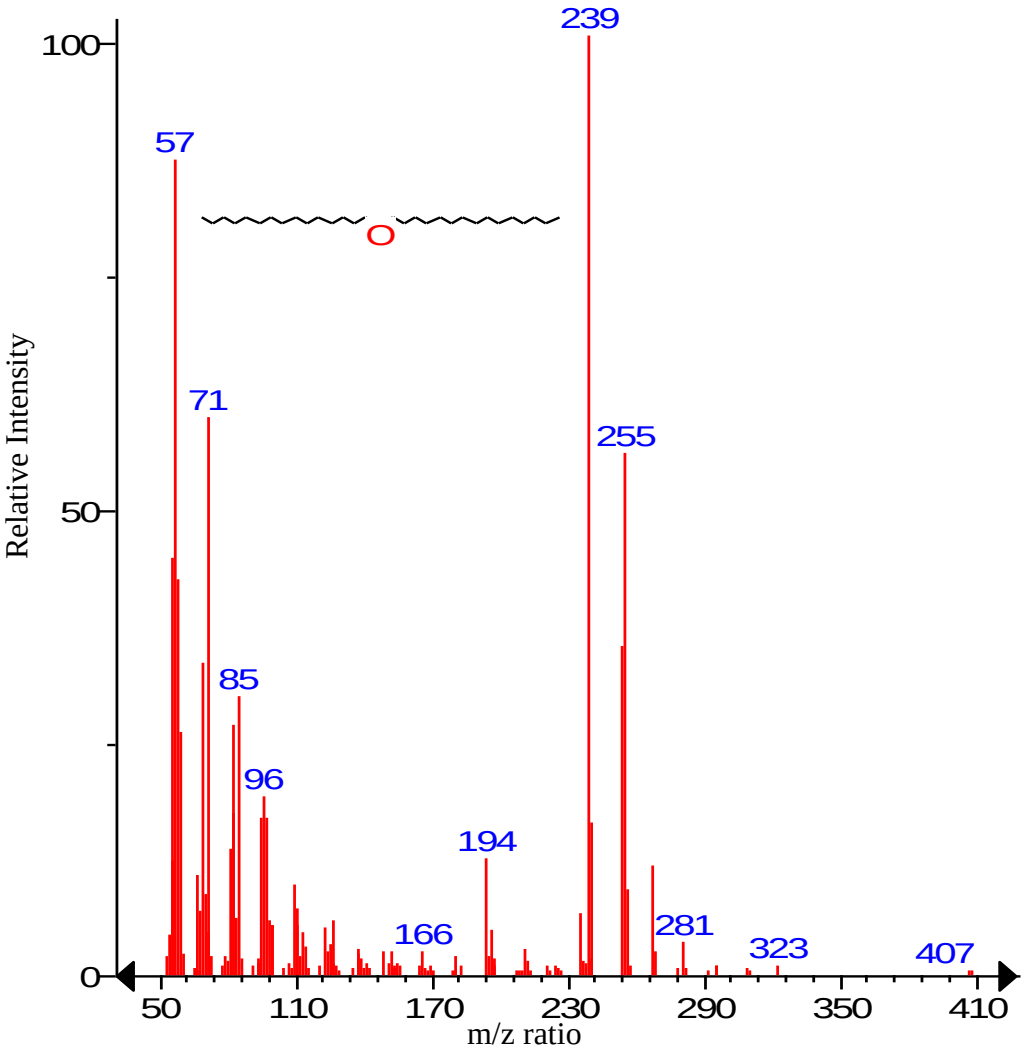

Figure 25. Hydrocarbon compounds and structure (top center) with specific m/z ratios identified, hentriacontanone $C_{31}H_{62}O$, in the Chattanooga Shale, Greene County, well permit # 3800.

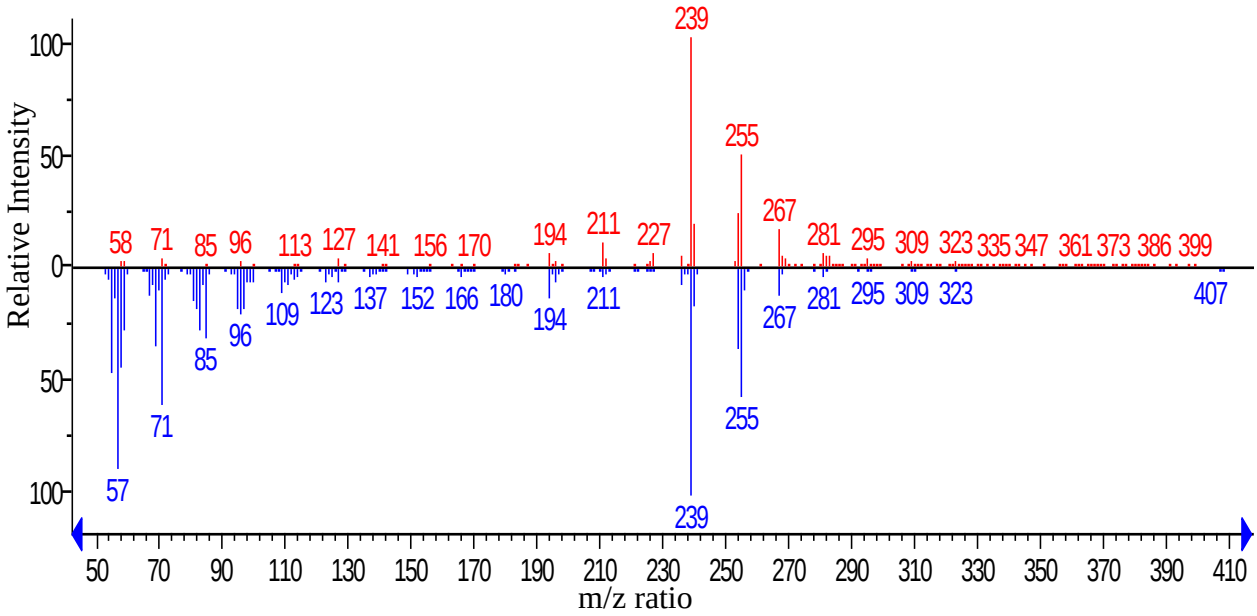

Figure 26. Standard spectral signature of hentriacontanone (blue) and actual spectral signature of organics extracted from the Chattanooga Shale, Greene County, well permit # 3800 (red).

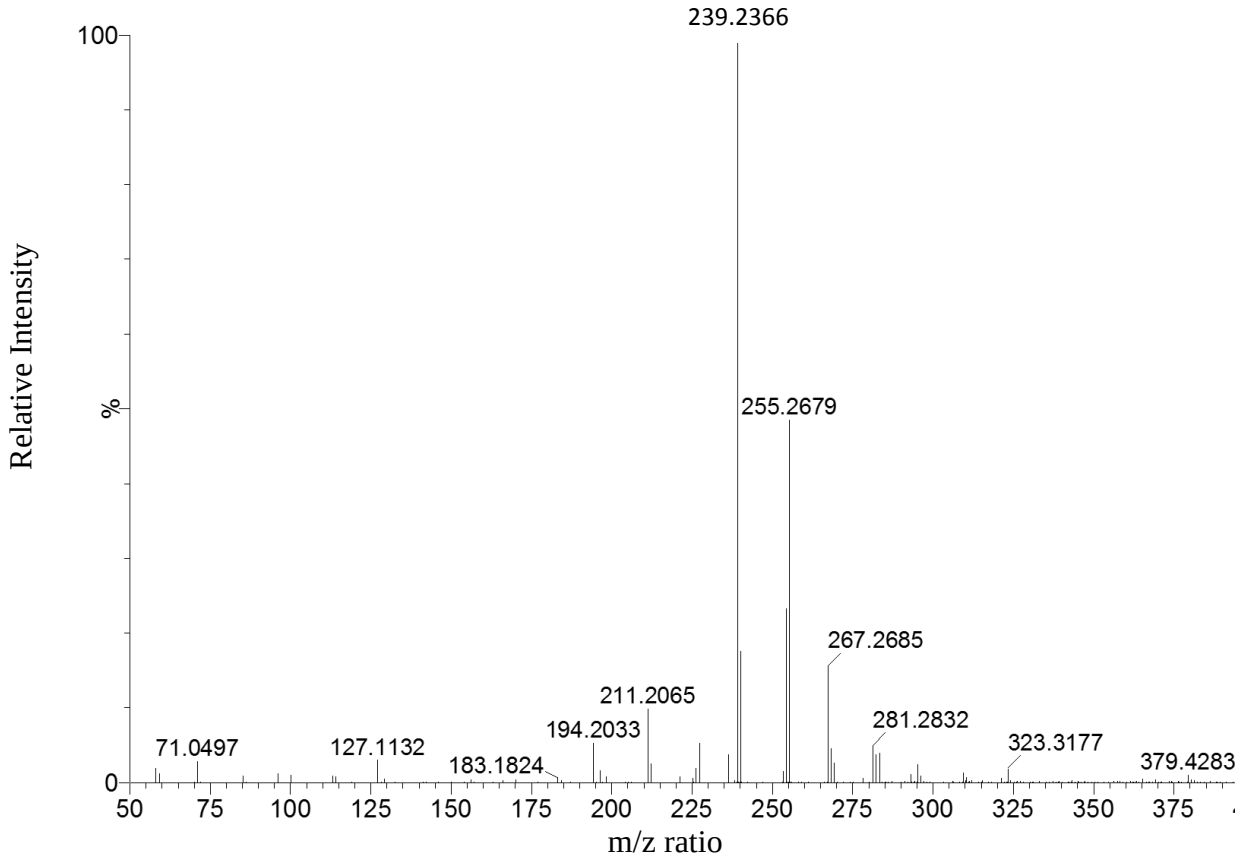

Figure 27. Mass to charge ratio (m/z) of organics extracted from the Chattanooga Shale, Greene County, well permit # 3800.

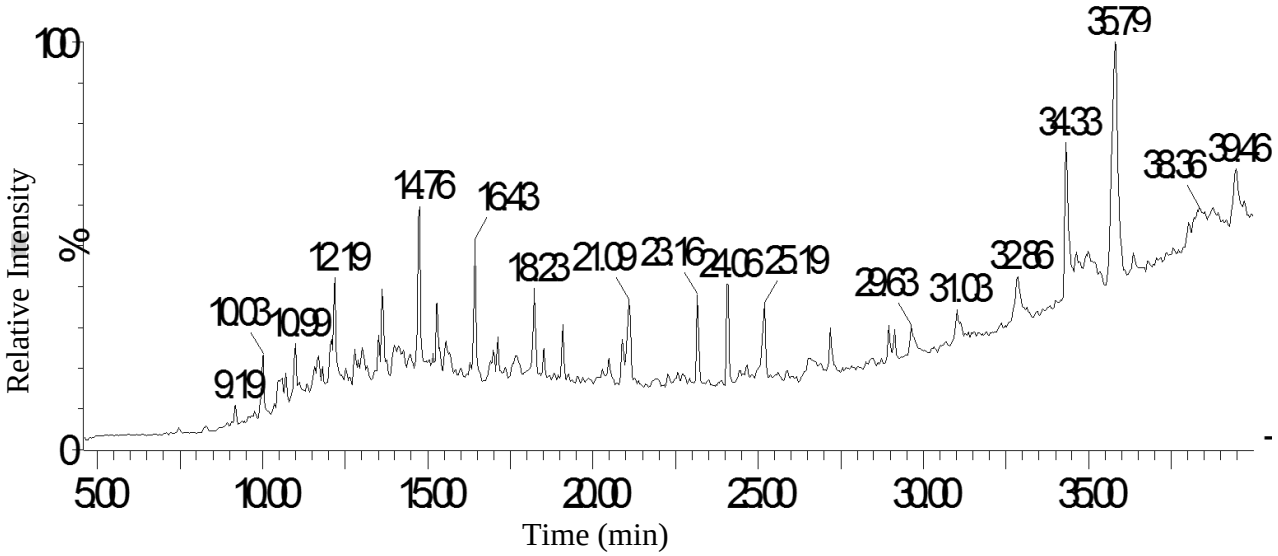

Figure 28. Full Scan gas chromatograph of extracted organics from the Chattanooga Shale, Greene County, well permit # 3800. The time peaks occur labeled atop of individual peaks.

Conasauga Shale, St. Claire County

Full scan GC-MS results for the Conasauga Shale, St. Claire County, well permit # 15720, indicate the presence of the hydrocarbon docosenamide ($C_{22}H_{43}NO$) (Figure 29). Docosenamide was identified through comparison of measured hydrocarbon spectral signatures and standard spectrum in the database library (Figure 30). The spectral signature shows that the extracted organics are dominated by compounds with mass to charge ratios (m/z) of 59, 72, 126, 320, and 337 (Figure 31). Full scan spectral also show the absence of hydrocarbon compounds with very light molecular weight (< 9 minutes), indicating this group of light hydrocarbon has been degraded in the geologic past (Figure 32). Other lighter sections of the hydrocarbon compounds (between 9 to 15 minutes) are still prevalent in this sample, indicating this group of hydrocarbon has remained stable since Late Cambrian (Figure 32). The remainder of the chromatograms shows presence of heavier compounds, as indicated by the occurrence of highest peaks after 15 minutes.

Degradation of petroleum hydrocarbons by natural microbes is a complex process that depends on the nature of the hydrologic environments and the composition of the hydrocarbons present. Preferential degradation of the lighter sections of the hydrocarbon compounds will occur when microbial interactions occur (Natter et al., 2012). With the lighter sections of hydrocarbon compounds (between 9 and 15 minutes) still prevalent it implies that little or no microbial degradation occurred in low-permeability shales.

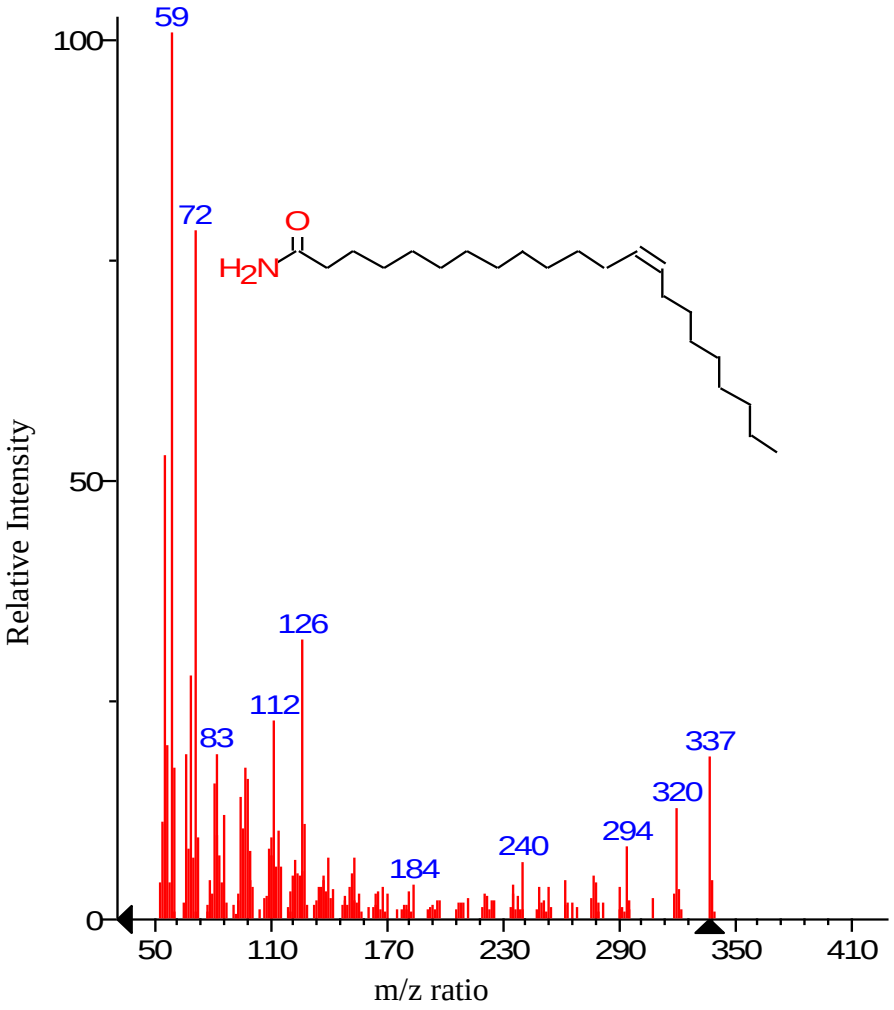

Figure 29. Hydrocarbon compounds and structure (top center) with specific m/z ratios identified, docosenamide $C_{22}H_{43}NO$, in the Conasauga Shale, St. Claire County, well permit # 15720.

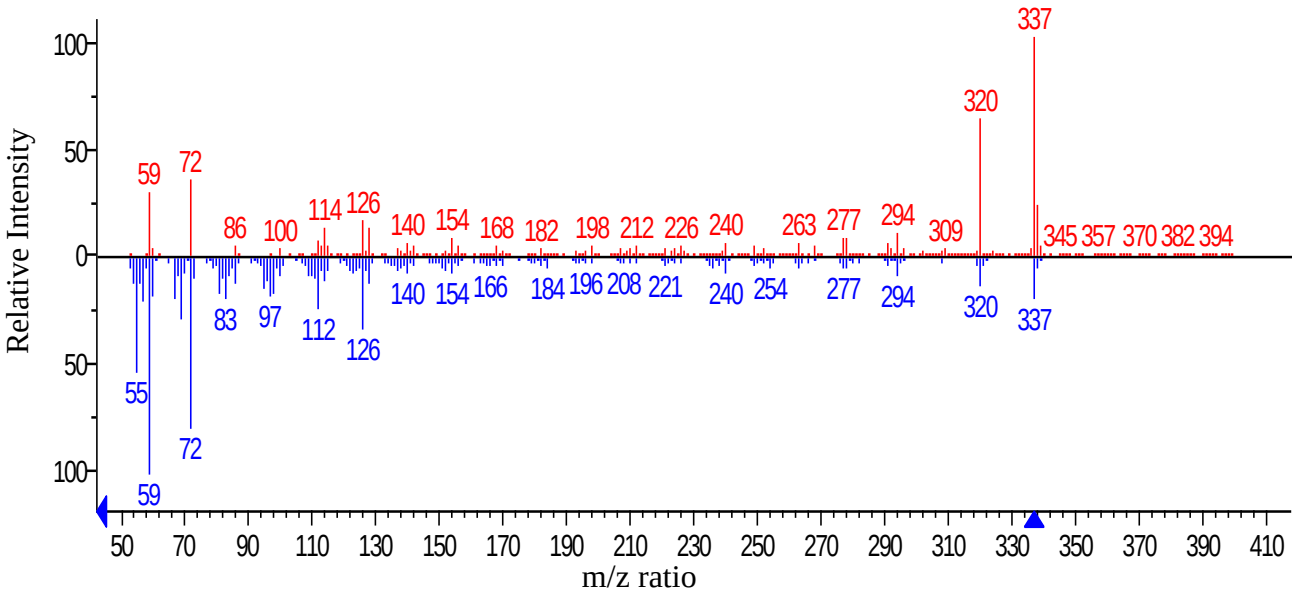

Figure 30. Standard spectral signature of docosenamide hydrocarbon (blue), and actual spectral signature of hydrocarbon extracted from the Conasauga Shale, St. Claire County, well permit # 15720 (red).

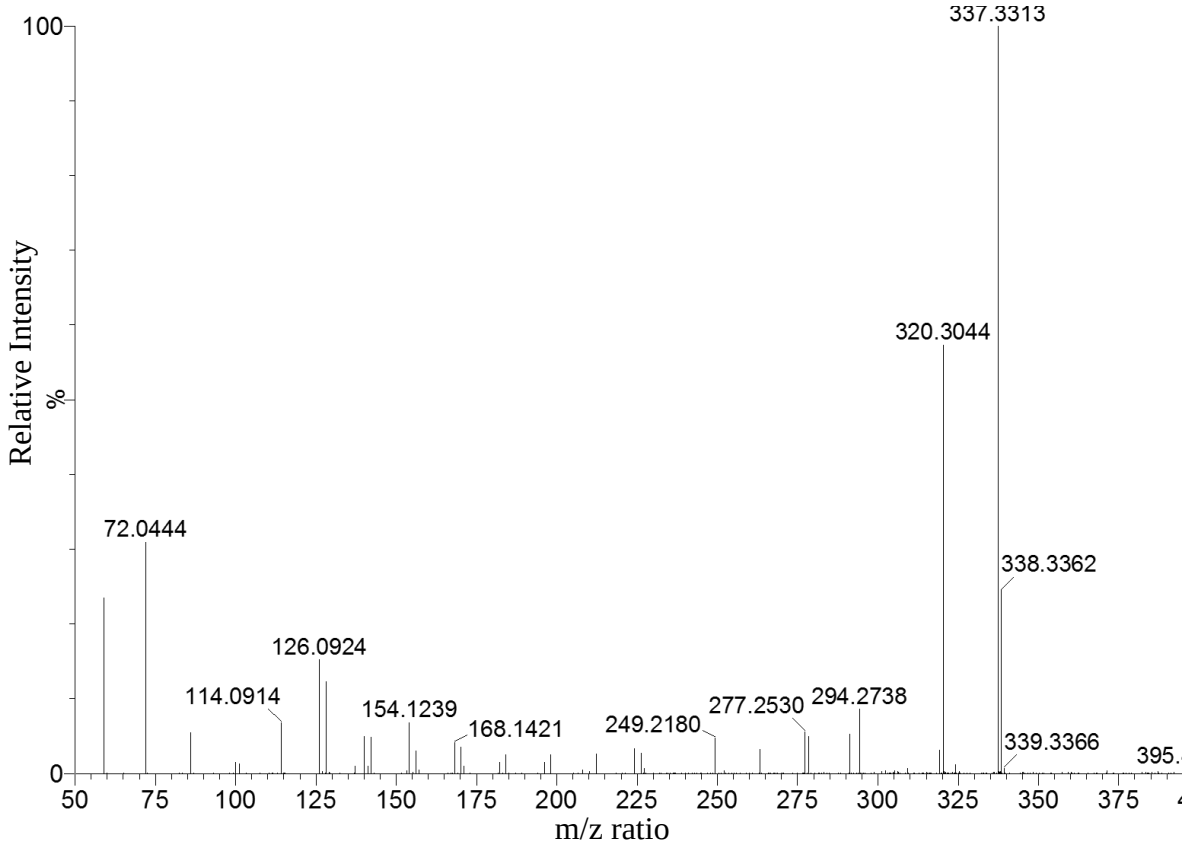

Figure 31. Mass to charge ratios of major organics extracted from the Conasauga Shale, St. Claire County, well permit # 15720.

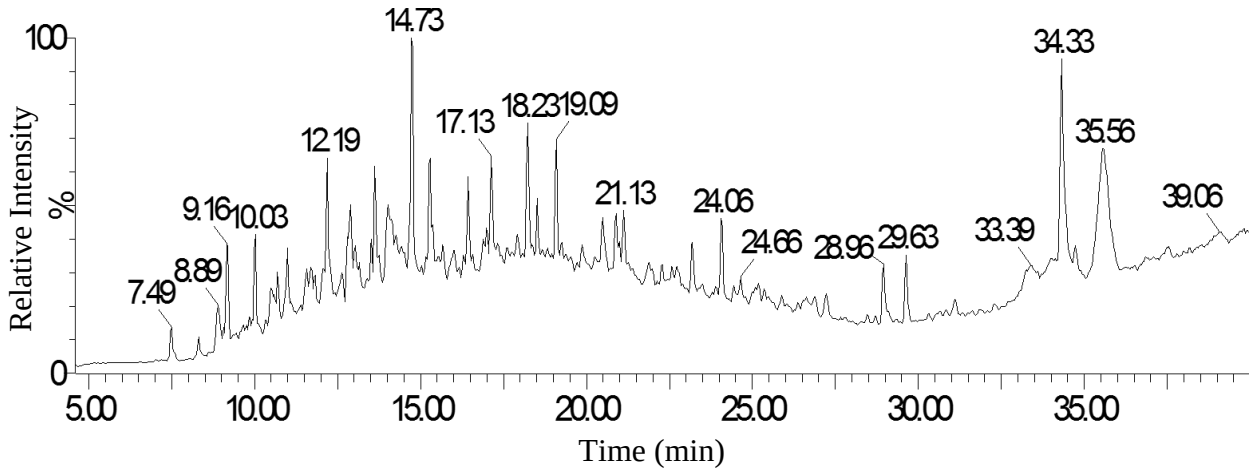

Figure 32. Full scan gas chromatogram of extracted organics from the Conasauga Shale, St. Claire County, well permit # 15720. The time peaks occur is labeled on top of individual peaks.

Neal (Floyd) Shale, Pickens County

Full scan GC-MS results for the Neal (Floyd) Shale, Pickens County, well permit # 14289, indicate the presence of tetradecandioic acid, bis(trimethylsilyl) ester ($C_{20}H_{42}O_4Si_2$) (Figure 33). Tetradecandioic acid, bis(trimethylsilyl) ester was identified by a comparison of the spectral signature of the hydrocarbon to an idealized hydrocarbon spectral signature from the database library (Figure 34). Strongest correlations between the ideal spectral signature and actual spectral signature are present at m/z ratios of 204 and 387 (Figure 34). The spectral signature shows that the extracted organics are dominated by compounds with mass a charge ratio of 368 (Figure 35). Hydrocarbon compounds with very light molecular weight (< 7 minutes) are not presented in the chromatograph, indicating the group of the lightest hydrocarbon has been degraded in the geologic past (Figure 36). The complete gas chromatogram has a high percentage of relatively lighter compounds, as indicated by the occurrence of high peaks between 6 and 16 minutes, whereas the remainder of the chromatogram shows multiple high-intensity peaks representing heavier compounds over the 18-36 minute range (Figure 36).

Degradation of the lightest section of hydrocarbon compounds in Neal (Floyd) Shale would be the result of microbial interactions. It is these interactions that are responsible for the non-peak sections of the chromatograph from 0 to 7 minutes (Figure 36). This line of evidence suggests that microbial degradation had occurred mostly to the lightest organic compounds in the past.

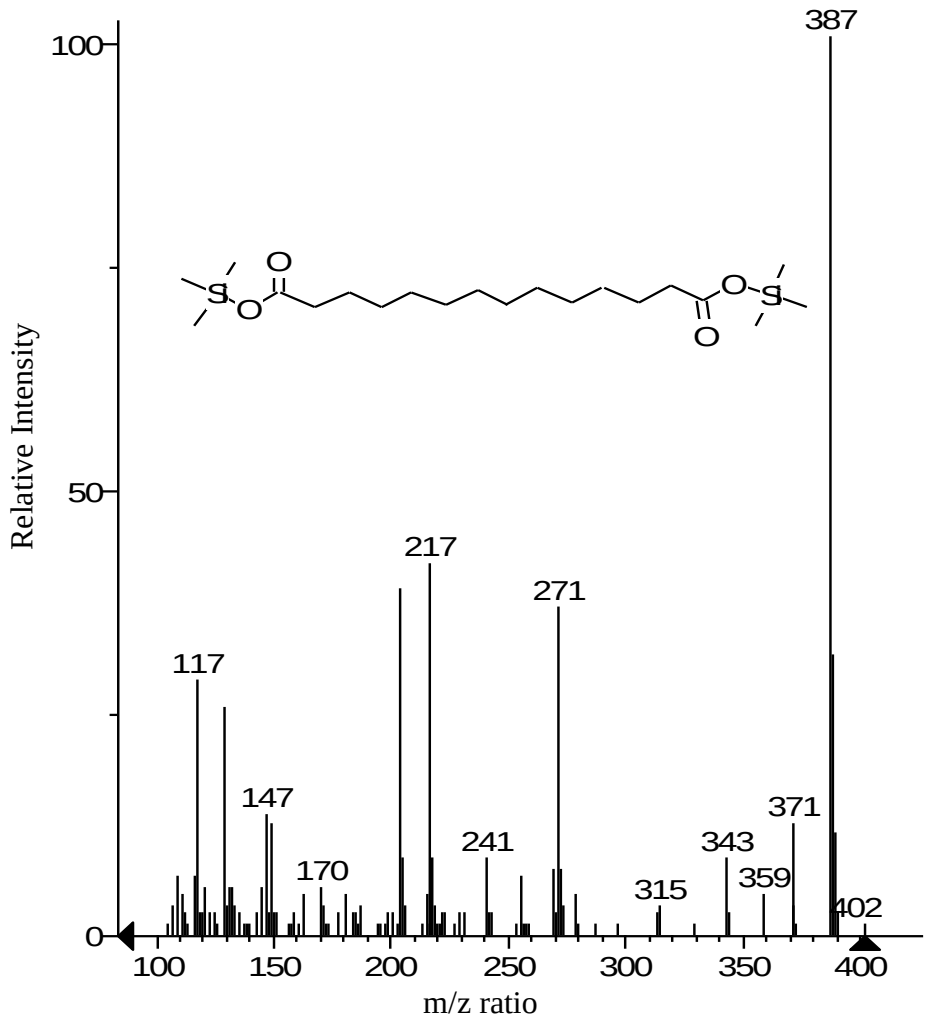

Figure 33. Hydrocarbon compounds and structure (top center) with specific m/z ratios identified, tetradecandioic acid, bis(trimethylsiyl) ester $C_{20}H_{42}O_4Si_2$, in the Neal (Floyd) Shale, Pickens County, well permit # 14289.

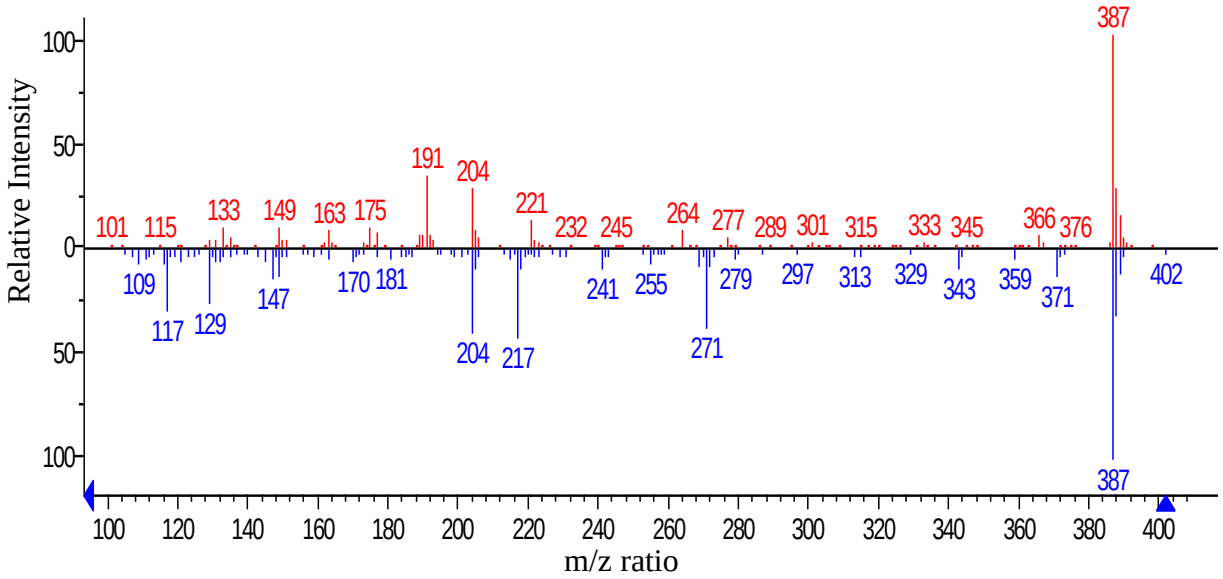

Figure 34. Standard spectral signature (blue) of tetradecandioic acid, bis(trimethylsilyl) ester, and actual spectral signature of organic compounds (red) extracted from the Neal (Floyd) Shale, Pickens County, well permit # 14289.

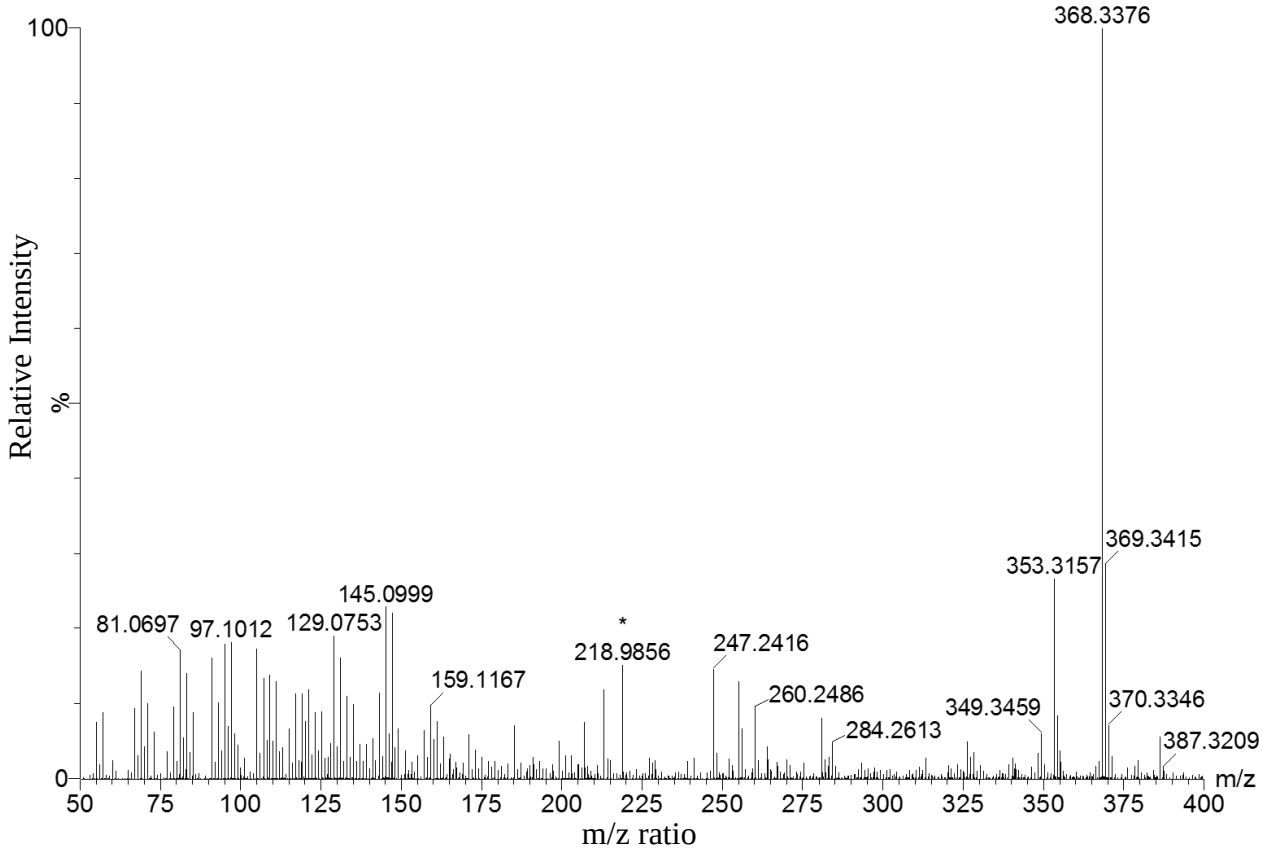

Figure 35. Mass to charge ratio (m/z) of organics extracted from the Neal (Floyd) Shale, Pickens County, well permit # 14289.

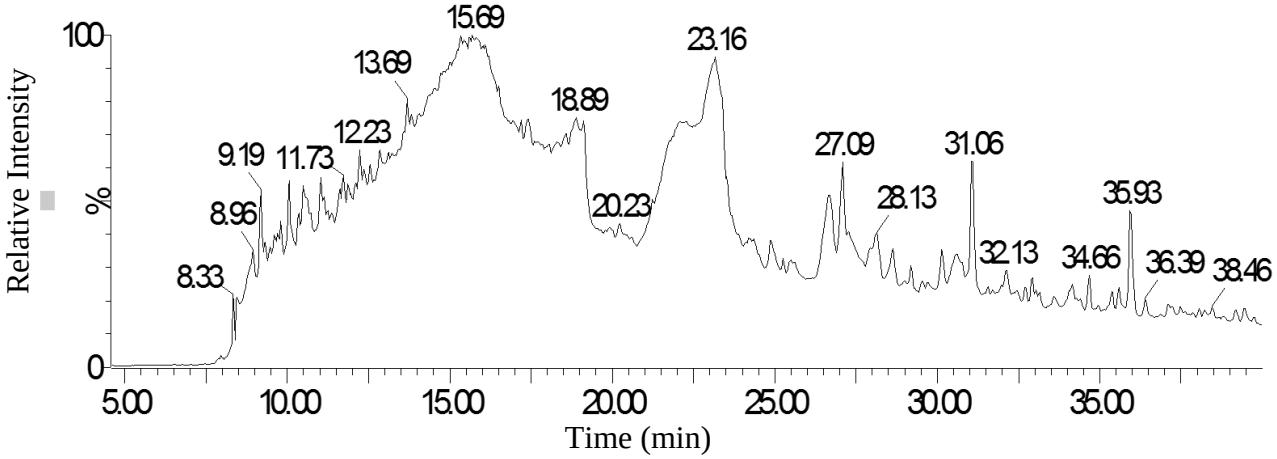

Figure 36. GC-MS full scan chromatograph of the Neal (Floyd) Shale, Pickens County, well permit # 14289.Time peaks occurred labeled atop of individual peaks.

Petroleum Biomarkers

Special geochemical biomarkers such as terpanes/hopanes (m/z 191) and steranes (m/z 217 and m/z 218) can be used to trace the source and biotransformation of hydrocarbons in sedimentary rocks. GC-MS single ion mode (SIM) analysis for m/z ratios of 191, 217, and 218 were conducted on organic compounds extracted from the Neal (Floyd) Shale, Pickens County, Chattanooga Shale, Greene County, and the Conasauga Shale, St. Claire County. From this, geochemical correlations of organic carbon sources can be conducted.

Chattanooga Shale, Greene County, Well Permit # 3800

The m/z 191gas fragmentograph for the Chattanooga Shale indicate large peaks occurring at 4.0, 5.5, 8, 9.1, 9.5, and 11.0 minutes (Figure 37a). The largest abundance of m/z 191 is located at 4 minutes with a relative intensity over 1000. Abundances in the remaining peaks vary from 100 to 550 above background. This gas fragmentograph is analogous to the m/z 191 gas fragmentograph for the Conasauga Shale (Figure 37b). The presence of terpanes/hopanes compounds after 18 minutes forms a plateau pattern in the gas fragmentograph of the Chattanooga Shale (Figure 37a). The main peaks in this gas fragementograph, abundances of m/z 191, and the plateau from 18 to 23.5 minutes all match those of the Conasauga Shales (Figure 37b).

Results for the m/z 217 gas fragmentograph show isolated peaks with very low intensity throughout the entire spectrum (Figure 38a-b). Signatures of m/z ratio 217 throughout the entire gas fragmentograph are very low with a maximum abundance of three above background values. The presence of steranes compounds after 19 minutes for the Chattanooga Shale (Figure 38a)

forms a plateau pattern in the gas fragmentograph. The main peaks in this gas fragementograph, abundances of m/z 217, and the plateau from 9 to 10.5 minutes match those of the Conasauga Shales (Figure 38b).

Results for m/z ratio 218 shows there are limited peaks with significant intensity present throughout the entire gas fragromentograph (Figure 39a). Abundances are very low, with a maximum of four above background values. A plateau exists from 9 to 10 minutes and after 19 minutes. Results of this gas fragmentograph are similar to that seen in the Conasauga Shale (Figure 39b).

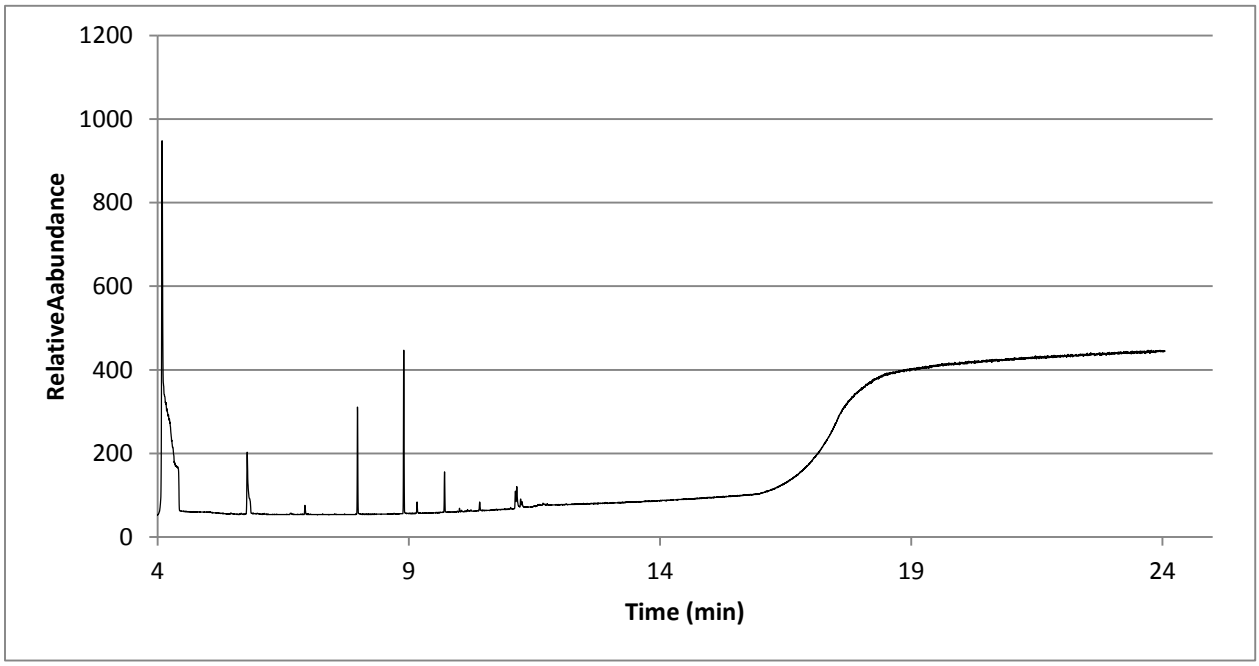

Figure 37a. Gas fragmentograph of m/z 191 petroleum biomarker from the Chattanooga Shale, Greene County.

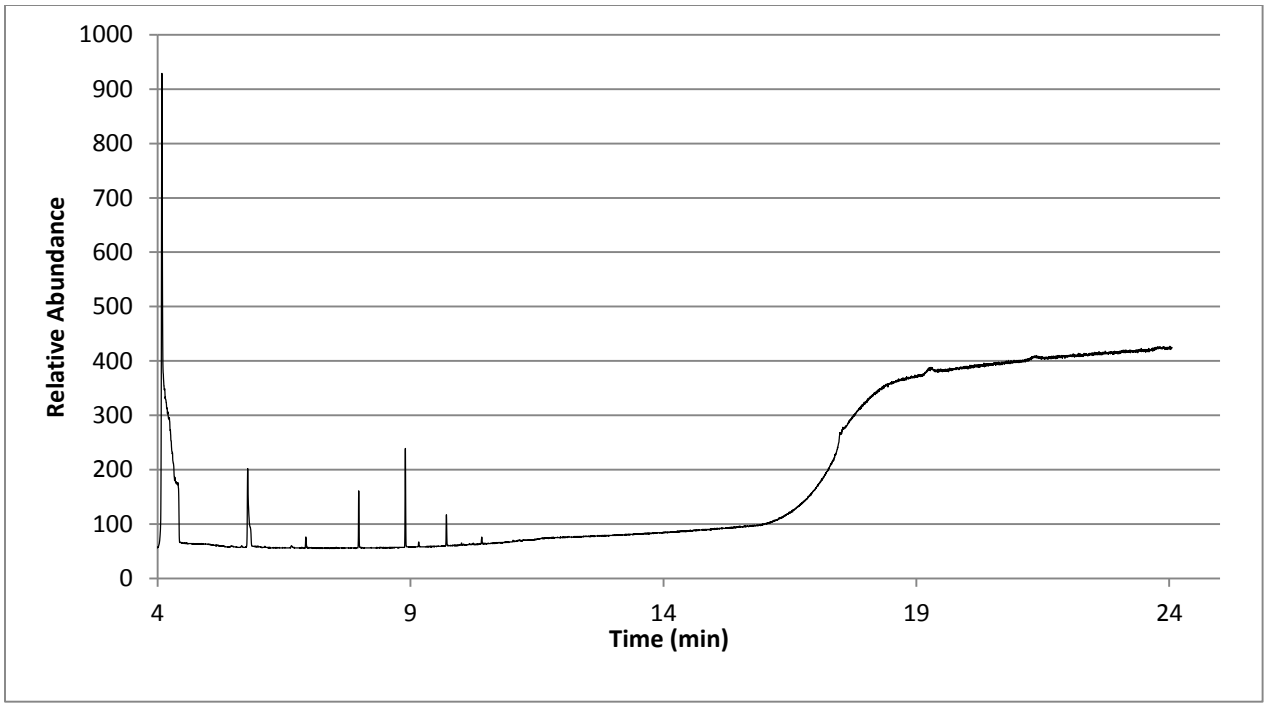

Figure 37b. Gas fragmentograph of m/z 191 petroleum biomarker from the Conasauga Shale, St. Claire County.

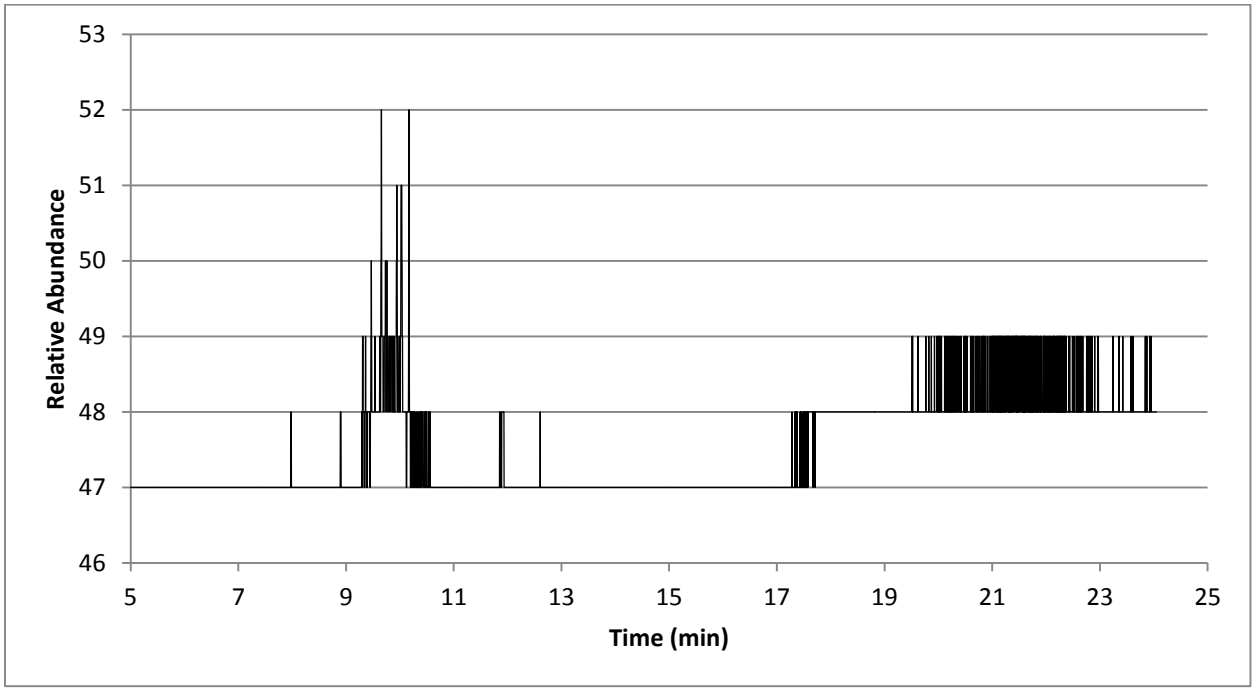

Figure 38a. Gas fragmentograph of m/z 217 petroleum biomarker from the Chattanooga Shale, Greene County.

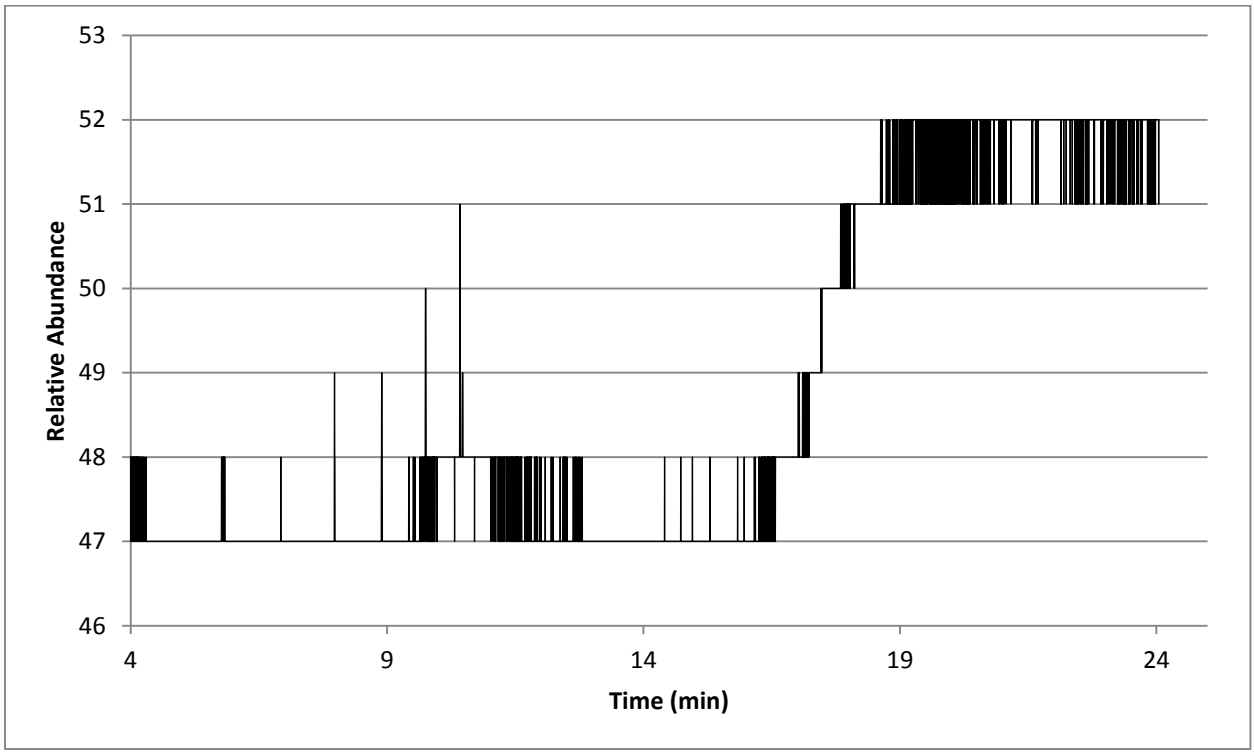

Figure 38b. Gas fragmentograph of m/z 217 petroleum biomarker from the Conasauga Shale, St. Claire County.

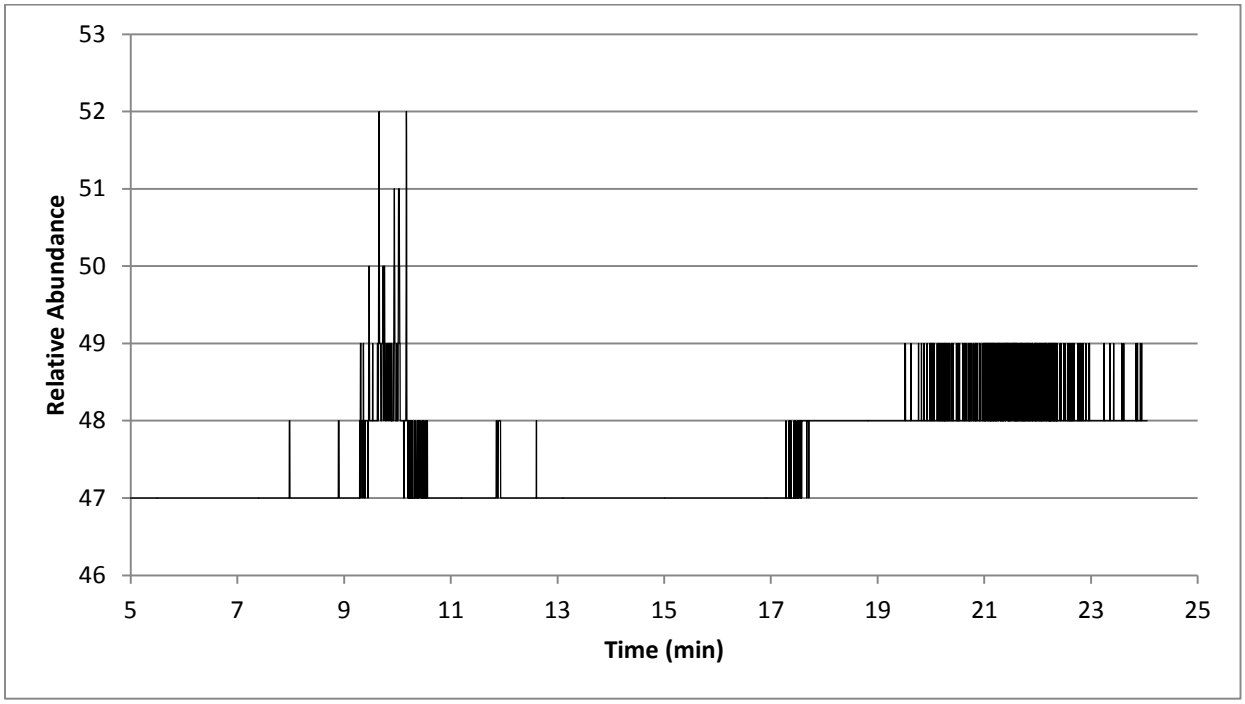

Figure 39a. Gas fragmentograph of m/z 218 petroleum biomarker from the Chattanooga Shale, Greene County.

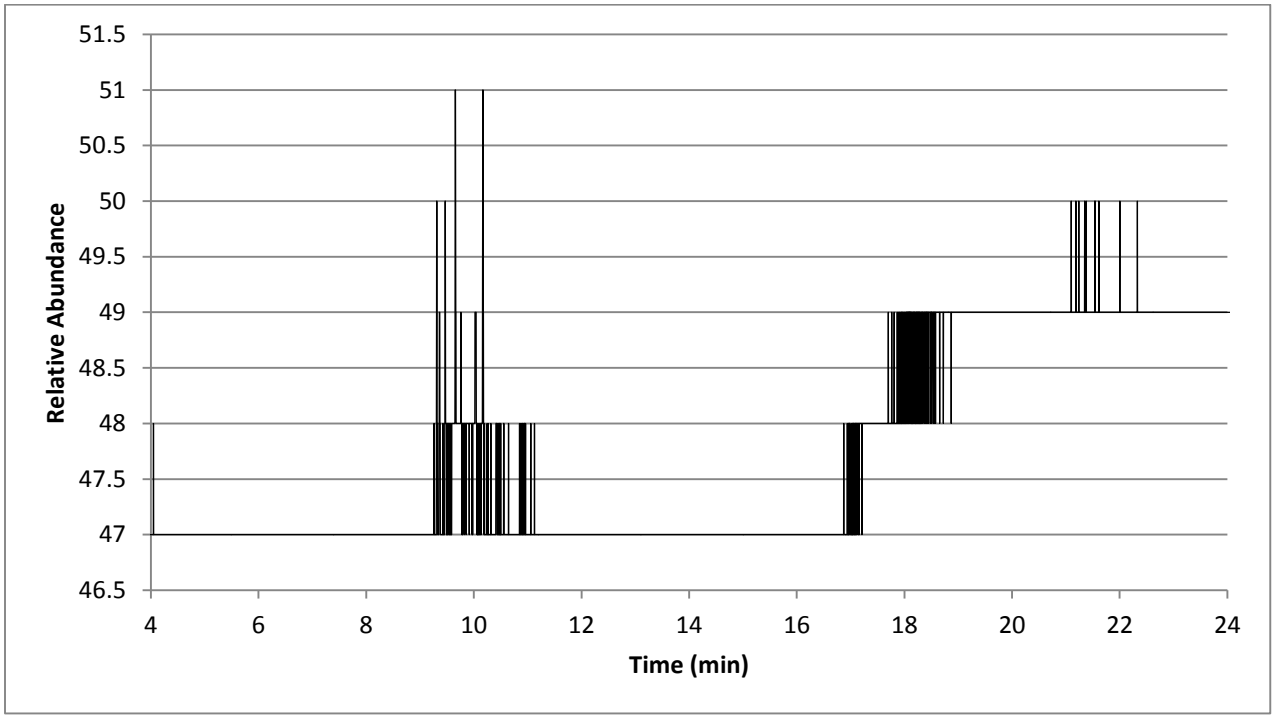

Figure 39b. Gas fragmentograph of m/z 218 petroleum biomarker from the Conasauga Shale, St. Claire County

Conasauga Shale, St. Claire County, Well Permit # 15720

The gas fragmentograph m/z ratio 191 for the Conasauga Shale, St. Claire County reveals high intensity spikes at 4.0, 5.5, 8.0, and 9.25 minutes (Figure 37b). The largest m/z 191 abundance is found at 4.0 minutes with relatively intensity of 1000. Other major spikes in the m/z 191 fragmentograph range from 225 to 325. The presence of other terpanes/hopanes compounds after 18 minutes forms a plateau pattern in the gas fragmentograph. This gas fragmentograph matches the gas fragmentograph m/z 191 for the Chattanooga Shale (Figure 37a).

Gas fragmentograph results for m/z ratios of 217 and 218 indicate very low abundances of sterane biomarkers for the entirety of the spectrum (Figures 38b, 39b). The largest abundances are only 1-2 above the background values. The largest spike in the fragmentograph occurs from 9 minutes to 11 minutes. These gas fragmentographs are similar to those of the Chattanooga Shale (Figures 38, 39), which also show very low abundances of sterane biomarkers.

Similarities in all three biomarker gas fragmentographs of m/z 191, 217, and 218 (Figure 37 a-b, 38a-b, 39 a-b) suggest that the Chattanooga Shale and Conasauga Shale share the same source of organic carbon.

Neal (Floyd) Shale, Pickens County, Well Permit # 14289

The gas fragmentograph m/z 191 of the Neal (Floyd) Shale (Figure 40) indicates abundances of terpanes/hopanes biomarkers from 8 to 20 minutes. There is a cyclic exponentially decaying nature to the abundance of m/z 191 starting at 8 minutes and ending at 20 minutes. Higher intensity of peaks is present between 8 and 12 minutes. The m/z 191 gas fragmentograph of Neal (Floyd) Shale, showing more distinct, high intensity peaks of different compounds, varies greatly those from those of the Conasauga Shale and Chattanooga Shale (Figure 37)

The gas fragmentograph of m/z ratio 217 indicates significant enrichment in sterane biomarkers from 10 to 14 minutes (Figure 41). High intensity peaks also appear at 8.0, 8.5, and 19.5 minutes. The lighter section of the sterane compounds, less than 8 minutes, are void of peaks. Gas fragmentograph of m/z 217 in the Neal (Floyd) Shale, show higher abundances of sterane compounds, which is markedly different from those of the Conasauga Shale and Chattanooga Shale (Figure 38).

The gas fragmentograph of m/z ratio 218 indicate significant enrichment at 12 minutes (Figure 42). High intensity peaks also appear at 9.5-10, 11, 12.8, and 14.5 minutes. Lighter sections of the sterane compounds, less than 8 minutes, are devoid of peaks. The general gas fragmentograph pattern, showing enrichment of sterane biomarkers, is significantly different from those of the Conasauga Shale and Chattanooga Shale (Figure 39).

This study shows that petroleum biomarkers of terpanes/hopanes (m/z 191) and steranes (m/z 217 and m/z 218) can be analyzed using gas chromatography to fingerprint sources of

organic matter in shales. Both GC-MS full-scan and single ion analyses provide enhanced specificity and peak intensity that can separate diagnostic biomarkers. Significant differences in all three biomarkers exist between the younger Neal (Floyd) Shale and two older Conasauga Shale and Chattanooga Shale in the Black Warrior Basin. This is an indication that while the Conasauga Shale and Chattanooga Shale share common sources of organic carbon, those in the younger Neal (Floyd) Shale are likely derived from a different source (Carroll et al., 1995).

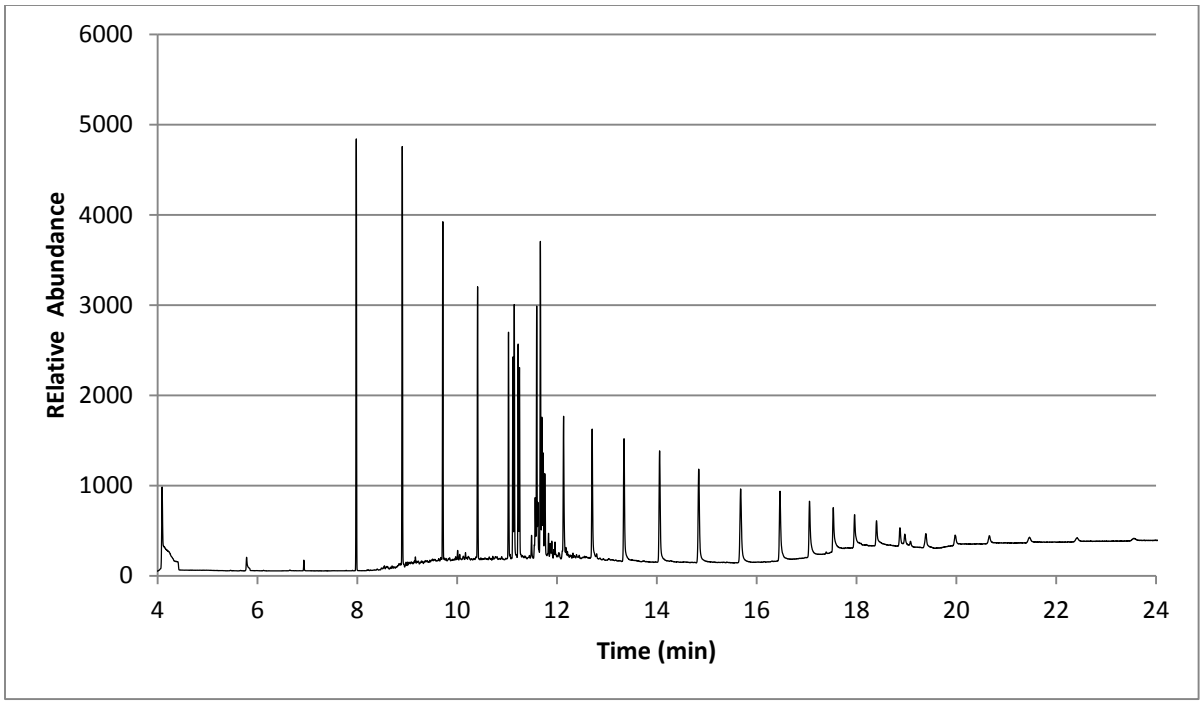

Figure 40. Gas fragmentograph of m/z 191petroleum biomarker from the Neal (Floyd) Shale, Pickens County.

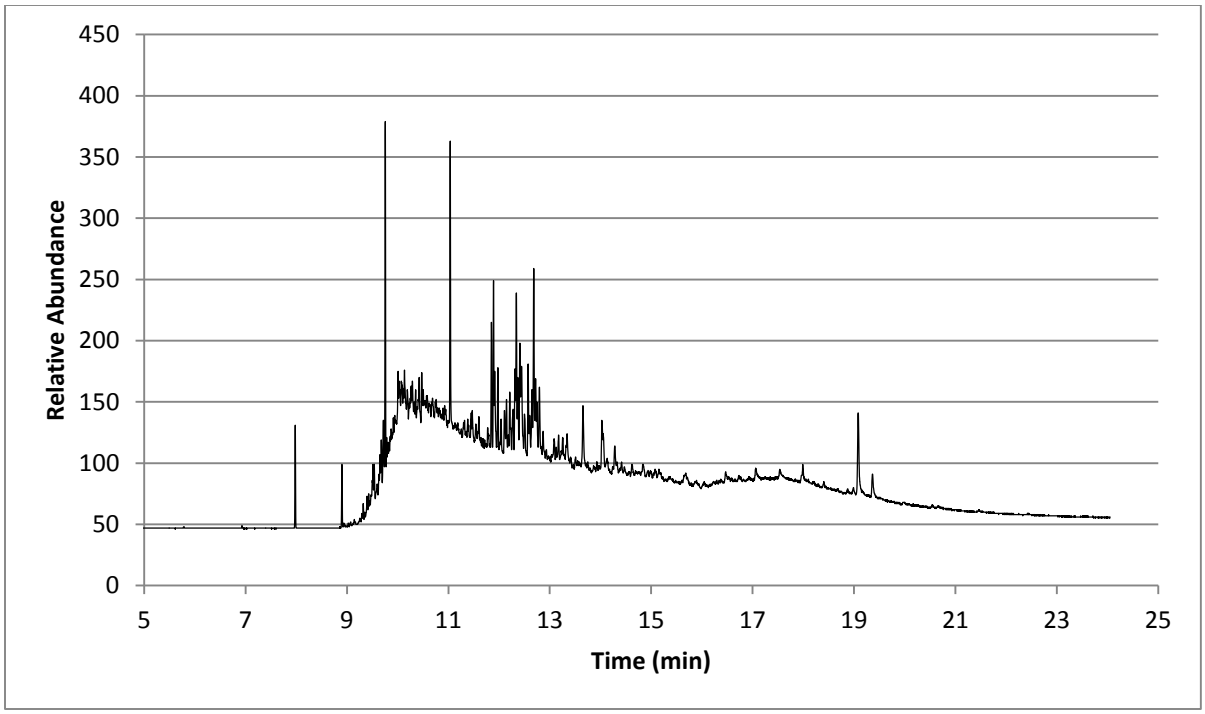

Figure 41. Gas fragmentograph of m/z 217 petroleum biomarker from the Neal (Floyd) Shale, Pickens County.

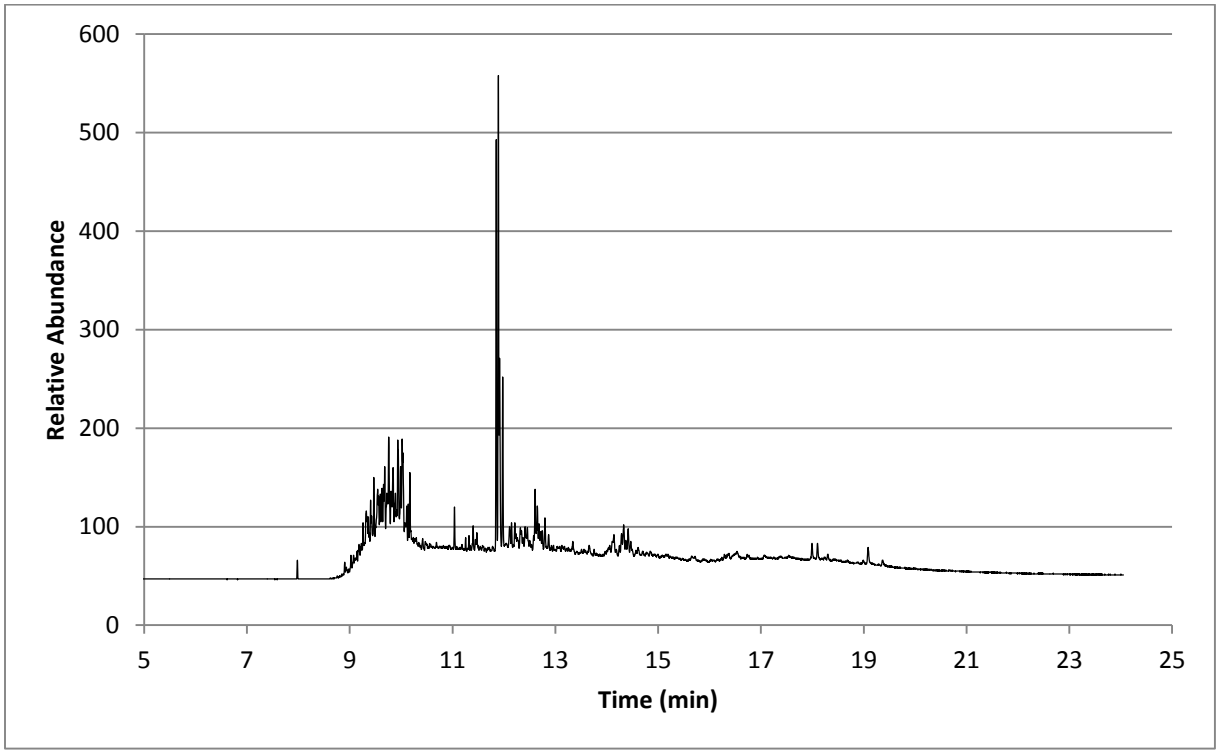

Figure 42. Gas fragmentograph of m/z 218 petroleum biomarker from the Neal (Floyd) Shale, Pickens County.

Reconstruction of Hydro-Stratigraphic Sections

Gamma ray logs collected from 31 of the 39 wells were correlated using PETRA software (Figure 43, Table 6). Counties in Alabama for this correlation included Lamar, Fayette, Tuscaloosa, Pickens, Greene, Hale, Sumter, and Jefferson Counties. The panel diagrams generated by Petra correlate the tops of the Neal (Floyd) Shale and Chattanooga Shale. The spatial distribution of correlated three-dimensional surfaces is presented in Figure 44. Three-dimensional surfaces, representing the physical tops of the Neal (Floyd) Shale and Chattanooga Shale, were created by correlating geophysical gamma logs (Table 6) in conjunction with previously interpreted well logs, and geologic sections (Figure 44 a-d). These surfaces present stratigraphic framework and give a visual representation of spatial distribution of shales, from a head on view of both gas-shales, as they progress into the depositional center of the Black Warrior Basin (Figure 44 a-d).

The Chattanooga shale is characterized by relatively high gamma ray counts, or higher radioactivity, as compared to the lower values seen in the overlying Neal (Floyd) Shale. Also, surfaces of both shales are deepen toward the southeast margin of the basin where it boarders the Appalachian thrust system. This reconstructed stratigraphy and basin geometry is consistent with the previous geologic interpretation of the basin (Pashing et al., 2011).

Along the south-eastern margin of the basin a large deposition center is present, as recognized by a large depression in the surfaces. A minor deposition center is located along the eastern margin of the basin (Figure 44 a-d).

Missing from this surface model is the deeper Conasuaga Formation. There were only a few wells drilled into the appropriate depth and thus limited geophysical logs are available to allow stratigraphic reconstruction of the Consasuage Formation within the Black Warrior Basin.

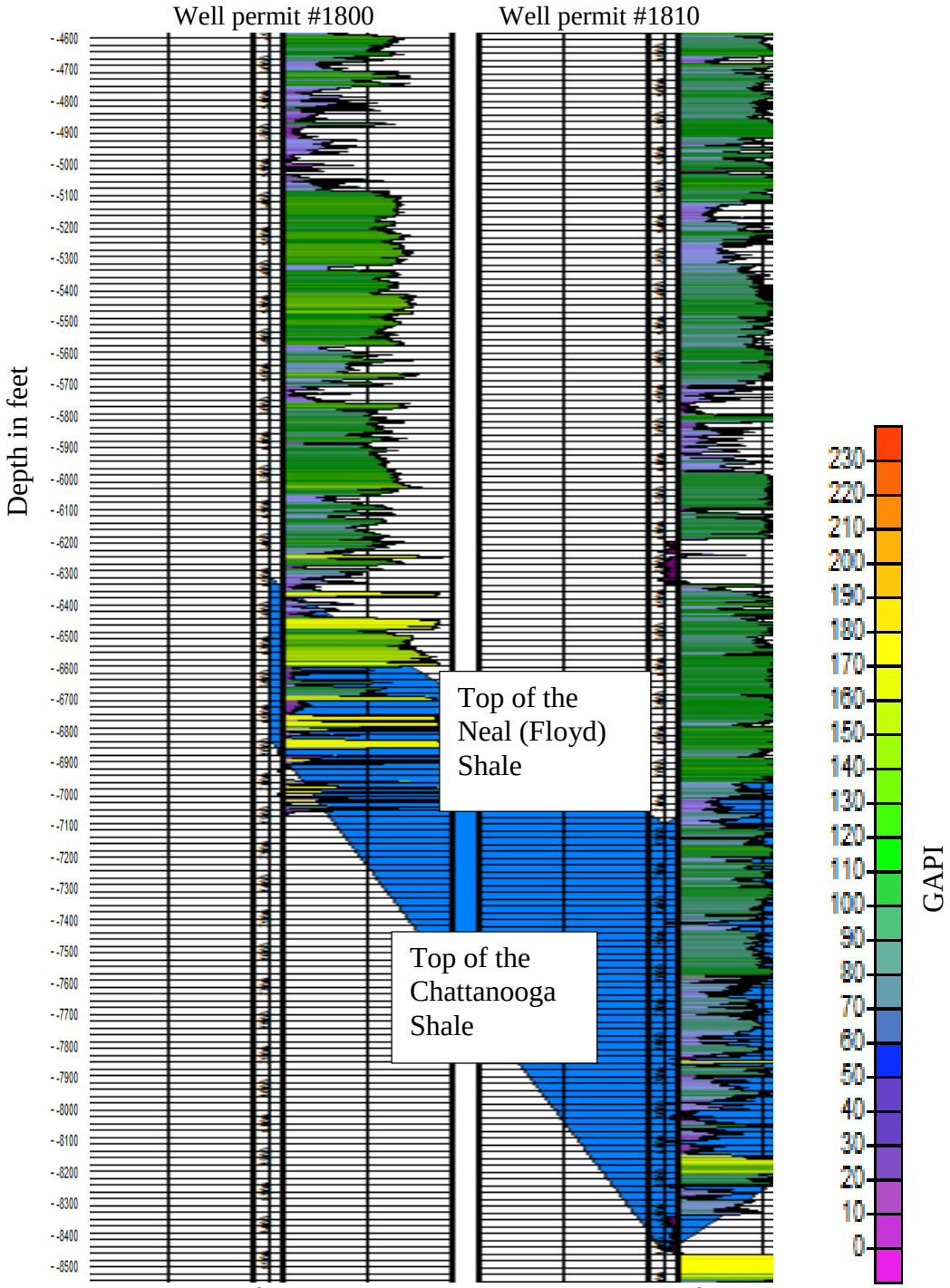

Figure 43. Panel diagram of wells with permit number's 1800 (left), and1810 (right) correlating the top of the Neal (Floyd) Shale and top of the Chattanooga Shale. Area above the top of the Neal (Floyd) Shale contains units not correlated in geophysical logs. Blue area corresponds to the body of the Neal (Floyd) Shale and the Tuscumbia Limestone and Fort Payne Chert undifferentiated. Colors seen in the wells indicate measured gamma ray intensities of the individual wells (scale on right of diagram). Horizontal scale 1:10,000.

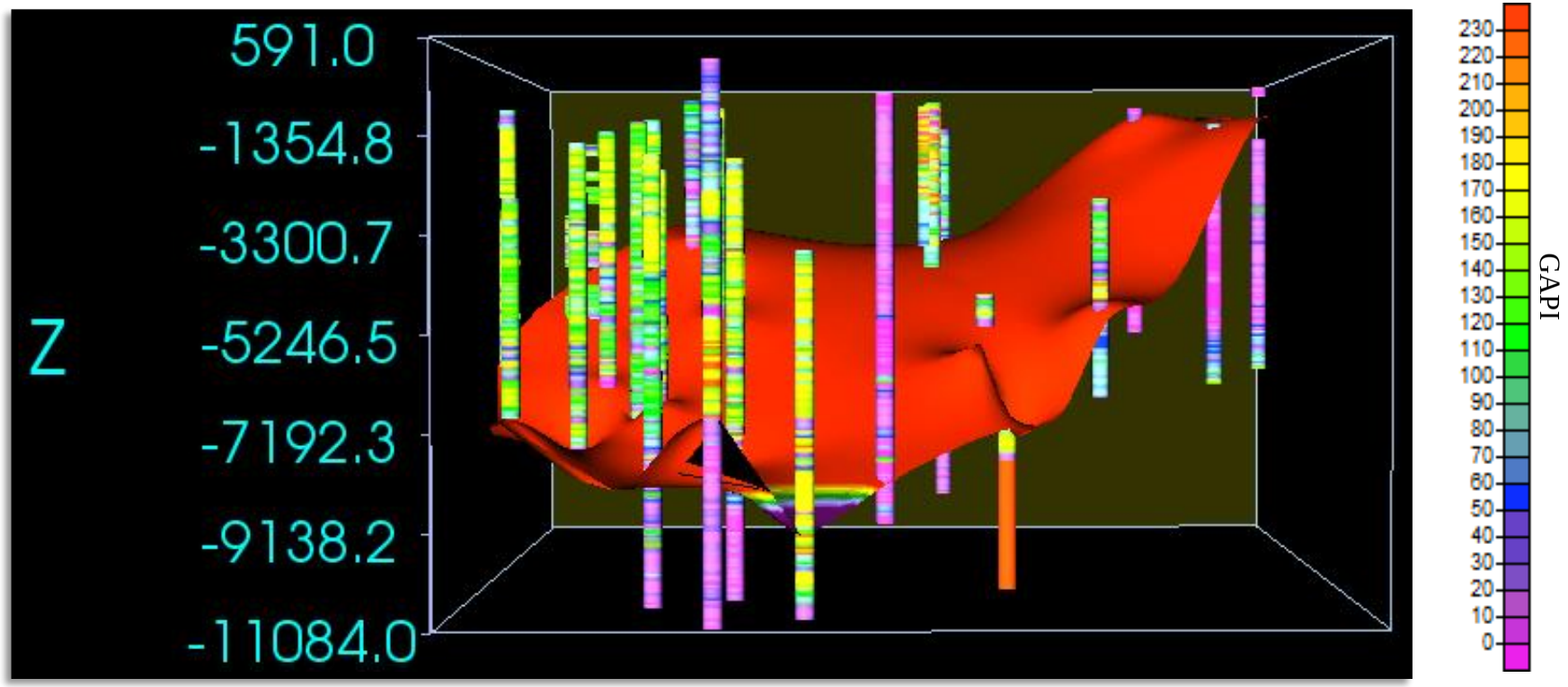

0 ———————— 100,000 feet. Horizontal scale.

Figure 44a. Three-dimensional spatial distribution of the interpreted top of the Chattanooga Shale in the Black Warrior Basin. Layer color scaled for interpolated gamma ray intensities for the Chattanooga Shale. Geophysical logs are present as long cylindrical tubes and color scaled for measured gamma ray intensity (See Appendix 1 for well log locations). Vertical exaggeration is 30. Shale surface is seen head on with North going into the page. Depth (Z axis) is

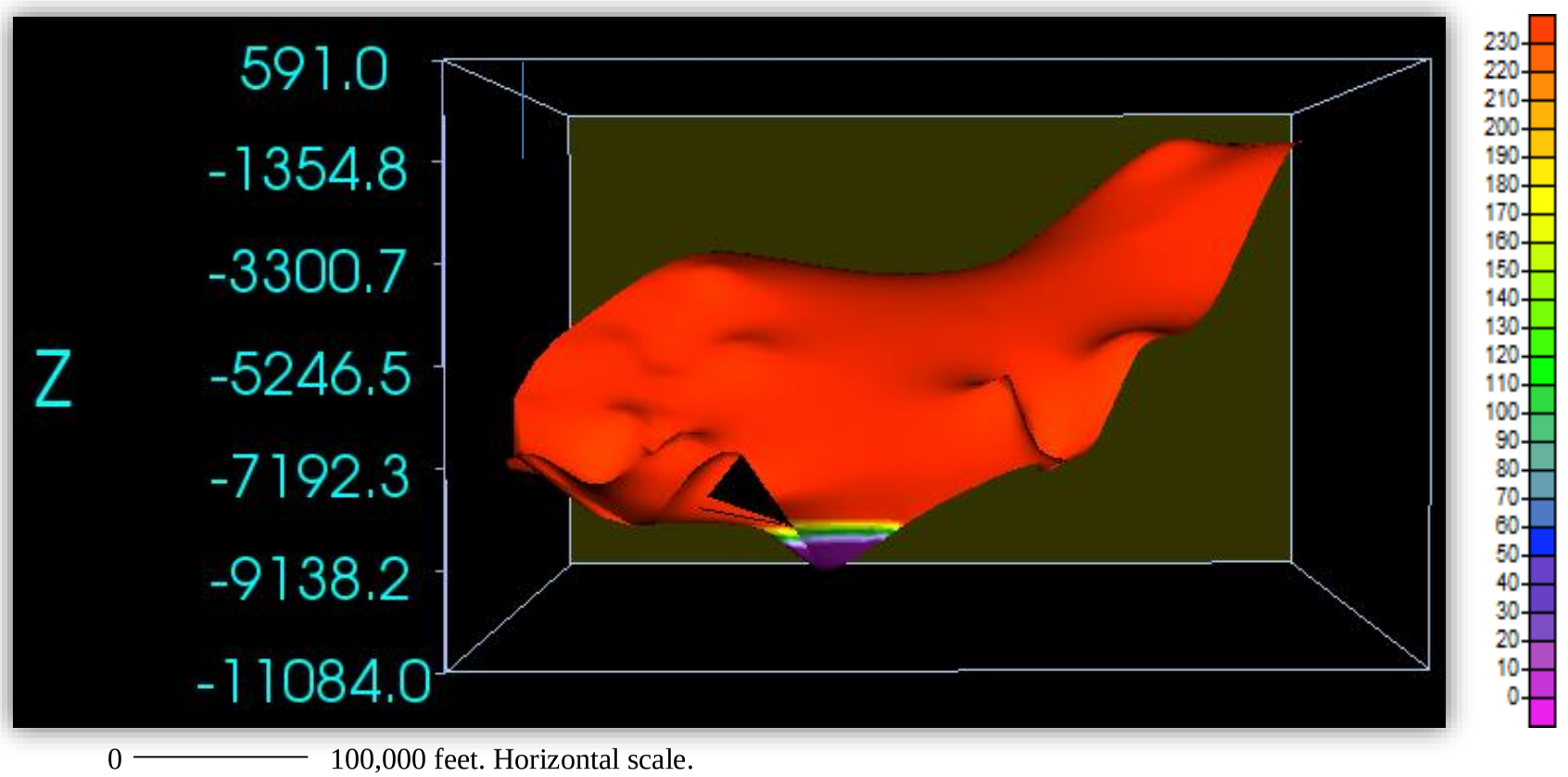

Figure 44b. Three-dimensional spatial distribution of the interpreted physical top of the Chattanooga Shale throughout the Black Warrior Basin. Layer color scaled for interpolated gamma ray intensities for the Chattanooga Shale. Vertical exaggeration is set to 30. Shale surface is seen head on with North going into the page. Depth (Z axis) is in feet

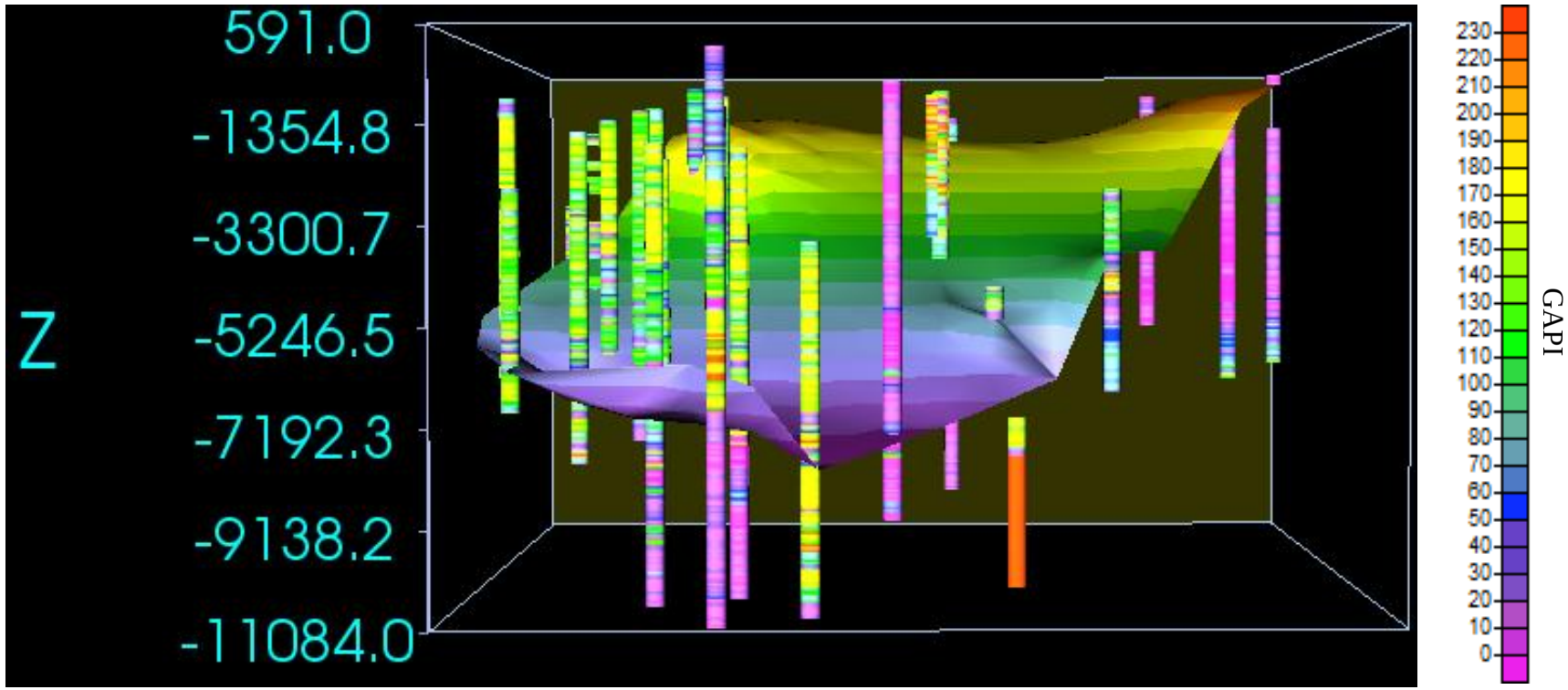

0 ———————— 100,000 feet. Horizontal scale.

Figure 44c. Three-dimensional spatial distribution of the interpreted physical top of the Neal (Floyd) Shale in the Black Warrior Basin. Layer color scaled for interpolated gamma ray intensities for the Neal (Floyd) Shale. Geophysical logs are present as long cylindrical tubes and color scaled for measured gamma ray intensity (See Appendix 1 for well log locations). Vertical exaggeration is 30. Shale surface is seen head on with North going into the page. Depth (Z axis) is in feet.

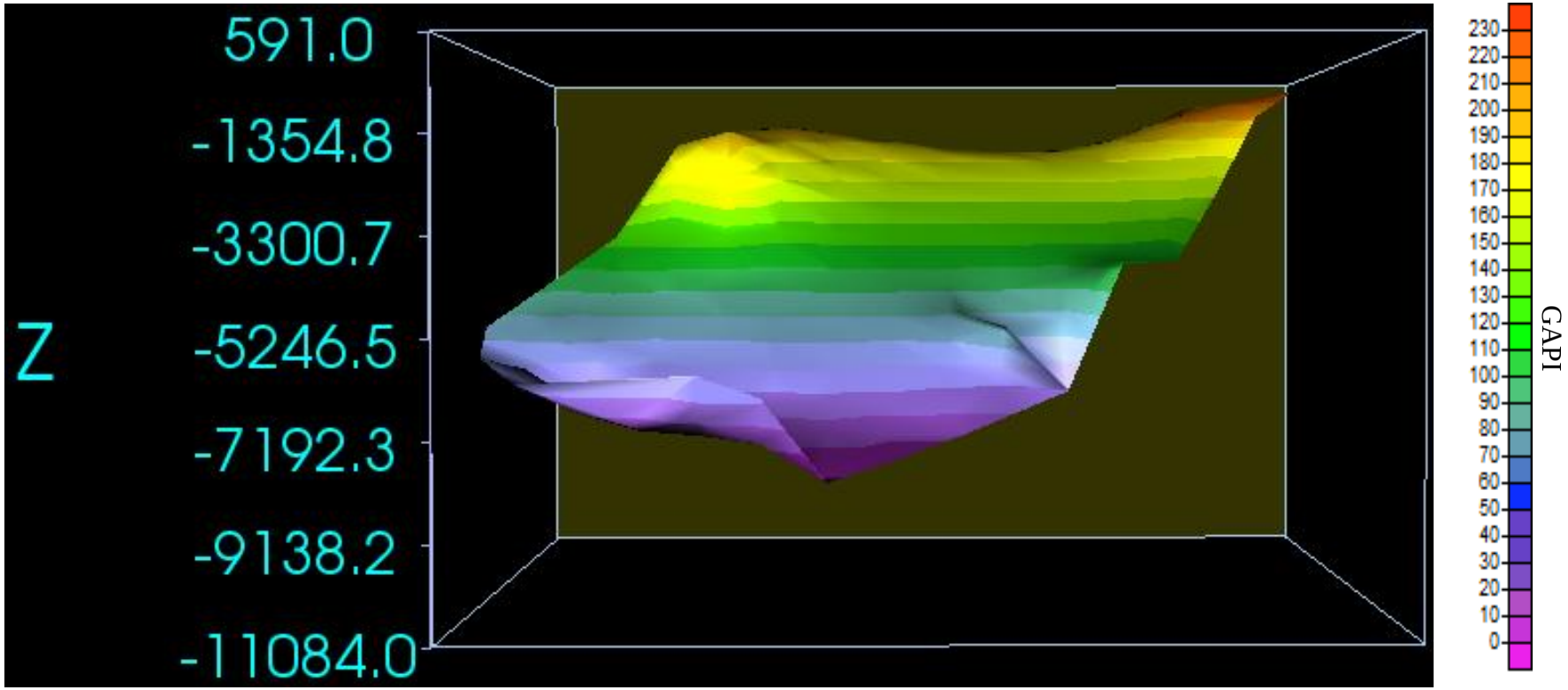

0 ———— 100,000 feet. Horizontal scale.

Figure 44d. Three-dimensional spatial distribution of the interpreted physical top of the Neal (Floyd) Shale throughout the Black Warrior Basin. Layer color scaled for interpolated gamma ray intensities for the Neal (Floyd) Shale. Vertical exaggeration is set to 30. Shale surface is seen head on with North going into the page. Depth (Z axis) is in feet

Basin Hydrologic Evolution, Overpressurization, and Thermal Maturation

A numerical model, Basin2 (Bethke et al., 1993), was used to simulate thermal maturation and fluid migration of the Black Warrior basin in the geologic past. The input file for simulation is shown in Appendix A. The model calculates the groundwater flow that arises from sediment compaction, the transfer of heat by conduction and advection, and the maturity of petroleum source beds through time. The modeling results along a north-to-south transect (Figure 45) were presented. The basin was modeled with both open and closed boundary conditions. The closed system assumes that the basin's margins are bounded by impermeable basement rocks or faults while the open system allows fluids to move outside of the basin. Reconstructed present-day stratigraphy is presented in Figure 46. Each stratigraphic unit in the calculations is composed of varying fractions of three common rock types: sandstone, carbonate, and shale. The evolution of porosity and permeability of each rock type is calculated using the correlations provided by Bethke et al., (1993).

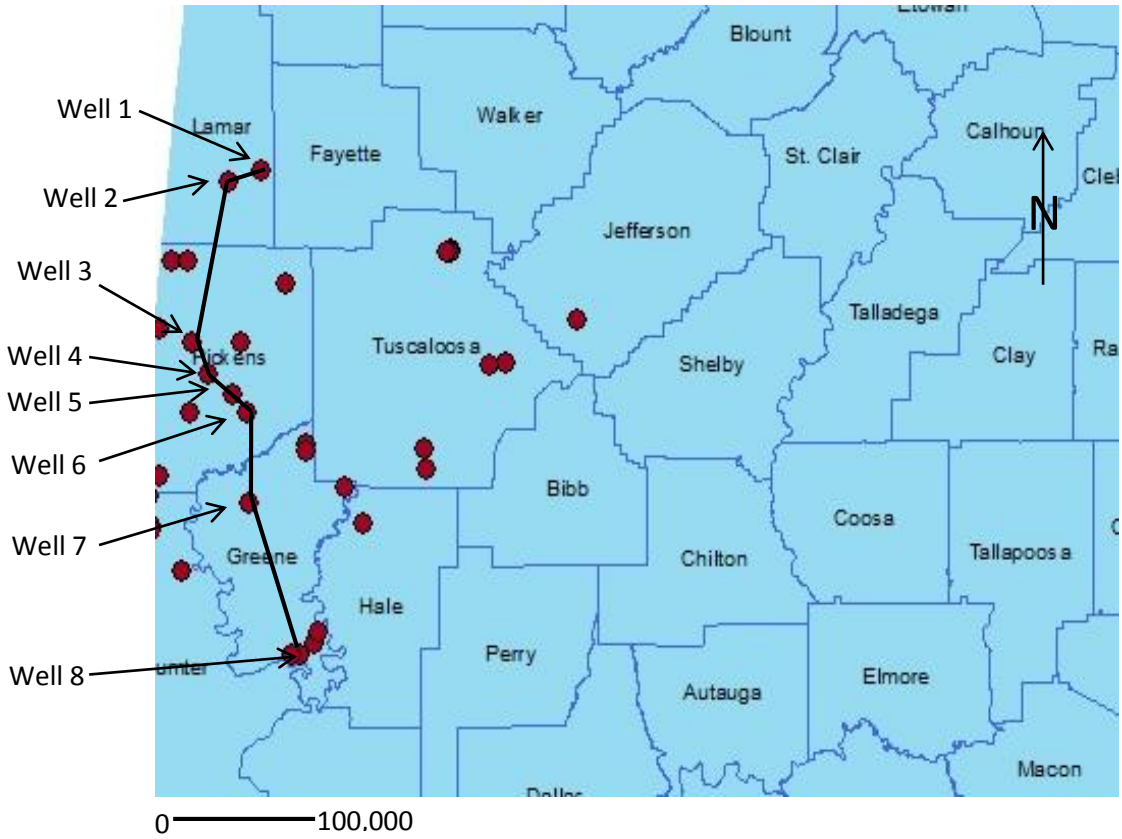

Figure 45. Transect modeled in the Black Warrior Basin utilizing Basin2 software. Well 1 is permit # 3097,well is permit # 2527, well 3 is permit # 14319, well 4 is permit # 14371, well 5 is permit # 5787, well 6 is permit # 1800, well 7 is permit # 10010, well 8 is permit # 3800.

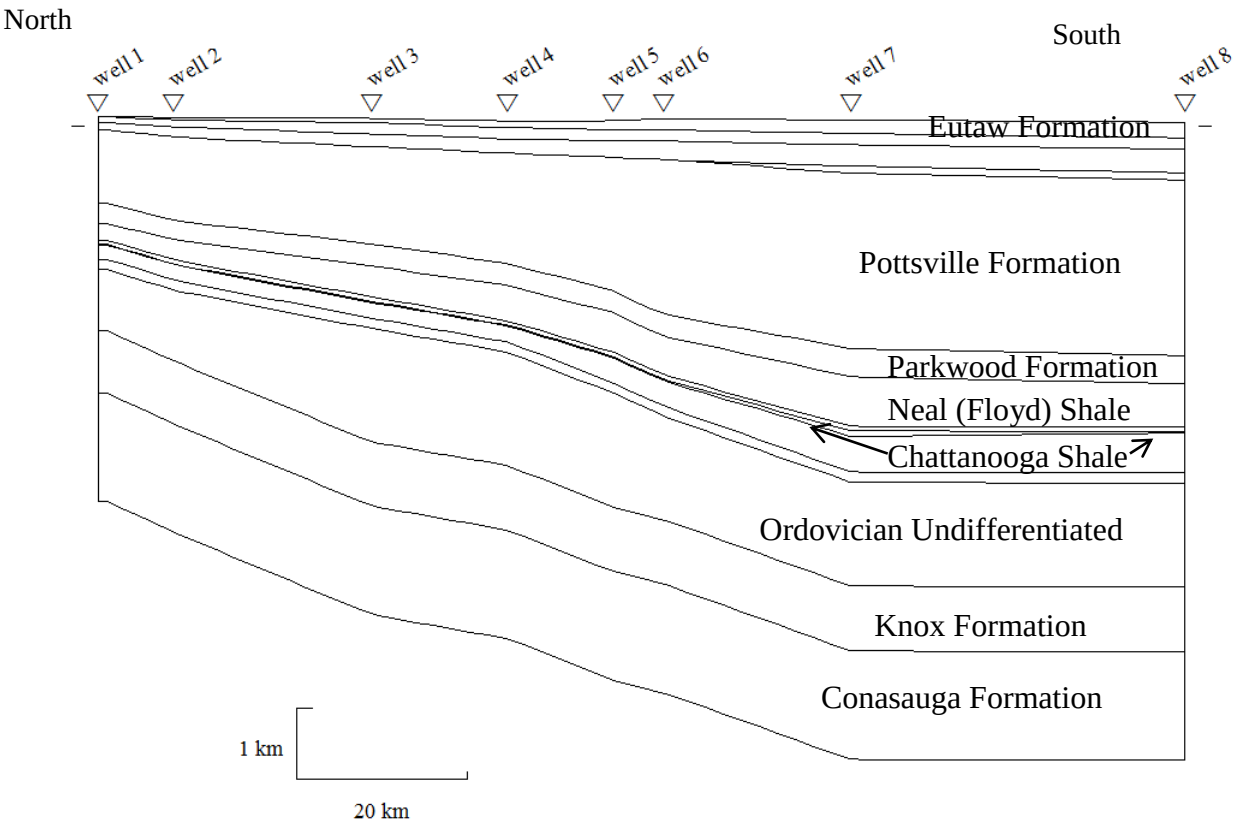

Figure 46. Stratigraphic-cross section of the Black Warrior Basin (see transect location in Figure 45), created in Basin2, presenting all formations of interest in the modeling results.

Modeling Results

The modeling results indicate that the first overpressurization episode in the Black Warrior Basin occurred during the deposition of the Knox Formation (Figure 47 a-b) in which the Conasauga Formation became overpressurized to approximately 45 atm above hydrostatic condition, when the sides of the basin were closed to groundwater flow (Figure 47a), and 30 atm above hydrostatic condition when the sides of the basin were open to groundwater flow (Figure 47b). During this time the Conasauga Formation reached the oil window (as defined by TTI values ranging from 15-160; Figure 47 a-b). Results are present in both close (Figure 47a) and open (Figure 47b) boundary conditions. The variation occurs in fluid flow directions predicted by the model under different boundary conditions, as the open system allows fluid flow to migrate across of the basin's margins. Groundwater is driven upward and in the lateral directions (in case of open flow boundaries) by compaction.

A second, slightly larger overpressurization occurred during the deposition of the Ordovician undifferentiated unit (Figure 48 a-b). Ovepressurization occurred primarily in the Conasauga Formation and reached approximately 70 atm above hydrostatic when the sides of the basin were closed to flow (Figure 48a). When the sides of the basin were open to groundwater flow, overpressurization reached approximately 70 atm above the hydrostatic (Figure 48b). Overpressurization was reduced along the margins of the basin as opposed to the closed flow system in which overpressurization is maintained at slightly higher values through the basin, specifically along the basin margins (Figure 48a). During this time the Conasauga Formation reached the oil window (Figure 48 a-b). Flow during this time was driven by compaction.

Overpressurization occurred in the Conasauga Formation during the deposition of the Parkwood Formation (Figure 49 a-b). When the margins of the basin were closed to groundwater flow overpressurization reached approximately 30 atm, above the hydrostatic, and was centered under well 7 and well 8 (Figure 49a). When the sides of the basin are open to groundwater flow overpressurization reached approximately 25 atm above the hydrostatic and was centered under well 7 (Figure 49b). The Conasauga Formation reached the gas window (TTI = 1000-5000) during the deposition of the Parkwood Formation (Figure 49 a-b). Fluid flow was driven by compaction process during this time.

The largest overpressurization of the Black Warrior Basin occurred during the deposition of the thick Pottsville Formation (Figure 50 a-b). When the sides of the basin are closed to groundwater flow modeling results indicate overpressurization reached approximately 240 atm above the hydrostatic. The overpressurization was centered under well 8 near basin's southern margin (Figure 50a). When the sides of the basin were open to groundwater flow modeling results indicate that overpressurization reached approximately 190 atm above the hydrostatic. Overpressurization shifted north (away from open boundary in the south) and is centered under well 7 (Figure 50b). The Chattanooga Shale and Neal (Floyd) Shale both reached oil window during this time (Figure 50 a-b). Modeling results indicate that the Chattanooga Shale was within the oil window from well 3 to well 5 and the Neal (Floyd) Shale was within the oil window from well 5 to well 8 (Figure 50 a-b). Fluid flow is driven from compaction in both modeling results. However, in the closed flow system compaction and overpressure are the highest near basin's deposition center with fluid flow being directed upward and laterally (northward) towards well 1 (Figure 50a). In the open flow system the compaction and overpressure center is shift northward

due to the open flow boundary present along the southern margin; in this flow regime fluid flow was directed upward and laterally towards basin's northern and southern margins (Figure 50b).

During the erosion of the Upper Pottsville Formation the Chattanooga Shale and Neal (Floyd) Shale reached the gas window, as defined by TTI values ranging from 1000-5000 (Figure 51 a-b). The Chattanooga Shale is thermally mature from well 5 to well 6 while the Neal (Floyd) Shale is thermally mature from well 7 to well 8. As indicated by both open and closed flow systems, there was no overpressurization of the basin during this time due to the lack of active sedimentation and compaction. There was no active groundwater flow during this erosion period.

During deposition of the Eutaw Formation the Black Warrior Basin experienced its last overpressurization event (Figure 52 a-b). The magnitude of overpressure (up to 18 atm) is much smaller with respect to those developed during the deposition of the thicker Pottsville Formation. Modeling results indicate that an overpressurization of 18 atm above hydrostatic occurred when the basin margins were closed to groundwater flow (Figure 52a). This overpressurization was centered along the southern margin of the basin (Figure 52a). When the basin margins were open to groundwater flow modeling results indicate an overpressurization of 10 atm above the hydrostatic (Figure 52b). Also, overpressurization has shifted northward under well 7 (Figure 52b). Both the Chattanooga Shale and Neal (Floyd) shale were in the gas window during this time (Figure 52 a-b). The Chattanooga Shale fell into the gas window from well 4 to well 6 while the Neal (Floyd) Shale fell into the gas window from well 6 to well 8. The driving hydraulic force was compaction during this time. However, in the closed system compaction and overpressure is maximized along the deposition center near the southern margin, which drives fluid updip northward (Figure 52a). In the open system, compaction and overpressure center

shifted north under well 7, fluid is driven updip and laterally towards both northern and southern margins (Figure 52b).

Overpressure created by sedimentation and compaction in the geologic past has largely dissipated (Figure 53 a-b) in the present-day. This implies that the overpressure condition observed in the Big Canoe Creek Field (Pashin, personal communication) is likely created or maintained by gas generation (Hansom and Lee, 2008) since the Chattanooga Shale and Neal (Floyd) Shale are currently in the gas window, in locations from well 3 to well 5 and from well 5 to well 7, respectively (Figure 53 a-b). This modeling result is consistent with measured vitrinite reflectance values for these two shales. Measured vitrinite reflectance values for the Conasauga shale in the Big Canoe Creek Field ranged from 1.1 to 1.9 (Pashin et al., 2011), indicating that they have reached thermal maturation for gas generation.

At present, the basin tilts to the south and groundwater flow is driven southward by gravity and topographic relief. In this gravity-driven flow system, local groundwater flow system dominates in the shallow basin with recharge areas at local topographic highs and discharge areas at adjacent topographic low. Recharge is occurring near well one, well three, well six, and well seven. Discharge is occurring at well 2, well 4, well 5, and well 8 (Figure 53 a-b). A regional flow system develops in the deeper basin with consistent southward flow directions. In the closed flow system fluid flow moves down dip and discharge or converges toward the surface near well 8 along the basin's southern margin (Figure 53a). However, in the open flow system all fluid flow is directed towards the southern margin where it discharges out of the basin instead of towards the surface (Figure 53b).

Figure 54 shows calculated evolution of oil thermal maturity (expressed as TTI) of three shales near basin's southern deposition center over geologic time. The Conasauga Formation

reached the onset of oil generation at 505 m.y. (TTI = 15), peak oil generation (TTI = 75) at 490 m.y., and reached the end of oil generation (TTI = 160) by 480 my. The Chattanooga Formation reached the onset of oil generation at 330 m.y. (TTI = 15), peak oil generation (TTI = 75) at 329 m.y., and reached the end of oil generation (TTI = 160) by 328 m.y. The Neal (Floyd) Formation reached the onset of oil generation at 330 m.y. (TTI = 15), peak oil generation (TTI = 75) at 328 m.y., and reached the end of oil generation (TTI = 160) by 325 m.y.

Figure 55 illustrates the calculated fraction of oil generation in each of the shales near basin's southern deposition center through geologic time. In the Conasauga Formation 100% of the possible oil generation occurred at 478 m.y. In the Chattanooga Shale and Neal (Floyd) Shale had 100% oil generation at 324.8 m.y. These values correlate with calculated TTI values for oil generation for the Conasauga Formation, Chattanooga Shale, and Neal (Floyd) Shale presented in Figure 55.

Figure 56 illustrates the calculated evolution of gas maturation (expressed as TTI) of the three shales near basin's southern deposition center over geologic time. The Conasauga Formation reached the onset of gas generation (TTI = 1000) at approximately 470 m.y. and reached a TTI of 5000 at 410 m.y. The Chattanooga Shale reached the onset of gas generation at 305 my reached a TTI of 5000 at 148 m.y. The Neal (Floyd) Shale reached the onset of gas generation at 275 my reached a TTI of 5000 at 40 m.y.

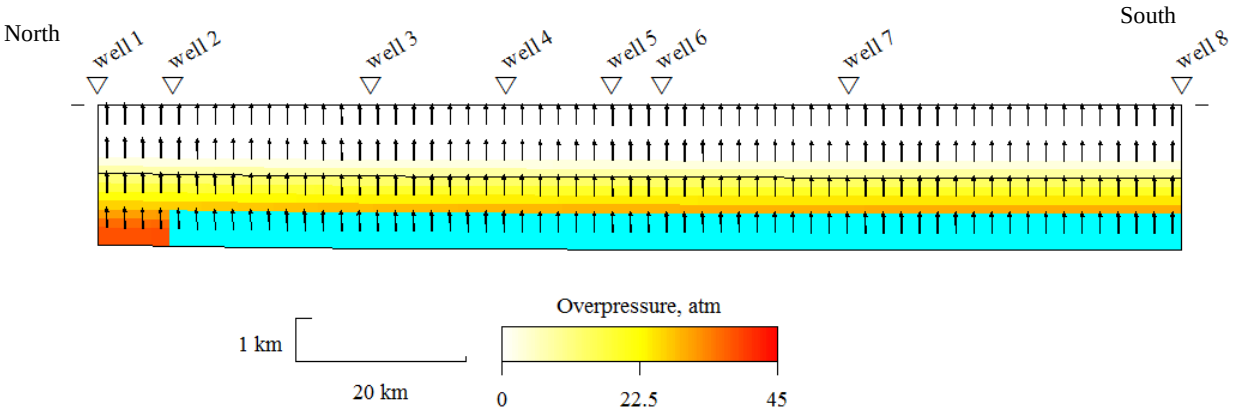

Figure 47a. Calculated distribution of overpressurization in the Black Warrior Basin during deposition of the Knox Formation. Refer to Figure 46 for stratigraphy. The Conasauga Formation reached the oil window, TTI of 15-160, represented by the color mask (blue). The sides of the basin are closed to groundwater flow. Arrows indicate the direction of fluid flow.

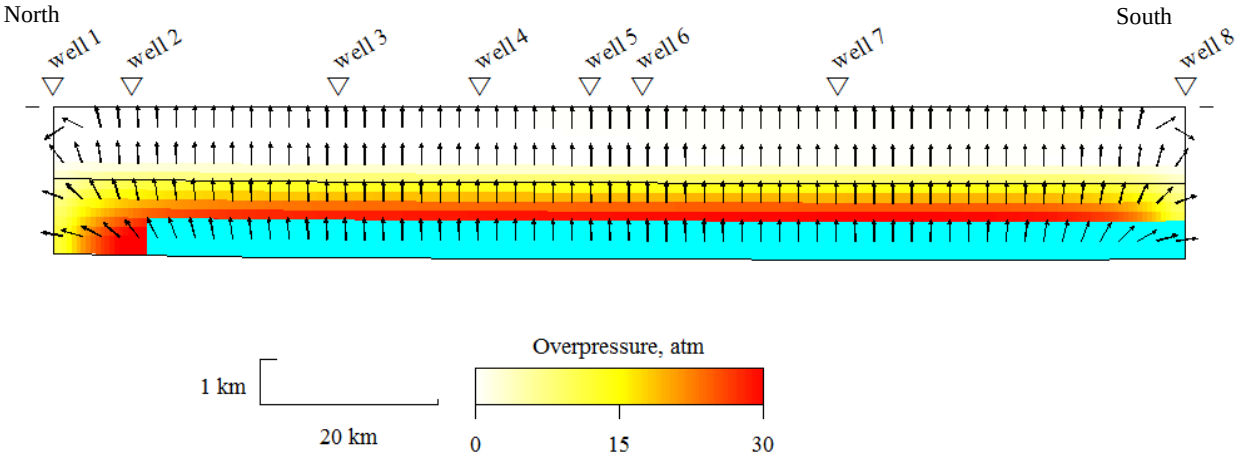

Figure 47b. Calculated distribution of overpressurization in the Black Warrior Basin during deposition of the Knox Formation. Refer to Figure 46 for stratigraphy. The Conasauga Formation reached the oil window, TTI of 15-160, represented by the color mask (blue). The sides of the basin are open to groundwater flow. Arrows indicate the direction of fluid flow.

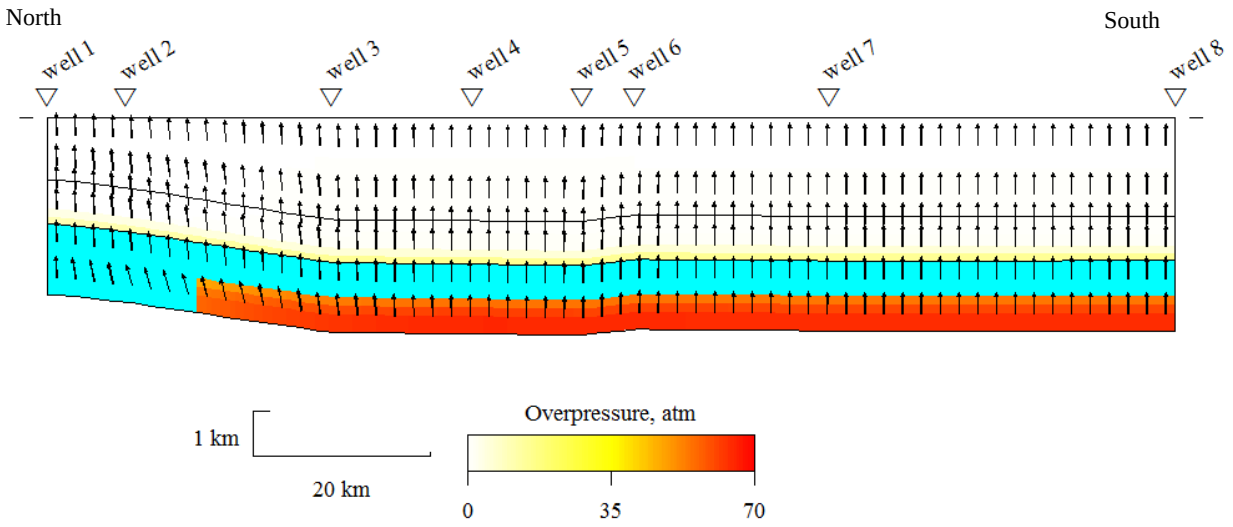

Figure 48a. Calculated distribution of overpressurization in the Black Warrior Basin during deposition of the Ordovician undifferentiated unit. Refer to Figure 46 for stratigraphy. The Conasauga Formation reached the oil window, TTI of 15-160, represented by the color mask (blue). The sides of the basin are closed to groundwater flow. Arrows indicate the direction of fluid flow.

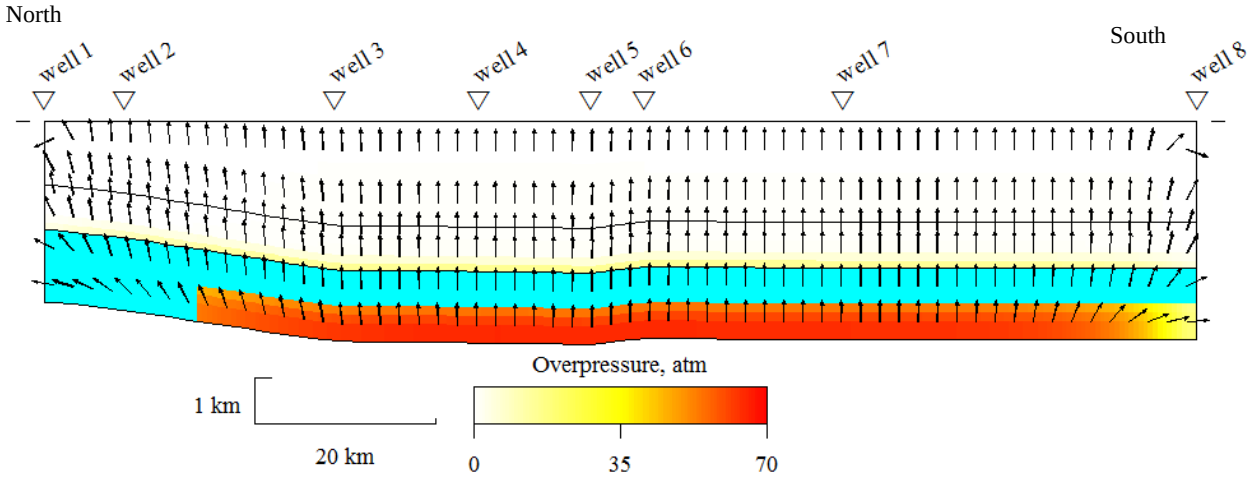

Figure 48b. Calculated distribution of overpressurization in the Black Warrior Basin during deposition of the Ordovician undifferentiated unit. Refer to Figure 46 for stratigraphy. The Conasauga Formation reached the oil window, TTI of 15-160, represented by the color mask (blue). The sides of the basin are open to groundwater flow. Arrows indicate the direction of fluid flow.

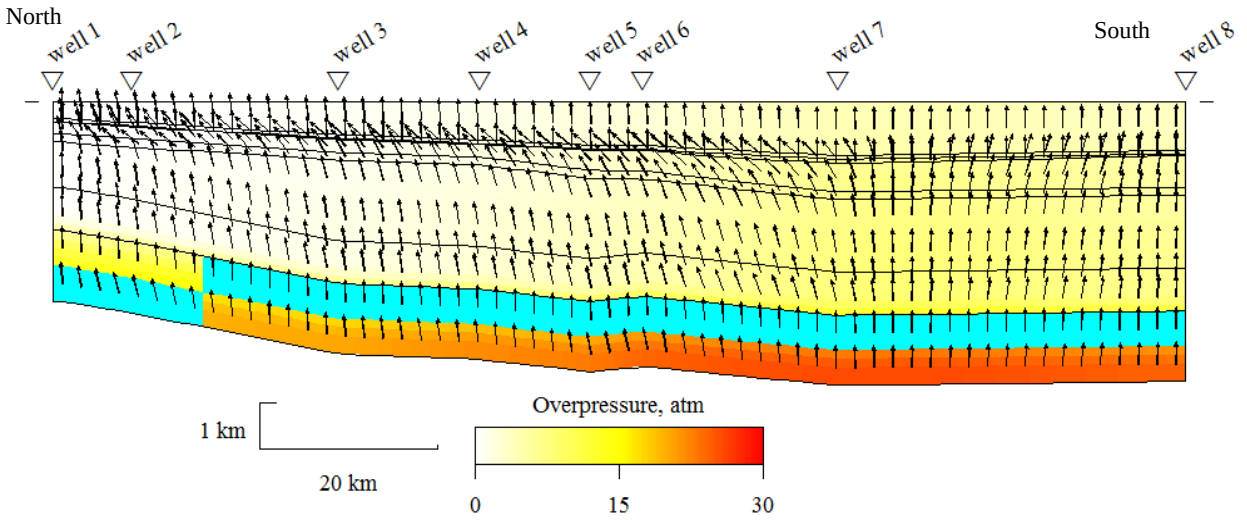

Figure 49a. Calculated distribution of overpressurization in the Black Warrior Basin during deposition of the Parkwood Formation. Refer to Figure 46 for stratigraphy. The Conasauga Formation reached the gas window, TTI of 1000-5000, represented by the color mask (blue). The sides of the basin are closed to groundwater flow. Arrows indicate the direction of fluid flow.

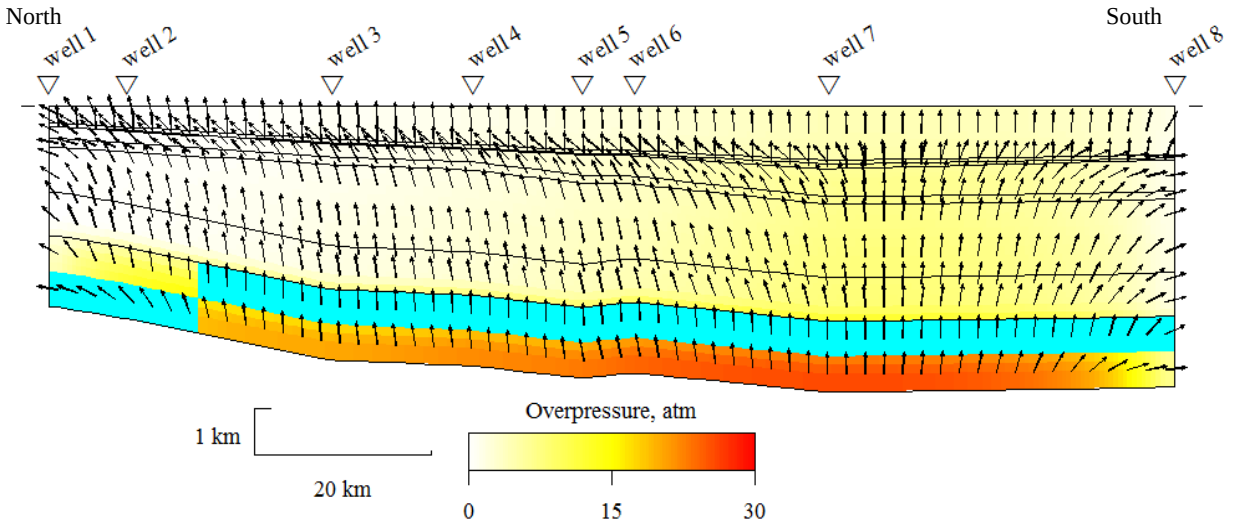

Figure 49b. Calculated distribution of overpressurization in the Black Warrior Basin during deposition of the Parkwood Formation. Refer to Figure 46 for stratigraphy. The Conasauga Formation reached the gas window, TTI of 1000-5000, represented by the color mask (blue). The sides of the basin are open to groundwater flow. Arrows indicate the direction of fluid flow.

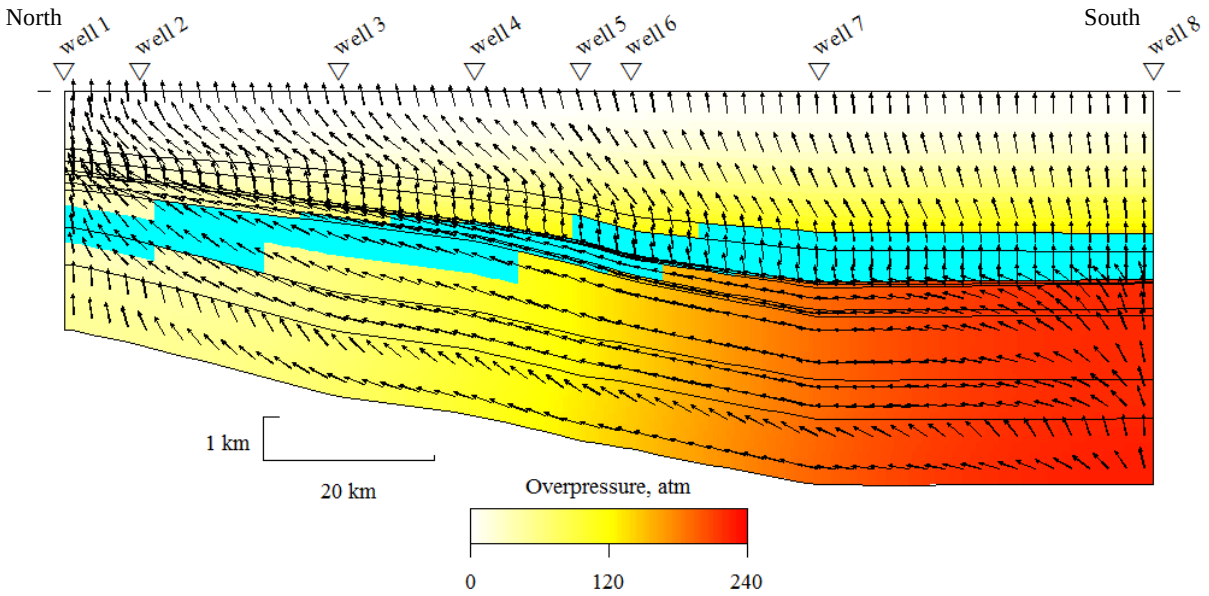

Figure 50a. Calculated distribution of overpressurization in the Black Warrior Basin during deposition of the Pottsville Formation. Refer to Figure 46 for stratigraphy. The Neal (Floyd) Shale and the Chattanooga Shale reached the oil window, TTI of 15-160, represented by the color mask (blue). The sides of the basin are closed to groundwater flow. Arrows indicate the direction of fluid flow.

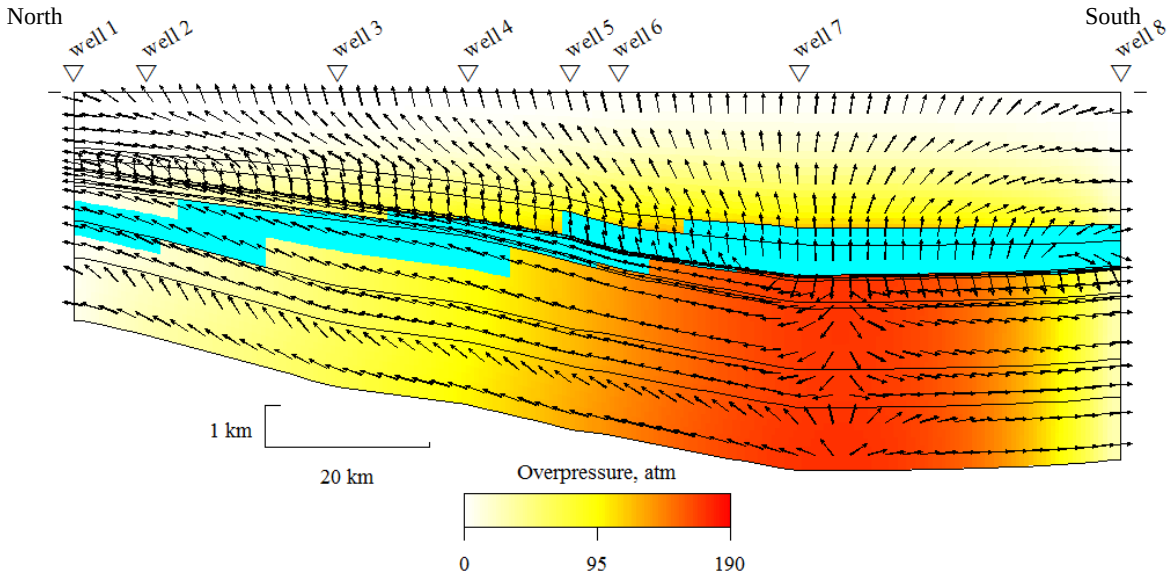

Figure 50b. Calculated distribution of overpressurization in the Black Warrior Basin during deposition of the Pottsville Formation. Refer to Figure 46 for stratigraphy. The Neal (Floyd) Shale and the Chattanooga Shale reached the oil window, TTI of 15-160, represented by the color mask (blue). The sides of the basin are open to groundwater flow. Arrows indicate the direction of fluid flow.

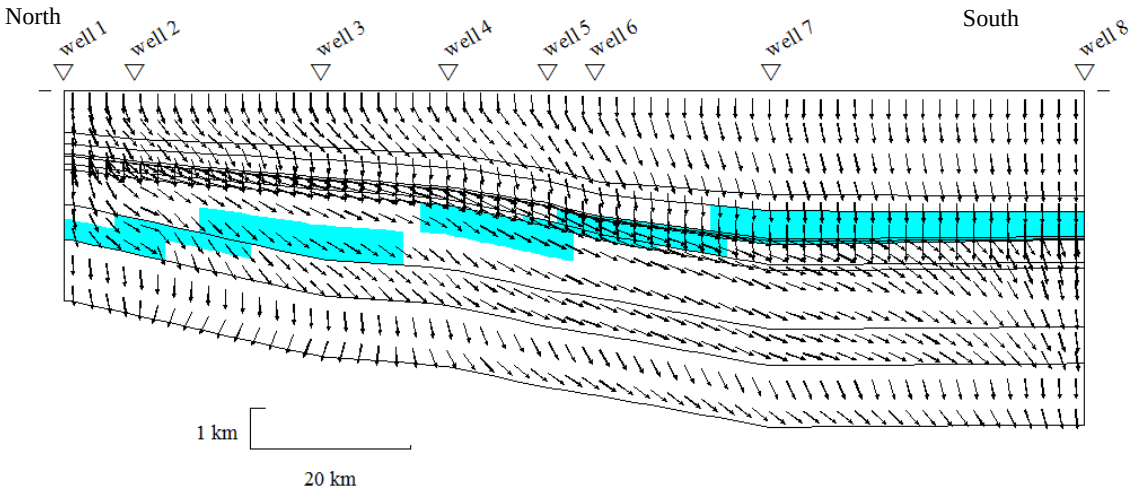

Figure 51a. Predicted Chattanooga Shale and Neal (Floyd) Gas-shale window (blue), TTI 1000-5000 reached during erosion of the Pottsville Formation. Refer to Figure 46 for stratigraphy. The sides of the basin are closed to groundwater flow. Arrows indicate the direction of fluid flow.

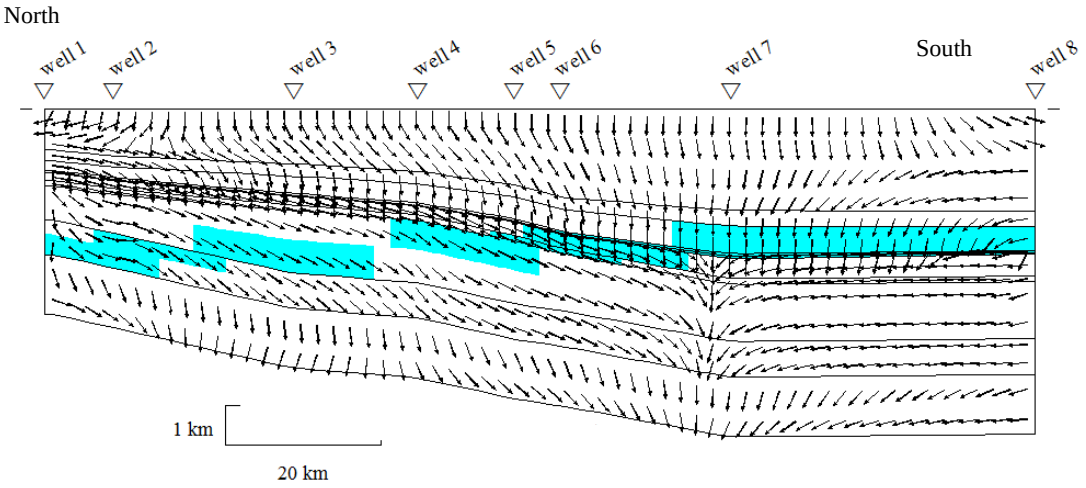

Figure 51b. Predicted Chattanooga Shale and Neal (Floyd) Gas-shale window (blue), TTI 1000-5000 reached during erosion of the Pottsville Formation. Refer to Figure 46 for stratigraphy. The sides of the basin are open to groundwater flow. Arrows indicate the direction of fluid flow.

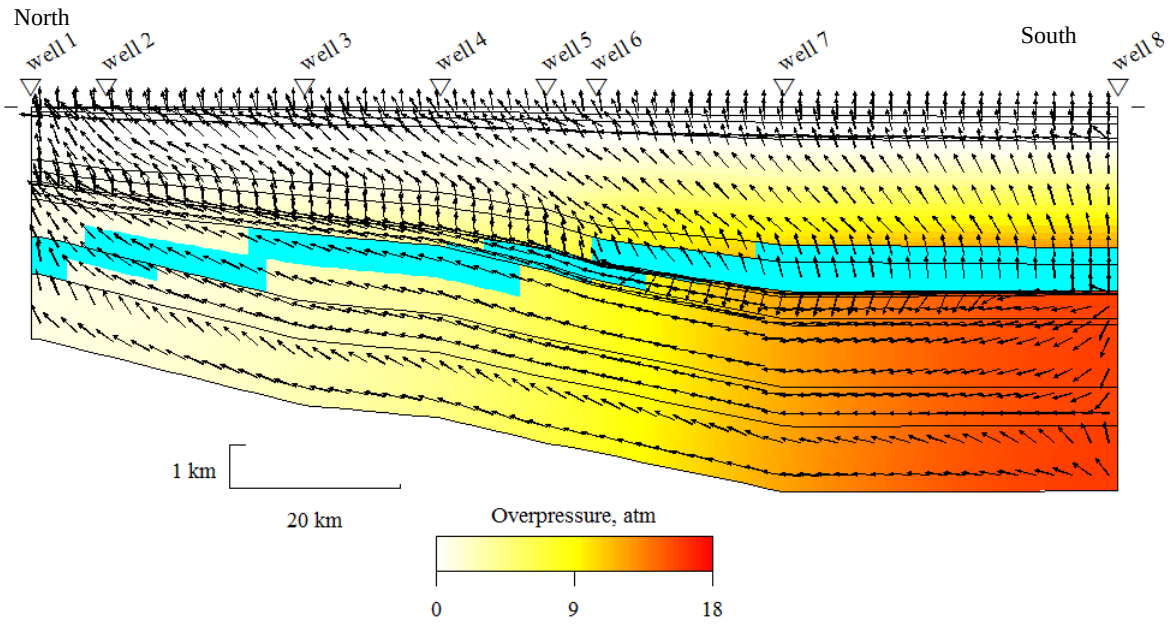

Figure 52a. Calculated distribution of overpressurization in the Black Warrior Basin during deposition of the Eutaw Formation. Refer to Figure 46 for stratigraphy. The Neal (Floyd) Shale and the Chattanooga Shale reached the gas window, TTI of 1000-5000, represented by the color mask (blue). The sides of the basin are closed to groundwater flow. Arrows indicate the direction of fluid flow.

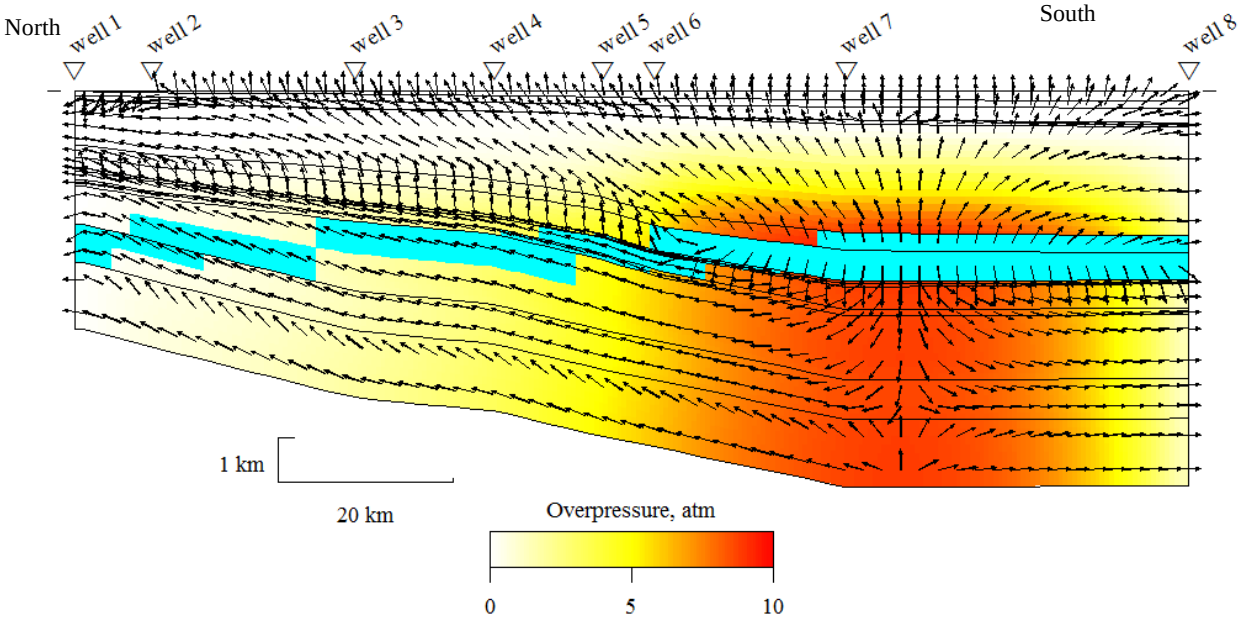

Figure 52b. Calculated distribution of overpressurization in the Black Warrior Basin during deposition of the Eutaw Formation. Refer to Figure 46 for stratigraphy. The Neal (Floyd) Shale and the Chattanooga Shale reached the gas window, TTI of 1000-5000, represented by the color mask (blue). The sides of the basin are open to groundwater flow. Arrows indicate the direction of fluid flow.

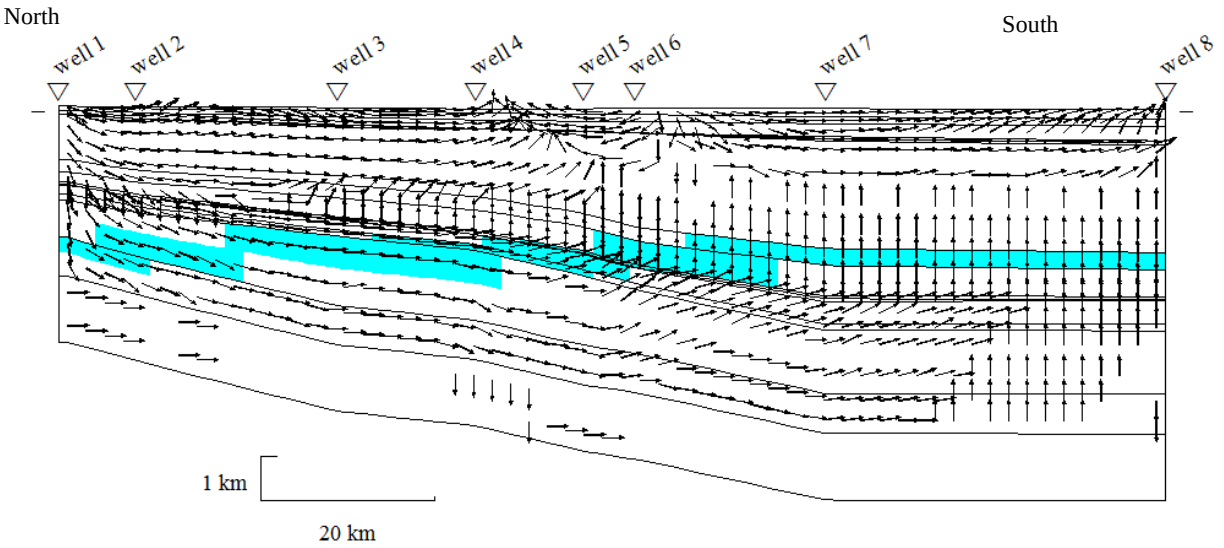

Figure 53a. Calculated present-day flow and gas window in the Black Warrior Basin. Refer to Figure 46 for stratigraphy. The Chattanooga Shale and Neal (Floyd) Shale are in the gas window, TTI 1000-5000, represented by the color mask (blue). The sides of the basin are closed to groundwater flow. Arrows indicate the direction of fluid flow.

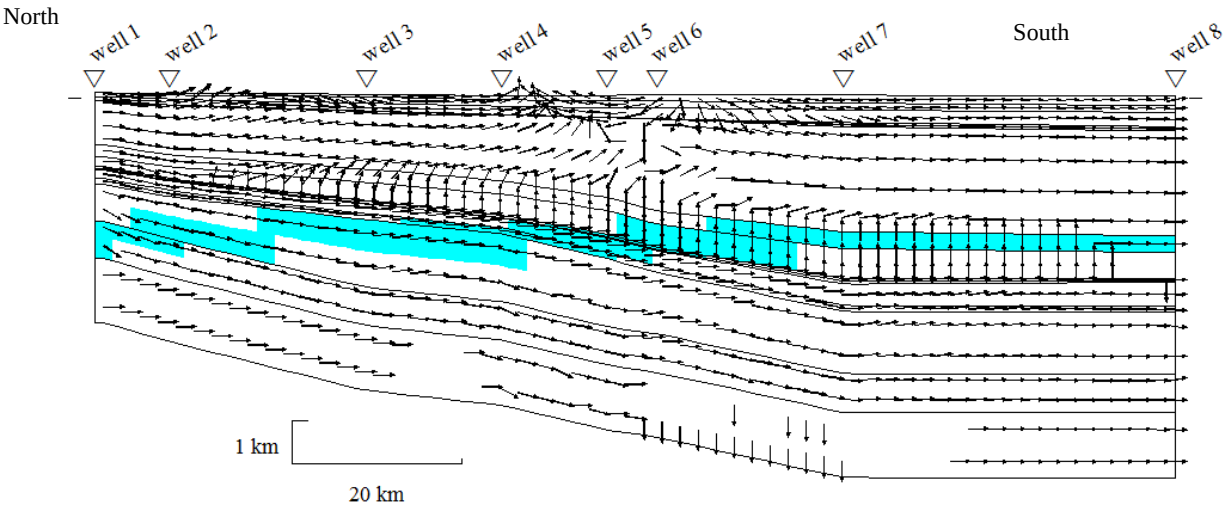

Figure 53b. Calculated present-day flow and gas window in the Black Warrior Basin. Refer to Figure 46 for stratigraphy. The Chattanooga Shale and Neal (Floyd) Shale are in the gas window, TTI 1000-5000, represented by the color mask (blue). The sides of the basin are open to groundwater flow. Arrows indicate the direction of fluid flow.

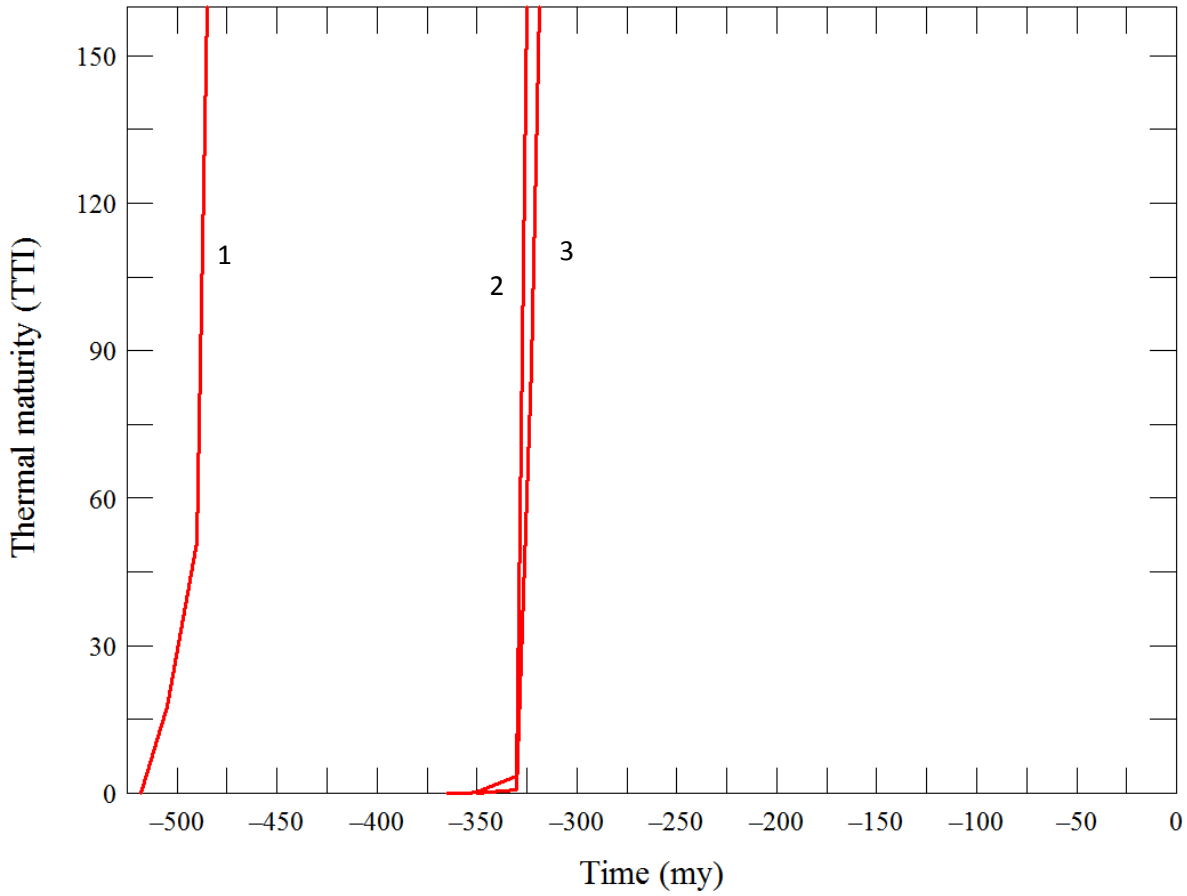

Figure 54. Calculated oil window thermal maturation through time, for the Conasauga Formation (1), Chattanooga Shale (2), and Neal (Floyd) Shale (3).

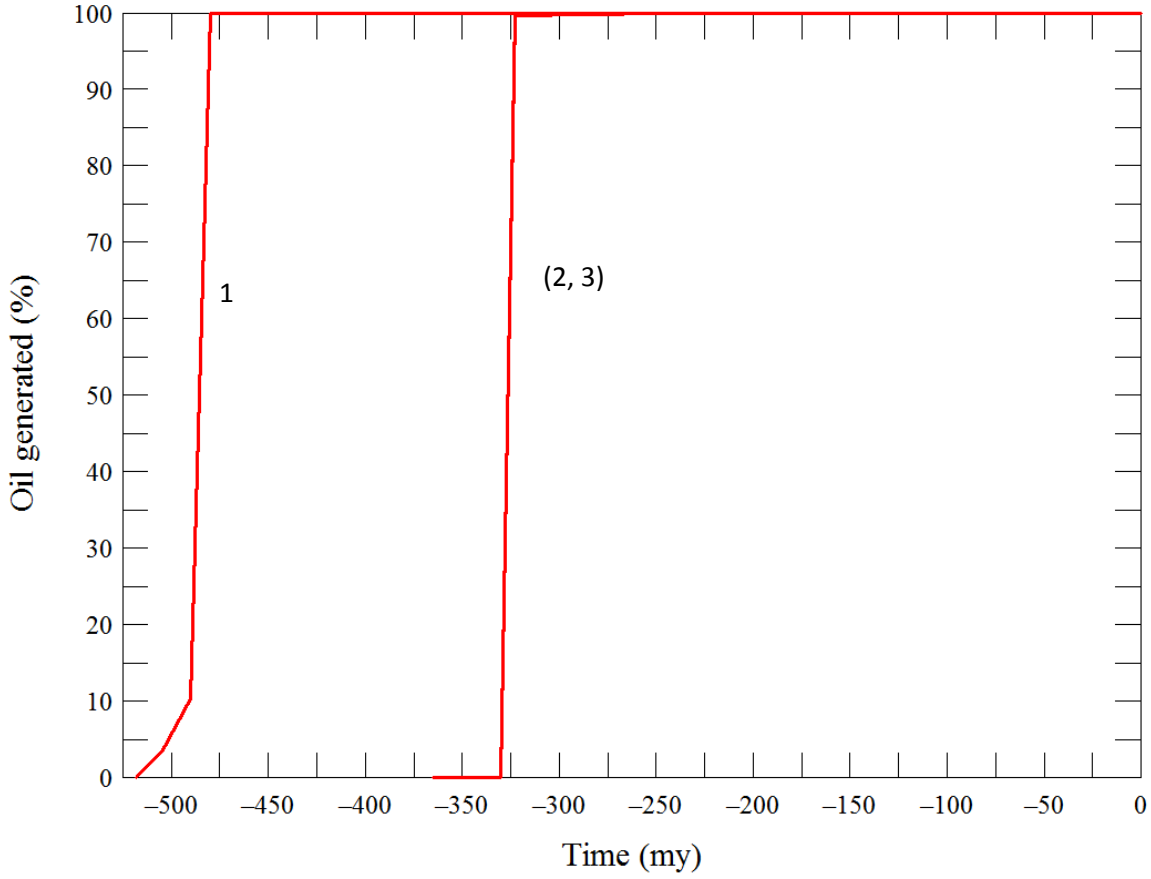

Figure 55. Calculated oil generated (%), through time, for the Conasauga Formation (1), Chattanooga Shale (2), and Neal (Floyd) Shale (3).

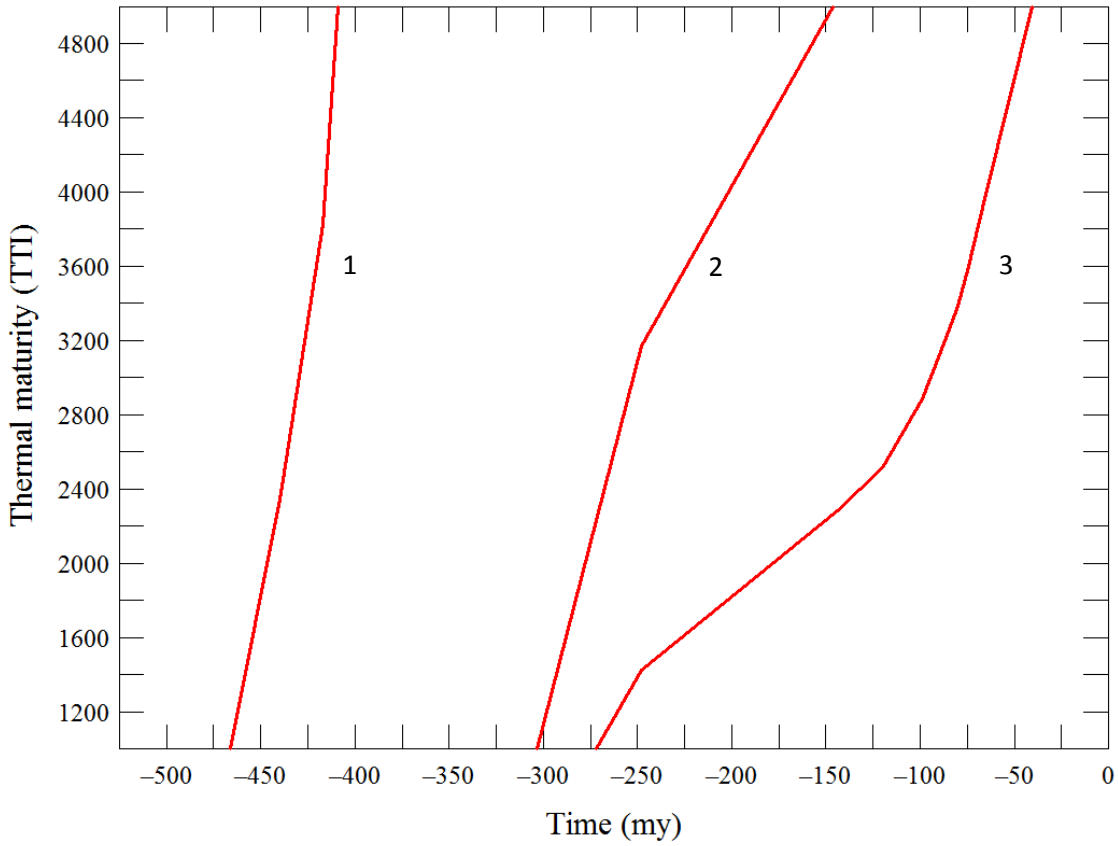

Figure 56. Calculated thermal maturation of gas generation (TTI> 1000) through time for the Conasauga Formation (1), Chattanooga Shale (2), and the Neal (Floyd) Shale (3).

Discussion Summary

Geochemical characterization of each of the shales indicates that there is a strong presence of potentially toxic elements (e.g., As, Pb, and Hg) in the non-carbonate sections and this correlates well to the abundance of metals-bearing minerals such as pyrite and Fe-oxides. If regulations are adopted in Alabama that mirror those of Colorado, Pennsylvanian, or Illinois, fracking operation may be suspended or banned should toxic metals be released and present in subsequent follow-up water testing.

GC-MS analysis of organic compounds extracted from three shales indicates that there are unique hydrocarbon signatures present in the Conasauga Shale, the Chattanooga Shale, and the Neal (Floyd) Shale. While the lightest sections of hydrocarbon compounds are degraded, heavier fractions persist in shales with extremely low porosity and permeability. Petroleum biomarker analysis indicates that the Conasauga Shale and the Chattanooga Shale share a similar source of organic carbon in the geologic past. However, the younger Neal (Floyd) Shale deposited during the Mississippian appears to have a different source of organic carbon. This contrast possibly reveals relative higher inputs of terrestrial organic matter in the basin during the Mississippian (Carroll et al., 1995). Significant temporal variability in organic matter reflects the changing sedimentary environments and climatic conditions, which requires further investigations.

Correlation of geophysical logs gives insight into the three-dimensional spatial distribution of both the Chattanooga Shale and the Neal (Floyd) Shale. Reconstructed surfaces created by PETRA indicate that there is a deposition center located in the southeastern section of

the Black Warrior Basin. Basin2 modeling results indicate that the Black Warrior Basin experienced five major overpressurization events and that the Conasauga Shale, Chattanooga Shale, and the Neal (Floyd) Shale had reached their thermal maturity to generate oil and gas. Modeling results also indicate that sediment compaction was the main mechanism that drove overpressurization of shales in the past. The compaction-induced overpressurization, however, has largely dissipated over time, the overpressures observed today are most likely maintained by active gas generation (Hansom and Lee, 2005). At present day subsurface fluids in the Black Warrior Basin migrates southwards, which is driven mainly by topographic relief.

Conclusions

This study was performed to analysis gas-shale production from a multidiscipline standpoint where both environmental and industrial concerns were addressed, and bridged, by addressing regulations and groundwater protection involving gas-shale production. To achieve this, several aspects of gas-shale were addressed: (1) understand how new regulations involving hydraulic fracturing may potentially affect the industrial practices of protecting groundwater supplies, (2) characterize the variations in gas-shale mineralogies, (3) quantify the concentration of trace elements (e.g., those with potential impacts to drinking water) and relate trace element concentrations to gas-shale mineralogy, (4) characterize and correlate key organic compounds (i.e., biomarkers) extracted from shales, (5) model the thermal history and hydrodynamic evolution of the basin.

Research goals were attained by completing extensive literature review of regulations concerning gas-shale production and groundwater protection. Elemental quantification of selected gas-shales was done by XRF analysis while mineralogy was done by XRD analysis. A full scan GC/MS and single ion GC/MS analysis was performed on selected gas-shale extracted

organics providing insight into hydrocarbons present as well as sources of organics. Lastly, the thermal and hydrodynamic histories of the gas-shales were modeled utilizing Basin2 modeling software.

- Illinois, Pennsylvania, and Colorado, have put forth the most extensive regulations involving hydraulic fracturing and the protection of USDWs. Each state requires baseline water testing of chloride, sulfate, arsenic, barium, calcium, chromium, iron, magnesium, selenium, cadmium, lead, manganese, mercury, and silver; subsequent follow-up testing is also required at regular time intervals up to ½ mile radius from the wellbore. These regulations will possibly be the standard adopted by states that have high yield gas-shale production. If these regulations become standardized throughout the United States it will enable regulatory bodies to asses a problem and determine the responsible party, if any.
- If Alabama gas-shale production increases and similar regulations as those in Colorado, Pennsylvania, and Illinois are adopted there could be additional expenditures above business as usual costs due to baseline and follow up water testing and potential contamination. This is due to the potential release of toxic trace elements due to the interactions of an oxidizing fluid and hosting geologic material.
- Elemental quantification of the Conasauga Formation, Devonian Shale, Chattanooga Shale, and Neal (Floyd) Shale resulted in elevated concentrations of trace elements in each, except in the Conasauga Formation in Shelby County, which is dominated by carbonate minerals. This would suggest that the

Conasauga Formation in Shelby County would pose the least amount of risk of trace elements contaminating the groundwater.

- The Chattanooga Shale in Greene County had the highest lead concentrations (98.25 ppm) and the Neal (Floyd) Shale in Greene County had the highest arsenic (20.8 ppm) and mercury (73.42ppm) concentrations. This would suggest that these two units would have the greatest potential for release of As and Pb if produced.
- Positive correlations exist between iron and arsenic concentrations ($R^2 = 0.36$), iron and lead concentrations ($R^2 = 0.36$), and sulfur and iron concentrations ($R^2 = 0.29$), implying that the iron- and sulfur-bearing minerals have strong geochemical affinity to adsorb trace metals onto their surfaces or crystalline structure. This suggests where ever large amounts of Fe-sulfides are present elevated concentrations of As and Pb could be expected.
- Aluminum enrichment factors of trace elements (i.e., As, Pb, Cu, and Hg) are very high in all of the shales. The greatest enrichments for arsenic and lead are found in the Chattanooga Shale in Greene County; the greatest enrichment for copper is found in the Conasauga Formation in Shelby County; the highest enrichment factor for mercury is found in the Devonian Shale in Hale County. Sulfur and Fe enrichment is also very high in each of the shales. This suggests that S and Fe bearing minerals work as sinks for the toxic trace metals.
- The presence of pyrite and iron oxides in each of the shales corresponds with the abundance of trace elements. The highest concentration of arsenic and lead are found in shales (i.e., Chattanooga Shale in Greene County and the Neal (Floyd)

Shale in Greene County) with the highest sulfide and iron oxide contents. The Conasauga Formation in Shelby County is dominated by carbonate minerals and lacks iron sulfide and iron oxide minerals. This corresponds to very low concentrations of sulfur, iron, as well as concentrations of arsenic and lead.

- Analysis of extracted organics from the Conasauga Formation, Chattanooga Shale in Greene County, and Neal (Floyd) Shale in Pickens County, indicate that docosenamide hydrocarbon is present in the Conasauga Formation, Hentraicontanone is present in the Chattanooga Shale, and Tetradecandioic acid, bis(trimethylsilyl) ester is present in the Neal (Floyd) Shale. This indicates that hydrocarbons had been generated in the geologic past in each of the shales and could potentially be production targets.
- Full scan GC-MS gas chromatographs indicate that microbial degradation had occurred mostly to the lightest organic compounds in the geological past. Biomarker analysis of m/z ratios 191, 217, and 218 indicate that the Conasauga Formation and the Chattanooga Shale share a similar source of organic carbon while those in the Neal (Floyd) Shale has a unique source of organic carbon represent a different source. This is most likely to a significant increase of land based plants during the Carboniferous.
- Biomarkers could be of significant importance if hydrocarbon if fugitive methane or other fugitive hydrocarbons are reported. This is due to the fingerprinting capability of biomarkers. It would enable a determination of the origin of that particular hydrocarbon to be determined by comparing the fugitive hydrocarbon

to a potential source. This would enable responsibility to be place, or removed, if contamination occurs.

- Correlations of geophysical gamma ray logs give an insight into the spatial distribution of these shales as they progress into the Black Warrior Basin. The major deposition center of the Black Warrior Basin is located at its southern margin.
- Modeling results indicate that the Black Warrior Basin experienced its first overpressurization event during the deposition of the Knox Formation. During this time the Conasauga Formation reached the oil window. A second overpressurization event occurred during the deposition of the Ordovician Undifferentiated unit. During this time the Conasauga Formation was in the oil window. A third overpressurization occurred during the deposition of the Parkwood Formation. During this time the Conasauga Formation fell into the gas window. The fourth and largest overpressurization event occurred during the deposition of the thick Pottsville Formation. During this time the Chattanooga Shale and the Neal (Floyd) Shale fell into the oil window. During the erosion of the Pottsville Formation the Chattanooga Shale and the Neal (Floyd) Shale fell into the gas window. A fifth overpressurization event occurred during the deposition of the Eutaw Formation. During this time the Chattanooga Shale and the Neal (Floyd) Shale reached the gas window.
- The Chattanooga Shale is currently overpressurized. Modeling results indicate that this is not from sedimentation. This is most likely due to hydrocarbons being present in the pore spaces of this shale.

- The Conasauga Formation began oil generation at 505 m.y. (TTI = 15), reached peak oil generation at 490 m.y. (TTI = 75), and ended oil generation at 480 m.y. (TTI = 160). At 478 m.y. 100% of possible oil generation in the Conasauga Formation had occurred. Onset of gas generation (TTI = 1000) occurred at 470 my and reached a TTI of 5000 at 410 m.y. That Chattanooga Shale began oil generation at 326 m.y. (TTI = 15), reached peak oil generation at 325.5 m.y. (TTI = 75), and ended oil generation at 325.25 my (TTI = 160). At 324.8 my 100% of possible oil generation in the Chattanooga Shale had occurred. Onset of gas generation (TTI = 1000) occurred at 305 m.y. and reached a TTI of 5000 at 148 m.y. The Neal (Floyd) Shale began oil generation at 326 m.y. (TTI = 15), reached peak oil generation at 325.5 m.y., and ended oil generation at 325 m.y. At 324.8 my 100% of possible oil generation in the Neal (Floyd) Shale had occurred. Onset of gas generation (TTI = 1000) occurred at 275 m.y. and reached a TTI of 5000 at 40 my.
- Thermal maturation modeling data is confirmed with the presence of hydrocarbons in each of the shales indicating they been thermally mature.
- Fluid flow modeled in the geologic past gives insight into the possible migration pathways of hydrocarbons in the Black Warrior Basin.
- Groundwater flow in the Black Warrior was mostly driven by compaction in the past. At present day the basin tilts to the south and groundwater flow is driven southward by gravity and topographic relief.

References

Alley, B., Beebe, A., Rodgers, J., & Castel, J. (2011) Chemical and physical characterization of produced waters from conventional and unconventional fossil fuel resources. *Chemosphere.*, **85**, 74-82.

Aunela-Tapola, L., Frandsen, F., & Hasanen, E. (1998) Trace metals emissions from the Estonian oil shale fired power plant. *Fuel Process Technologies.*, **21**, 490-494.

Beaulie, B., & Ramirez, R.E. (2013) Arsenic Remediation Field Study Using a Sulfate Reduction and Zero-Valent Iron PRB. *Groundwater Monitoring and Remediation*., **33**, 85-94.

Berman, A., & Engelderan, T. (2012). North American Energy Summit, *Panel 1. Baker Institute Energy Forum and PFC Energy*. http://www.youtube.com/watch?v=ZKRyq5RubOY

Bethke, C., Lee, M., Quinodoz, H., & Kreiling, W. (1993) Basin Modeling with Basin2: A guide to using Basin2, B2plot, B2video, and B2view, *University of Illinois Hydrogeology program*, 1- 225.

Bowker, K.A. (2002) Recent developments of the Barnet Shale play, Fort Worth basin, in B.E. Law and M. Wilson, eds., *Innovative Gas Exploration Concepts Symposium, Rocky Mountain Association of Geologist and Petroleum Technology Transfer Council*, October, 2002, Denver, Colorado, 16.

Bowker, K.A. (2003) Recent development of the Barnett Shale play, Fort Worth Basin, West *Texas Geological Society Bulletin.*, v **42**, 1-11.

Bradley, J., David R. , Naomi J., Mike B., & Williams A (2013). State of Illinois. *98th General Assembly. Hydraulic Fracturing Regulatory Act.* 2013.

Briskin, J., and Stephen Kraemer. (2013) United States. Environmental Protection Agency . *Well Construction/Operation and Subsurface Modeling*., Web

Carroll, R. E., Pashin, J. C., & Kugler, R. L. (1995) Burial history and source-rock characteristics of upper Devonian through Pennsylvanian strata, Black Warrior Basin, Alabama: *Alabama Geological Survey Circular.*, **187**, 1-29.

Cleaves, A.W., & Broussard, M.C. (1980) Chester and Pottsville depositional systems, outcrop and subsurface, in the Black Warrior basin of Mississippi and Alabama. *Gulf Coast Association of Geological Societies Transactions.*, **30**, 49-60.

Colorado. Colorado Oil and Gas Conservation Commission. (2012)*Complete Rules 100-1200 Series*.

Coveney, R., & Glascock, M. (1989) A review of the origins of metal-rich Pennsylvanian black shales, central U.S.A. with an inferred role for basinal brines. *Applied Geochemistry.*, **4**, 347-367.

Dale, L., & Fardy, J. (1984) Trace elements partitioning during the retorting of some Australian oil shales. *Environmental Science Technologies*., **18**, 887-889.

Drever, J. I. (1997) The geochemistry of natural waters surface and groundwater environments Upper Saddle River, Prentice Hall

Ingraffea. (2010) . *Facts on Fracking*., Nanticoke, Pennsylvania. Web. 15 Jul 2013. <http://www.youtube.com/watch?v=mSWmXpEkEPg>.

EIA (Energy Information Administration) (2006) *U.S. Crude oil, natural gas, and natural gas*

liquids reserves 2005 annual report., Appendix B, 10, http://www.eia.doe.gov/oil_gas/natural_gas/data_publications/crude_oil_natural_gas_reserves/cr.html.

Fisher, K., & Warpinski, N. (2011) Hydraulic fracture-height growth: real data, *Paper SPE 145949 presented at the Annual Technical Conference and Exhibition, Denver, Colorado.*, DOI*:10.2118/145949-MS.*

Groshong, R.H., Jr., Hawkins, W.B.Jr., Pashin, J.C., & Harry, D.L. (2010) Extensional structures of the Alabama promontory and Black Warrior foreland Basin: Styles and relationship to the Appalachian fold-thrust belt, in Tollo, R.P., Bartholomew, M.J., Hibbard, J.P., and Darabinos, P.M., eds., *From Rodinia to Pangea: Geological Society of America Memoir.*, **206,** 579-605.

Hansom, J., & Lee, M.-K.. (2005) Effects of hydrocarbon generation, basal heat flow, and sediment compaction on overpressure development: A numerical study. *Petroleum Geoscience.*, **11**, 353-360.

Haynes, C.D., Malone, P.G., & Camp, B.S. (2010) Exploration of the shallow Chattanooga Shale in north central Alabama: Tuscaloosa, *Alabama. University of Alabama, college of Continuing Studies, 2010 International coalbed and Gas-shale Symposium proceedings, paper.*, **1015**, 1-16.

Jarvie, D.M., Hill, R.J., Ruble, T.E., & Pollastro, R.M. (2007) Unconventional shale-gas systems: the Mississippian Barnett Shale of north central Texas as one model for thermogenic shale- gas assessment. *AAPG Bulletin.*, **91**, no. 4, 475- 499.

Kao, Y.-H., Wang, S.-W., Maji, S.K., Liu, C.-W., Wang, P.-L., Chang, F.-J., & Liao, C.-M. (2013) Hydrochemical, Mineralogical and Isotopic Investigation of Arsenic Distribution and Mobilization in the Guandu Wetland of Taiwan. *Journal of Hydrology.*, **498**, 274-286.

Karl, K., & Karl, W, H. (1961) Distribution of elements in some major units of the Earth's crust. *Geological Society of America Billiton*, **72**, 175-192.

King, G., 2010, Thirty years of gas shale fracturing: What have we learned? Paper SPE 133456 presented at the SPE Annual Technical Conference and Exhibition, September 19-22, 2010, Florence, Italy.

King, G., Hale, L., Shuss, J., & Dobkins, T. (2008) Increasing fracture path complexity and controlling downward fracture growth in the Barnett shale. *Paper 119896 presented at the SPE gas-shale Production Conference, November 16-18, 2008, Fort Worth, Texas*.

Kwon, O., Kronenberg, Gangi, A., Johnson, B., &Herbert, B. (2004a) Permeability of illite-bearing shale: 1. Anisotropy and effects of clay content and loading. *Journal of Geophysical Research* .,**109**, B10205.doi: 10.1029/2004/JB003052.

Kwon, O., Herbert, & Kronenberg, A. (2004b) Permeability of illite-bearing shale: 2. Influence of fluid chemistry on flow and functionally connected pores. *Journal of Geophysical Research*, **109**, B10206. DOI: 10.1029/2004B002055.

La Force, M.J., Hansel, C.M., & Fendorf, S. (2000) Arsenic speciation, seasonal transformations, and co-distribution with iron in a mine waste-influenced palustrine emergent wetland. *Environmental Science Technology.*, **34**, 3937-3943.

Lacombe, S., Sudickey, E., Frape, S., Unger, A. (1995) Influence of leak boreholes on cross-formational groundwater flow and contaminant transport. *Water Resources Research*, **31**, no 8, 1871-1882.

Lee, M.-K., Saunders, J.A., Wilkin, R.T. & Mohammad, S. (2005) Geochemical modeling of arsenic speciation and mobilization: Implications for bioremediation, in Advances in Arsenic

Research: Integration of Experimental and Observational Studies and Implications for Mitigation, O'Day et al. (eds.), *American Chemical Society Symposium Series.*, **915**, 398-413.

Lopatin, V. (1971) Temperature and geologic time as factors in coalification (in Russian), *Akademiia Nauk SSSR Izvestiya Seriy Geologiches-Kaya* ., **4**, 95-106.

Mandal, S.K., Dey, M., Ganguly, D., Sen, S., & Jana, T.K. (2009) Biogeochemical controls of arsenic occurrence and mobility in the Indian Sundarban mangrove ecosystem.. *Mar. Pollution Bulletin,*. **58**, 652-657.

Mandal, S.D., Majumder, N., Chowdhury, C., Ganguly, D., Dey, M., & Jana, T.K.. (2012) Adsorption kinetic control of As (III andV) mobilization and sequestration by Mangrove Sediment. *Environmental Earth Science*., 65, 2027-2036.

Miskimins, J. (2009) The importance of geophysical and petrophysical data intergration for the hydraulic fracturing of unconventional reservoirs. *The Leading Edge, Special Section: Unconventional Resources and CO_2 Monitoring., 844- 849.*

Myers T. (2012) Potential Contaminant Pathways from Hydraulically Fractured Shale to Aquifers. *Ground Water.*, **50**, no 6, 872-882.

Natter, M., Keevan, J., Wang, Y.,Keimowitz, A. R., Okeke, B. C., Son, A., & Lee, M. K. (2012) Level and Degradation of Deep-water Horizon Spilled Oil in Coastal Marsh Sediments and Pore-Water. *Environmental Science Technology.*, **46**, 5744-5755.

Neuzil, C. E. (1994) How permeable are clays and shales. *Water Resources Research,*. 30, no2, 145-150.

Neuzil, C. (1986) Groundwater flow in low-permeability environments. *Water Resources Research*, **22**, no 2, 145-150.

Pahin, J.C. (1993) Tectonics, paleoceanography, and paleoclimate of the Kaskaskia sequence in the Black Warrior basin of Alabama, in Pashin, J.C., ed. *New perspectives on the Mississippian System of Alabama, Alabama Geological Society 30th Annual Field Trip Guidebook*, 1-28.

Pashin, J. C. (1994) Cycles and stacking patterns in Carboniferous rocks of the Black Warrior foreland Basin. *Gulf Coast Association of Geological Societies Transactions*., **44**, 555-563.

Pashin, J.C. (2004) Cyclothems of the Black Warrior basin in Alabama: eustatic snapshots of foreland basin tectonism, in Pashin, J.C., and Gastaldo, R.A., eds., Sequence stratigraphy, paleclimate, and tectonics of coal-bearing strata, *American Association of Petroleum Geologists Studies in Geology.*, **51**, 199-217.

Pashin, J. C., Kopaska-Merkel, D. C., Arnold, A. C., & McIntyre, M. R. (2011) Geological foundation for production of natural gas resources from diverse shale formations: Sugarland, *Texas, Research Partnership to Secure Energy for America Final Report 07122.17.01; Geological Survey of Alabama Open-File Report 1110*, 156. Annual Conference and Exposition, New Orleans, Louisiana.

Pashin, J. C., & Groshong, R.H., Jr. (1998) Structural control of coalbed methane production in Alabama. *International journal of Coal Geology*., **38**, 89-113.

Pashin, J. C. (2008) Gas shale potential of Alabama, Tuscaloosa, Alabama, University of

Alabama, College of Continuing Studies. *2008 International Coalbed and Gas-shale Symposium Proceedings.*, paper 0808, 13.

Pashin, J.C., Gas-shale plays of the sourthern Appalachian thrust belt: Tuscaloosa, Alabama, University of Alabama, College of Continuing Studies, 2009 International Coalbed and Shale

Gas Symposium Proceedings, paper 0907, 14p.
Pashin, J.C., Grace, R.L.B., & Kopaska-Merkel, D.C. (2010) Devonian shale plays in the black Warrior basin and Appalachian thrust belt of Alabama: Tuscaloosa, Alabama, University of Alabama, College of Continuing Studies. *2010 International Coalbed and Gas-shale Symposium Proceedings*, paper 1016, 20.
Pennsylvania Department of Environmental Protection (PADEP), 2011, Marcellus Shale, http://www.dep.state.pa.us/dep/deputate/minres/oilgas/new_forms/marcellus/marcellus.htm
Pennsylvania. Pennsylvania Department of Environmental Protection. (2012) *Oil and Gas Title 58*.
Perkins, R., Mason, C., & Piper, D. (2012) Mobility of trace elements from the Sunbury Shale, eastern Kentucky. *Mineralogical Magazine*, **76**, i 6, 2220.
Rheams, K.F., and Neathery, T.L. (1988) Characterization and geochemistry of Devonian oil shale, north Alabama, northwest Georgia, and south-central Tennessee (a resource evaluation). *Alabama Geological Survey Bulletin.*, **128**, 214.
Saunders, J.A., Pritchett, M.A., & Cook, R.B. (1997) Geochemistry of biogenic pyrite and ferromanganese stream coatings: a bacterial connection?. *Geomicrobiology*, **14**, 203-217.
Saunders, J.A., Lee, M.-K., Shamsudduha, M., Dhakal, P., Uddin, A., Chowdury, M.T., & Ahmed, K.M. (2008) Geochemistry and Mineralogy of Arsenic in (Natural) Anaerobic Groundwaters. *Applied Geochemistry*, **23**, 3205-3214.
Smedley, P.L., &Kinniburgh, D,G. (2002) A review of the source, behavior and distribution of arsenic in natural waters. *Applied Geochemistry*., **17**, 517-568.
Smith, A. H., Marshall, G., Liaw, J.,& Ferreccio, C. (2012) Mortality in Young Adults Following in Utero and Childhood Exposure to Arsenic in Drinking Water. *Environmental Health Perspectives*, **120**, no 11, 1527 – 1531.
Soeder, D., &Kappel, W., 2009, Water Resources and Natural Gas Production from the MarcellusShale, *USGS fact shee.,t* 2009-3032.
Soeder, D. (1988) Porosity and permeability of eastern Devonian gas shale. *Society of Petroleum Engineers Formation Evaluation, Society of Petroleum Engineers*, **3**, no 2, 116-124. DOI: 10.2118/15213-PA.
Soerensen K., & Cant, N. (1988) The role of catalysis by mineral matter during oil shale retorting. *Fuel.*, **67**, 1344-1348.
Thomas, W. A. (1988) The Black Warrior basin, in Sloss, L.L., ed., Sedimentary cover— North American Craton. *Geological Society of America, The Geology of North America*, **D-2**, 471-492.
Thomas, W. A. (1977) Evolution of Appalachian-Ouachita salient and recesses from reentrants and promontories in the continental margin. *American Journal of Science*, **277**, 1233-1278.
Thomas, W. A., and Bayona, G. (2005) The Appalachian thrust belt in Alabama and Georgia: thrust-belt structure, basement structure, and palinspastic reconstruction. *Alabama Geologic Survey Monograph.*, **16**, 48.
Thomas, W.A. (2001) Mushwad: Ductile duplex in the Appalachian thrust belt in Alabama, American. *Association of Petroleum Geologist Bulletin*, **85**, 1847-1869.
United States. Environmental Protection Agency. Permitting Guidance for Oil and Gas Hydraulic Fracturing Activities Using Diesel Fuels –Draft: Underground Injection Control Program Guidance , <http://cluin.org/live/archive/>.

U.S. Environmental Protection Agency. (2002) http://www.epa.gov/osw/hazard/testmethods/pdfs/3570.pdf

Waples, W. (1980) Time and temperature in petroleum formation, application of Lopatin's method to petroleum exploration. *American Association of Petroleum Geologists Bulletin.*, **64**, 916-926.

Wang, G., &Carr, T. (2012) Methodology of organic-rich shale lithofacies identification and prediction: A case study from Marcellus Shale in the Appalachian basin. *Computers and Geosciences*, **49**, 151-163.

Wang, Z., & Stout, S.A. (2007) Oil Spill Environmental Forensics. *Academic Press: New York*.

Zhang, T., Ellis, G., Ruppel, S., Milliken, K., & Yang, R. (2012) Effect of organic-matter type and thermal maturity on methane adsorption in shale-gas systems. *Organic Geochemistry.*, **47**, 120-131.

APPENDIX 1. Input file for Basin2 modeling thermal history, overpressurization, and basin hydrology simulation. Input file describes three basic rock types and their associated hydraulic properties. Percentages of these particular rock types are then placed at defined thicknesses and amount at each well location used in the modeled transect. Thermal properties of the basin were set in this input as well as the boundary conditions of the model. For more detailed instruction of input parameters see Bethke et al. (1993).

```
start = -518 m.y.; end = 0 m.y.
nx = 60; dztarg = 800 m
y_LHS = 10 cm; y_RHS = 1 cm
press_increase = 5; temp_increase = 5
initial = steady; compaction = irreversible
tti = $TTI; vitrinite = on; arrhenius = on
tables = TTI
tables = X_oil
rock ss
  A_perm = 15.5; B_perm = -5 log_darcy; p_kxkz = 2.5
rock sh
  A_perm = 8; B_perm = -8 log_darcy; p_kxkz = 10
rock cn
  A_perm = 10; B_perm = -6.5 log_darcy; p_kxkz = 6
rock im
  A_perm = 4;  B_perm = -9 log_darcy; p_kxkz = 0
end_rock
width = 417485 ft
x_well(ft)  0   29117   105129   157473   198128   217199   289268   417485
left = closed; right = closed
heat_flow = 1.5 HFU;
X_average = geometric, Z_average = harmonic
strat 'Conasuaga Formation'
  t_dep = -518 m.y.
  column   thickness(ft)   X(ss)   X(sh)   X(cn)
  w(1:8)     5000          0.0     0.6     0.4
strat 'Knox Group'
  t_dep = -505 m.y.
  column   thickness(ft)   X(ss)   X(sh)   X(cn)
  w(1:8)      4000         0.0     0.0     1
strat 'erosion 1'
  t_dep = -490 m.y.
  column   thickness(ft)
  w(1:8)   -1500
```

strat 'Ordovician undifferentiated'
t_dep = -480 m.y.

column	thickness(ft)	X(ss)	X(sh)	X(cn)
w(1)	3500	0.0	0.0	1
w(2)	4000	0.0	0.0	1
w(3)	6000	0.0	0.0	1
w(4)	6000	0.0	0.0	1
w(5)	6000	0.0	0.0	1
w(6)	5500	0.0	0.0	1
w(7)	5500	0.0	0.0	1
w(8)	5500	0.0	0.0	1

strat 'erosion 2'
t_dep = -440 m.y.

column	thickness(ft)
w(1:8)	-1000

strat 'Silurian undifferentiated'
t_dep = -438 m.y.

column	thickness(ft)	X(ss)	X(sh)	X(cn)
w(1:2)	600	0.3	0.2	0.5
w(3:6)	600	0.0	0.0	1
w(7:8)	600	0.0	0.0	1

strat 'erosion 3'
t_dep = -417 m.y.

column	thickness(ft)
w(1:8)	-200

strat 'Unnamed Devonian carbonate and chert unit'
t_dep = -400 m.y.

column	thickness(ft)	X(ss)	X(sh)	X(cn)
w(1)	1000	0.0	0.0	1
w(2)	1050	0.0	0.0	1
w(3)	1075	0.0	0.0	1
w(4)	1075	0.0	0.0	1
w(5)	1500	0.0	0.0	1
w(6)	1500	0.0	0.0	1
w(7)	2000	0.0	0.0	1
w(8)	2200	0.0	0.0	1

strat 'erosion 4'
t_dep = -370 m.y.

column	thickness(ft)
w(1:8)	-500

strat 'Chattanooga Shale'
t_dep = -365 m.y.

column	thickness(ft)	X(ss)	X(sh)	X(cn)
w(1)	40	0.0	1	0.0
w(2)	40	0.0	1	0.0
w(3)	80	0.0	1	0.0

w(4)	45	0.0	1	0.0
w(5)	90	0.0	1	0.0
w(6)	90	0.0	1	0.0
w(7)	300	0.0	1	0.0
w(8)	90	0.0	1	0.0

strat 'erosion 5'
t_dep = -360 m.y.

column	thickness(ft)
w(1)	-30
w(2)	-30
w(3)	-48
w(4)	-30
w(5)	-40
w(6)	-40
w(7)	-100
w(8)	-40

strat 'Tuscumbia Limestone and Fort Payne Chert undifferentiated'
t_dep = -354 m.y.

column	thickness(ft)	X(ss)	X(sh)	X(cn)
w(1:8)	200	0.0	0.0	1

strat 'Bangor Limestone and Floyd Shale Undifferentiated'
t_dep = -350 m.y.

column	thickness(ft)	X(ss)	X(sh)	X(cn)
w(1)	700	0.3	0.5	0.2
w(2)	900	0.2	0.6	0.2
w(3)	1400	0.0	0.8	0.2
w(4)	1600	0.0	0.9	0.1
w(5)	1800	0.0	1	0.0
w(6)	1800	0.0	1	0.0
w(7)	2300	0.0	1	0.0
w(8)	2000	0.0	1	0.0

strat 'Parkwood Formation'
t_dep = -330 m.y.

column	thickness(ft)	X(ss)	X(sh)	X(cn)
w(1)	900	0.3	0.4	0.3
w(2)	850	0.3	0.4	0.3
w(3:6)	1000	0.1	0.9	0.0
w(7:8)	1300	0.2	0.8	0.0

strat 'Pottsville Formation'
t_dep = -323 m.y.

column	thickness(ft)	X(ss)	X(sh)	X(cn)
w(1)	4000	0.5	0.5	0.0
w(2)	4500	0.4	0.6	0.0
w(3)	5500	0.3	0.7	0.0
w(4)	6500	0.3	0.7	0.0
w(5)	7500	0.2	0.8	0.0

```
   w(6)       8500              0.2    0.8    0.0
   w(7:8)     9500              0.4    0.6    0.0
strat 'erosion 6'
   t_dep = -248 m.y.
   column   thickness(ft)
   w(1:2)     -1000
   w(3)       -1500
   w(4:8)     -2000
strat 'lower Creataceous undiff'
   t_dep = -144 m.y.
   column   thickness(ft)   X(ss)   X(sh)   X(cn)
   w(1:6)     100              1      0       0
   w(7:8)     400              0.8    0       0.2
strat 'erosion 7'
   t_dep = -120 m.y.
   column   thickness(ft)
   w(1:8)     -100
strat 'Coker Formation'
   t_dep = -99 m.y.
   column   thickness(ft)   X(ss)   X(sh)   X(cn)
   w(1)       500              0.5    0.5    0
   w(2)       650              0.5    0.5    0
   w(3)       750              0.6    0.4    0
   w(4)       800              0.5    0.5    0
   w(5)       900              0.5    0.5    0
   w(6)       1000             0.5    0.5    0
   w(7)       1100             0.5    0.5    0
   w(8)       1200             0.5    0.5    0
strat 'erosion 8'
  t_dep = -90 m.y.
  column   thickness(ft)
  w(1:8)     -100
strat 'Gordo Formation'
  t_dep = -80 m.y.
  column   thickness(ft)   X(ss)   X(sh)   X(cn)
  w(1:2)     300              0.4    0.6    0.0
  w(3:8)     500              0.5    0.5    0.0
strat 'erosion 9'
  t_dep = -85 m.y.
  column    thickness(ft)
  w(1:8)      -100
strat 'Eutaw Formation'
  t_dep = -75 m.y.
  column   thickness(ft)   X(ss)   X(sh)   X(cn)
  w(1)       0                0.0    0.0    0.0
  w(2)       100              0.5    0.5    0.0
```

```
  w(3)       200                0.5     0.5     0.0
  w(4)       300                0.5     0.5     0.0
  w(5)       400                0.5     0.5     0.0
  w(6)       500                0.5     0.5     0.0
  w(7)       600                0.5     0.5     0.0
  w(8)       700                0.5     0.5     0.0
strat 'Deposition Hiatus'
  t_dep = -65 m.y.
  column    thickness(ft)
  w(1:8)       0
strat 'present day'
  t_dep = 0 m.y.
thickness = 0
  column    water_depth(ft)
  w(1)       -470
  w(2)       -369
  w(3)       -351
  w(4)       -226
  w(5)       -242
  w(6)       -336
  w(7)       -273
  w(8)       -175
```